

2014-09-02

Phenotypic Association between the Outer Membrane Protein OmpW and the Small Multi-Drug Resistance Protein EmrE in Escherichia coli

Beketskaia, Maria

Beketskaia, M. (2014). Phenotypic Association between the Outer Membrane Protein OmpW and the Small Multi-Drug Resistance Protein EmrE in Escherichia coli (Master's thesis, University of Calgary, Calgary, Canada). Retrieved from <https://prism.ucalgary.ca>. doi:10.11575/PRISM/27333
<http://hdl.handle.net/11023/1712>

Downloaded from PRISM Repository, University of Calgary

UNIVERSITY OF CALGARY

Phenotypic Association between the Outer Membrane Protein OmpW and the Small
Multi-Drug Resistance Protein EmrE in *Escherichia coli*

by

Maria S. Beketskaia

A THESIS

SUBMITTED TO THE FACULTY OF GRADUATE STUDIES
IN PARTIAL FULFILMENT OF THE REQUIREMENTS FOR THE
DEGREE OF MASTER OF SCIENCE

GRADUATE PROGRAM IN BIOLOGICAL SCIENCES

CALGARY, ALBERTA

AUGUST, 2014

© Maria S. Beketskaia 2014

Abstract

In *Escherichia coli*, the small multidrug resistance (SMR) transporter protein EmrE confers host resistance to a broad range of toxic quaternary cationic compounds (QCCs) via proton motive force in the cytoplasmic membrane. Biologically produced QCCs also act as EmrE osmoprotectant substrates within the cell and participate in host pH regulation and osmotic tolerance. Although *E. coli* EmrE is one of the most well-characterized SMR members, it is unclear how the substrates that it transports into the periplasmic space escape across the outer membrane (OM) in Gram-negative bacteria. We tested the hypothesis that *E. coli* EmrE relies on an unidentified OM protein (OMP) to complete the extracellular release of its QCC. By conducting pH-based phenotypic growth screens, complementation and methyl viologen (MV) resistance assays, we have confirmed that EmrE relies on the presence of an OMP, specifically OmpW, to complete its extracellular substrate efflux across the OM.

Preface

This thesis work has been published in the Journal of Bacteriology (Beketskaia MS, Bay DC, Turner RJ. 2014. Outer membrane protein OmpW participates with small multidrug resistance protein member EmrE in quaternary cationic compound efflux. J. Bacteriol. 196:1908-1914.) and the first author of the paper is also the author of this thesis and the person responsible for the data collection and analysis. Also, this work has been presented during the poster sessions at the 2014 General Meeting of the American Society for Microbiology (Beketskaia MS, Bay DC, Turner RJ. 2014. Outer membrane protein OmpW participates with the Small Multidrug Resistance protein EmrE in quaternary cationic compound resistance. The 114th General Meeting of the American Society for Microbiology (ASM 2014), Boston, Massachusetts, USA.) and the 2014 Annual Conference of the Canadian Society for Molecular Biosciences (Beketskaia MS, Bay DC, Turner RJ. 2014. 57th Annual Conference of the Canadian Society for Molecular Biosciences – Membrane Proteins in Health and Disease (CSMB 2014), Banff, Alberta, Canada.).

Acknowledgements

I would like to start off by thanking my supervisor, Dr. Raymond J. Turner. Thank you for believing in me, Dr.T! This work would have not been possible without your support, encouragement and guidance. A huge thank you to my committee members, Dr. Michael F. Hynes and Dr. Elke M. Lohmeier-Vogel, for your time, feedback and interest throughout this journey. Additionally, I would like to thank Dr. Anthony B. Schryvers and Dr. Doug G. Storey for their time and contribution to my thesis defence.

I must also thank all of my lab mates in the Turner lab, who have first became my friends and then became like family, for their help and advice. Thank you guys for providing the best-est research environment that I could have asked for. Also, a very special thank you to Dr. Denice C. Bay for her vision, expertise and inexhaustible patience. Denice, thank you for being my security blanket.

Dedication

I dedicate this thesis to my family, Sergey, Irina, Anastasia and Viktor.

Table of Contents

Abstract	ii
Preface.....	iii
Acknowledgements.....	iv
Dedication	v
Table of Contents	vi
List of Tables	ix
List of Figures and Illustrations	x
List of Symbols, Abbreviations and Nomenclature	xv
 CHAPTER ONE: INTRODUCTION.....	 1
1.1 Cell Envelope of Gram-Negative Bacteria	1
1.1.1 The Outer Membrane	1
1.1.2 The Peptidoglycan Cell Wall.....	4
1.1.3 The Cytoplasmic Membrane	4
1.2 Bacterial Stress Responses.....	5
1.2.1 Osmotic Stress and Bacterial Osmoregulation	5
1.2.2 pH Stress and Bacterial Alkali Tolerance	8
1.3 Antibiotic Resistance in Bacteria.....	9
1.3.1 Efflux-Mediated Multidrug Resistance	10
1.3.2 The Small Multidrug Resistance Family	12
1.3.3 Ethidium multidrug resistance protein E.....	14
1.4 Research Hypothesis and Goals.....	19
 CHAPTER TWO: GENERAL EXPERIMENTAL METHODS AND MATERIALS	 20
2.1 Bacterial Strains	20
2.2 Growth Conditions and Chemicals	23
2.3 Plasmids and Constructs	24
2.4 Preparation of Competent <i>E. coli</i> Cells	26
2.5 Bacterial Transformation	27
2.6 DNA Purification from <i>E. coli</i> Cells	27
2.6.1 Genomic DNA isolation	27
2.6.2 Plasmid DNA isolation.....	28
2.7 <i>E. coli</i> DNA Amplification	30
2.7.1 Polymerase Chain Reaction (PCR)	30
2.7.2 Purification of Polymerase Chain Reaction Products	32
2.8 Agarose Gel Electrophoresis	32
2.8.1 DNA Analysis and Separation.....	33
2.8.2 DNA Purification from Agarose Gel.....	33
2.9 DNA Restriction with Endonucleases	35
2.10 DNA Ligation	36
2.10.1 Blunt end ligation	36
2.10.2 Sticky End Ligation.....	38

CHAPTER THREE: DEVELOPMENT OF A PHENOTYPIC SCREENING METHOD TO IDENTIFY OUTER MEMBRANE PROTEIN CANDIDATES INVOLVED IN EMRE-MEDIATED SUBSTRATE EFFLUX	40
3.1 Introduction.....	40
3.2 Materials and Methods.....	41
3.2.1 pH 7 to 9 M9 Growth Curves of Selected <i>E. coli</i> Outer Membrane Protein Gene Deletion Mutants	41
3.3 Results and Discussion	43
3.4 Summary	54
CHAPTER FOUR: PH-BASED PHENOTYPIC GROWTH SCREENS OF SELECTED <i>E. COLI</i> OUTER MEMBRANE PROTEIN GENE DELETION MUTANTS	56
4.1 Introduction.....	56
4.2 Materials and Methods.....	56
4.2.1 Neutral/alkaline pH Growth Phenotype Screens of Candidate OMP Mutants	56
4.2. Percentage Growth Recovery by pEmrE-transformed Strains	57
4.3. Results and Discussion	58
4.3.1 Only the ompW Gene Deletion Restored Host Alkali Tolerance and Rescued the Loss-of-Growth Phenotype Induced by EmrE at pH 9	58
4.4 Summary	66
CHAPTER FIVE: PLASMID COMPLEMENTATION ALKALINE GROWTH ASSAYS OF <i>E. COLI</i> Δ EMRE AND Δ OMPW STRAINS.....	67
5.1 Introduction.....	67
5.2 Materials and Methods.....	68
5.2.1 pMS119EHC Vector Construction.....	68
5.2.2 Construction of pOmpW, pOmpA and pLamB Clones.....	70
5.2.3 Plasmid Complementation Alkaline Growth Assays of <i>E. coli</i> Δ ompW and Δ emrE Mutants	72
5.2.4 Percentage Growth Recovery by Plasmid Pair Co-transformed Δ ompW and Δ emrE Strains	73
5.3 Results and Discussion	75
5.3.1 Complementation of <i>E. coli</i> Δ ompW Strain by pEmrE and pOmpW Reproduced the Loss-of-Growth Phenotype Under Alkaline Minimal Growth Conditions.....	75
5.3.2 Reverse complementation of <i>E. coli</i> Δ emrE strain by pEmrE and pOmpW also replicated the loss-of-growth phenotype under alkaline minimal growth conditions.....	78
5.4 Summary	79
CHAPTER SIX: TOXIC QUATERNARY CATIONIC COMPOUND MINIMUM INHIBITION CONCENTRATION ASSAYS	81
6.1 Introduction.....	81
6.2 Materials and Methods.....	81
6.3 Results and Discussion	83

6.3.1 E. coli Δ ompW and WT Strains Transformed with Both pEmrE and pOmpW Conferred Host Resistance to High Concentrations of MV	83
6.3.2 Co-expression of emrE and ompW gGenes in E. coli Δ ompW and WT Strains did not Increase Host Resistance to Acriflavine, EtBr or CTAB.	86
6.1 Summary	89
CHAPTER SEVEN: FINAL DISCUSSION, CONCLUDING REMARKS AND FUTURE DIRECTIONS	
7.1 Summary of Thesis Results	91
7.2 Functional Association between OmpW and EmrE: Connecting the Dots	92
7.3 Future Directions	95
REFERENCES	97

List of Tables

Table 2.1. The <i>E. coli</i> K-12 single-gene knockout Keio collection mutants (133) and cloning strain DH5 α (134) used within this thesis.....	21
Table 2.1. <i>E. coli</i> K-12 single-gene knockout Keio collection mutants (133) and cloning strain DH5 α (134) used within this thesis continued	22
Table 2.2. Plasmids used and constructed within this thesis	25
Table 2.3. Contents of a 50 μ L polymerase chain reaction	30
Table 2.4. General polymerase chain reaction cycling program used	31
Table 2.5. Contents of restriction endonuclease digestion reaction mix	36
Table 2.6. Contents of 35 μ L overhang blunting reaction mix.....	37
Table 2.7. Contents of a 20 μ L blunt end DNA ligation reaction mix	38
Table 2.8: Contents of a 20 μ L “sticky” end DNA ligation reaction mix.....	39
Table 6.1. Methyl viologen minimum inhibitory concentrations for culture dilutions of <i>E. coli</i> $\Delta ompW$ and WT strain plasmid co-transformants grown on M9 medium agar for 16 hrs	84
Table 6.2. Methyl viologen minimum inhibitory concentrations for culture dilutions of <i>E. coli</i> $\Delta ompW$ and WT strain plasmid co-transformants grown on M9 medium agar for 24 hrs	85
Table 6.3. Methyl viologen minimum inhibitory concentrations for culture dilutions of <i>E. coli</i> $\Delta ompW$ and WT strain plasmid co-transformants grown on M9 medium agar for 48 hrs	86
Table 6.4. Acriflavine minimum inhibitory concentrations for culture dilutions of <i>E. coli</i> $\Delta ompW$ and WT strain plasmid co-transformants grown on M9 medium agar for 16 and 24 hrs	88
Table 6.5. Ethidium bromide minimum inhibitory concentrations for culture dilutions of <i>E. coli</i> $\Delta ompW$ and WT strain plasmid co-transformants grown on M9 medium agar for 16 and 24 hrs	88
Table 6.6. Cetyltrimethylammonium bromide minimum inhibitory concentrations for culture dilutions of <i>E. coli</i> $\Delta ompW$ and WT strain plasmid co-transformants grown on M9 medium agar for 16 and 24 hrs	89

List of Figures and Illustrations

Figure 1.1. Schematic representation of Gram-positive and Gram-negative cell envelopes (adapted from reference (4)): LTA = lipoteichoic acid; CAP = covalently attached protein; WTA = wall teichoic acid; IMP = integral membrane protein; LP = lipoprotein; OMP = outer membrane protein; LPS/LOS = lipopolysaccharide/lipooligosaccharide; CM = cytoplasmic membrane; OM = outer membrane.	2
Figure 1.2. Diagrammatic comparison of the five major families of multidrug resistance transporters in bacteria (adapted from 82): MFS = major facilitator superfamily, SMR = small multidrug resistance superfamily, MATE = multidrug and toxic compound extrusion superfamily, RND = resistance-nodulation-cell division superfamily, ABC = ATP-binding cassette superfamily, OM = outer membrane and CM = cytoplasmic membrane.	11
Figure 1.3. Schematic representation of the ethidium multidrug resistance protein E (EmrE) from <i>E. coli</i> ; CM = cytoplasmic membrane; “E” represented the highly conserved glutamate residue located in the first transmembrane α -helix in all small multidrug resistance proteins	15
Figure 1.4. Schematic representation of the two proposed mechanism for EmrE-mediated substrate efflux in Gram-negative bacteria. According to the first hypothesis, indicated by the number 1, EmrE relies on an unidentified OMP to completely remove its substrate from the cell. According to the second hypothesis, indicated by the number 2, EmrE supplies substrate into the periplasm, where it can be accessed and removed completely from the cell by a multipartite transporter system.	18
Figure 3.1. Plasmid maps of the empty control vector (A) pMS119EHA (138) and the <i>emrE</i> gene expression construct (B) pEmrE (137).	42
Figure 3.2. Growth curve experiments with <i>E. coli</i> WT strain transformed with the pMS119EHA and pEmrE plasmids. Mean OD _{600nm} values (y axis) represent the growth of cultures measured every 2 hrs in pH 7 M9 medium at 37°C, over a 24-hr time frame (x axis) for the <i>E. coli</i> WT strain transformed with pMS119EHA (red) or pEmrE (green) or untransformed (black). Error bars represent the standard errors determined for each mean OD _{600nm} value (n=5).	45
Figure 3.3. Growth curve experiments with <i>E. coli</i> WT strain transformed with the pMS119EHA and pEmrE plasmids. Mean OD _{600nm} values (y axis) represent the growth of cultures measured every 2 hrs in pH 8 M9 medium at 37°C, over a 24-hr time frame (x axis) for the <i>E. coli</i> WT strain transformed with pMS119EHA (red) or pEmrE (green) or untransformed (black). Error bars represent the standard errors determined for each mean OD _{600nm} value (n=5).	46

- Figure 3.4. Growth curve experiments with *E. coli* WT strain transformed with the pMS119EHA and pEmrE plasmids. Mean OD_{600nm} values (y axis) represent the growth of cultures measured every 2 hrs in pH 9 M9 medium at 37°C, over a 24-hr time frame (x axis) for the *E. coli* WT strain transformed with pMS119EHA (red) or pEmrE (green) or untransformed (black). Error bars represent the standard errors determined for each mean OD_{600nm} value (n=5). 46
- Figure 3.5. Growth curve experiments with *E. coli* $\Delta ompA$ strain transformed with the pMS119EHA and pEmrE plasmids. Mean OD_{600nm} values (y axis) represent the growth of cultures measured every 2 hrs in pH 7 M9 medium at 37°C, over a 24-hr time frame (x axis) for the *E. coli* $\Delta ompA$ strain transformed with pMS119EHA (red) or pEmrE (green) or untransformed (black). Error bars represent the standard errors determined for each mean OD_{600nm} value (n=5). 47
- Figure 3.6. Growth curve experiments with *E. coli* $\Delta ompW$ strain transformed with the pMS119EHA and pEmrE plasmids. Mean OD_{600nm} values (y axis) represent the growth of cultures measured every 2 hrs in pH 7 M9 medium at 37°C, over a 24-hr time frame (x axis) for the *E. coli* $\Delta ompW$ strain transformed with pMS119EHA (red) or pEmrE (green) or untransformed (black). Error bars represent the standard errors determined for each mean OD_{600nm} value (n=5). 47
- Figure 3.7. Growth curve experiments with *E. coli* $\Delta ompX$ strain transformed with the pMS119EHA and pEmrE plasmids. Mean OD_{600nm} values (y axis) represent the growth of cultures measured every 2 hrs in pH 7 M9 medium at 37°C, over a 24-hr time frame (x axis) for the *E. coli* $\Delta ompX$ strain transformed with pMS119EHA (red) or pEmrE (green) or untransformed (black). Error bars represent the standard errors determined for each mean OD_{600nm} value (n=5). 48
- Figure 3.8. Growth curve experiments with *E. coli* $\Delta tolC$ strain transformed with the pMS119EHA and pEmrE plasmids. Mean OD_{600nm} values (y axis) represent the growth of cultures measured every 2 hrs in pH 7 M9 medium at 37°C, over a 24-hr time frame (x axis) for the *E. coli* $\Delta tolC$ strain transformed with pMS119EHA (red) or pEmrE (green) or untransformed (black). Error bars represent the standard errors determined for each mean OD_{600nm} value (n=5). 48
- Figure 3.9. Growth curve experiments with *E. coli* Δwza strain transformed with the pMS119EHA and pEmrE plasmids. Mean OD_{600nm} values (y axis) represent the growth of cultures measured every 2 hrs in pH 7 M9 medium at 37°C, over a 24-hr time frame (x axis) for the *E. coli* Δwza strain transformed with pMS119EHA (red) or pEmrE (green) or untransformed (black). Error bars represent the standard errors determined for each mean OD_{600nm} value (n=5). 49
- Figure 3.10. Growth curve experiments with *E. coli* $\Delta ompA$ strain transformed with the pMS119EHA and pEmrE plasmids. Mean OD_{600nm} values (y axis) represent the growth of cultures measured every 2 hrs in pH 8 M9 medium at 37°C, over a 24-hr time frame (x axis) for the *E. coli* $\Delta ompA$ strain transformed with

pMS119EHA (red) or pEmrE (green) or untransformed (black). Error bars represent the standard errors determined for each mean OD _{600nm} value (n=5).....	49
Figure 3.11. Growth curve experiments with <i>E. coli</i> $\Delta ompW$ strain transformed with the pMS119EHA and pEmrE plasmids. Mean OD _{600nm} values (y axis) represent the growth of cultures measured every 2 hrs in pH 8 M9 medium at 37°C, over a 24-hr time frame (x axis) for the <i>E. coli</i> $\Delta ompW$ strain transformed with pMS119EHA (red) or pEmrE (green) or untransformed (black). Error bars represent the standard errors determined for each mean OD _{600nm} value (n=5).....	50
Figure 3.12. Growth curve experiments with <i>E. coli</i> $\Delta ompX$ strain transformed with the pMS119EHA and pEmrE plasmids. Mean OD _{600nm} values (y axis) represent the growth of cultures measured every 2 hrs in pH 8 M9 medium at 37°C, over a 24-hr time frame (x axis) for the <i>E. coli</i> $\Delta ompX$ strain transformed with pMS119EHA (red) or pEmrE (green) or untransformed (black). Error bars represent the standard errors determined for each mean OD _{600nm} value (n=5).....	50
Figure 3.13. Growth curve experiments with <i>E. coli</i> $\Delta tolC$ strain transformed with the pMS119EHA and pEmrE plasmids. Mean OD _{600nm} values (y axis) represent the growth of cultures measured every 2 hrs in pH 8 M9 medium at 37°C, over a 24-hr time frame (x axis) for the <i>E. coli</i> $\Delta tolC$ strain transformed with pMS119EHA (red) or pEmrE (green) or untransformed (black). Error bars represent the standard errors determined for each mean OD _{600nm} value (n=5).	51
Figure 3.14. Growth curve experiments with <i>E. coli</i> Δwza strain transformed with the pMS119EHA and pEmrE plasmids. Mean OD _{600nm} values (y axis) represent the growth of cultures measured every 2 hrs in pH 8 M9 medium at 37°C, over a 24-hr time frame (x axis) for the <i>E. coli</i> Δwza strain transformed with pMS119EHA (red) or pEmrE (green) or untransformed (black). Error bars represent the standard errors determined for each mean OD _{600nm} value (n=5).	51
Figure 3.15. Growth curve experiments with <i>E. coli</i> $\Delta ompA$ strain transformed with the pMS119EHA and pEmrE plasmids. Mean OD _{600nm} values (y axis) represent the growth of cultures measured every 2 hrs in pH 9 M9 medium at 37°C, over a 24-hr time frame (x axis) for the <i>E. coli</i> $\Delta ompA$ strain transformed with pMS119EHA (red) or pEmrE (green) or untransformed (black). Error bars represent the standard errors determined for each mean OD _{600nm} value (n=5).....	52
Figure 3.16. Growth curve experiments with <i>E. coli</i> $\Delta ompW$ strain transformed with the pMS119EHA and pEmrE plasmids. Mean OD _{600nm} values (y axis) represent the growth of cultures measured every 2 hrs in pH 9 M9 medium at 37°C, over a 24-hr time frame (x axis) for the <i>E. coli</i> $\Delta ompW$ strain transformed with pMS119EHA (red) or pEmrE (green) or untransformed (black). Error bars represent the standard errors determined for each mean OD _{600nm} value (n=5).	52
Figure 3.17. Growth curve experiments with <i>E. coli</i> $\Delta ompX$ strain transformed with the pMS119EHA and pEmrE plasmids. Mean OD _{600nm} values (y axis) represent	

- the growth of cultures measured every 2 hrs in pH 9 M9 medium at 37°C, over a 24-hr time frame (x axis) for the *E. coli* $\Delta ompX$ strain transformed with pMS119EHA (red) or pEmrE (green) or untransformed (black). Error bars represent the standard errors determined for each mean OD_{600nm} value (n=5)..... 53
- Figure 3.18. Growth curve experiments with *E. coli* $\Delta tolC$ strain transformed with the pMS119EHA and pEmrE plasmids. Mean OD_{600nm} values (y axis) represent the growth of cultures measured every 2 hrs in pH 9 M9 medium at 37°C, over a 24-hr time frame (x axis) for the *E. coli* $\Delta tolC$ strain transformed with pMS119EHA (red) or pEmrE (green) or untransformed (black). Error bars represent the standard errors determined for each mean OD_{600nm} value (n=5). 53
- Figure 3.19. Growth curve experiments with *E. coli* Δwza strain transformed with the pMS119EHA and pEmrE plasmids. Mean OD_{600nm} values (y axis) represent the growth of cultures measured every 2 hrs in pH 9 M9 medium at 37°C, over a 24-hr time frame (x axis) for the *E. coli* Δwza strain transformed with pMS119EHA (red) or pEmrE (green) or untransformed (black). Error bars represent the standard errors determined for each mean OD_{600nm} value (n=5). 54
- Figure 4.1. Growth recovery screens of 11 plasmid-transformed *E. coli* OMP strains in neutral pH 7 M9 media after 16 hrs at 37°C. The percentages of growth recovery, shown as a bar chart, represent the change in the mean (n = 5) 16 hr OD_{600nm} values (growth) of each strain transformed with pEmrE compared to results for the vector pMS119EHA. All strains except the WT, $\Delta ompC$ and Δpal pEmrE transformants failed to show statistically significant reductions ($P \leq 0.005$) in growth between the pEmrE-transformed strain and the empty control vector (pMS119EHA)-containing strain. 61
- Figure 4.2. Growth recovery screens of 11 plasmid-transformed *E. coli* OMP strains in alkaline pH 8 M9 media after 16 hrs at 37°C. The percentages of growth recovery, shown as a bar chart, represent the change in the mean (n = 5) 16 hr OD_{600nm} values (growth) of each strain transformed with pEmrE compared to results for the vector pMS119EHA. All strains except the $\Delta ompF$, $\Delta ompW$ and Δslp pEmrE transformants showed statistically significant reductions ($P \leq 0.005$) in growth between the pEmrE-transformed strain and the empty control vector (pMS119EHA)-containing strain. 63
- Figure 4.3. Growth recovery screens of 11 plasmid-transformed *E. coli* OMP strains in neutral pH 9 M9 media after 16 hrs at 37°C. The percentages of growth recovery, shown as a bar chart, represent the change in the mean (n = 5) 16-h OD_{600nm} values (growth) of each strain transformed with pEmrE compared to results for the vector pMS119EHA. Percent growth recovery value for the Δpal mutant is not shown, since this strain failed to grow at pH 9. All strains except the $\Delta ompW$ pEmrE transformant showed statistically significant reductions ($P \leq 0.005$) in growth between the pEmrE-transformed strain and the empty control vector (pMS119EHA)-containing strain. 65

Figure 5.1. Plasmid map of the Cm-resistant control vector pMS119EHC.....	69
Figure 5.2. Plasmid maps of the <i>ompW</i> gene expression construct (A) pOmpW, <i>ompA</i> expression construct (B) pOmpA and <i>lamb</i> gene expression construct (C) pLamB.....	71
Figure 5.3. Plasmid complementation of the <i>E. coli</i> $\Delta ompW$ strain cultured using alkaline (pH 9) M9 growth phenotype assays. The percent growth recovery of plasmid co-transformed $\Delta ompW$ strains is shown as a bar chart, reflecting the change in mean ($n = 5$) 16-hr OD _{600nm} values (growth) between the pEmrE-transformed strain and the pMS119EHA strain. Statistically significant reduction in percent growth recovery values ($P \leq 0.005$) was observed only for pEmrE + pOmpW co-transformant and is indicated by an asterisk. Dashed line indicates the cutoff value ($30\% \times 2 = 60\%$) used to determine significant complementation.....	76
Figure 5.4. Plasmid complementation of the <i>E. coli</i> $\Delta emrE$ strain cultured using alkaline (pH 9) M9 growth phenotype assays. The percent growth recovery of plasmid co-transformed $\Delta emrE$ strains is shown as a bar chart, reflecting the change in mean ($n = 5$) 16-h OD _{600nm} values (growth) between the pOmpW-transformed strain and the pMS119EHC strain. Statistically significant reduction in percent growth recovery values ($P \leq 0.005$) was observed only for the pEmrE + pOmpW co-transformant and is indicated by an asterisks. Dashed line indicates the cutoff value ($30 \times 2 = 60\%$) used to determine significant complementation. ...	79

List of Symbols, Abbreviations and Nomenclature

Symbol	Definition
ABC	ATP-binding cassette
Amp	Ampicillin
ATP	Adenosine triphosphate
°C	Degrees Celsius
C	Carboxyl-terminus
CAP	Covalently attached protein
CM	Cytoplasmic membrane
Cm	Chloramphenicol
CTAB	Cetyltrimethylammonium bromide
Δ	Deletion
Δp	Electrochemical proton gradient
dd	Double distilled
DMSO	Dimethyl sulfoxide
E	Glutamate
EDTA	Ethylenediaminetetraacetic acid
EmrE	Ethidium multidrug resistance protein E
EtBr	Ethidium bromide
GlcNAc	N-acetylglucosamine
Hrs	Hours
IE	Inoculum effect
IMP	Integral membrane protein
IPTG	Isopropyl β -D-1-thiogalactopyranoside
kb	Kilobase
kDa	Kilodalton
LB	Lysogeny broth
LDAO	Lauryl dodecyl amine oxide
LOS	Lipooligosaccharide
LP	Lipoprotein
LPS	Lipopolysaccharide
LTA	Lipoteichoic acid
M9	Minimal 9 salts
MATE	Multidrug and toxic compound extrusion
MDR	Multidrug resistance
MFP	Membrane fusion protein
MFS	Major facilitator superfamily
MIC	Minimum inhibitory concentration
MOPS	3-morpholinopropane-1-sulfonic acid
MurNAc	N-acetylmuramic acid
MV	Methyl viologen
N	Amino-terminus

Symbol	Definition
n	Sample size
NaAC	Sodium acetate
NH ₄ Ac	Ammonium acetate
OD _{600nm}	Optical density at 600nm
OM	Outer membrane
OMP	Outer membrane protein
PCR	Polymerase chain reaction
PSMR	Paired small multidrug resistance
QCC	Quaternary cationic compounds
RND	Resistance–nodulation–cell division
rpm	Revolutions per minute
rrn	Ribosomal RNA operon
SMP	Small multidrug pumps
SMR	Small multidrug resistance
SUG	Suppressor of <i>groEL</i> mutation
TBE	Tris–borate–EDTA
TM	Transmembrane
T _m	Melting temperature
v/v	Volume/volume
WT	Wild type
WTA	Wall teichoic acid
w/v	Weight/volume

Chapter One: **Introduction**

1.1 Cell Envelope of Gram-Negative Bacteria

Over 100 years ago, Christian Gram developed a differential staining technique that allowed him to classify nearly all bacteria into two large groups, currently known as Gram-positive and Gram-negative, according to cell envelope composition and structure (1). As shown in Figure 1.1, the cell envelope of Gram-negative bacteria, such as *Escherichia coli*, contains three morphologically defined layers (2, 3). The most exterior layer, which consists of lipids, polysaccharides and proteins, is called the outer membrane (OM) and serves as a barrier to permeation. Internal to the OM, is a thin yet ridged layer of peptidoglycan (polymeric chains of *N*-acetylmuramic acid and *N*-acetylglucosamine linked by short peptides), which is located in the aqueous periplasmic space. Lastly, the innermost layer is a lipid-protein cytoplasmic membrane (CM), which regulates the movement of metabolites in and out of the cytoplasm and provides a platform for energy from respiration. Starting from the outside of the cell and proceeding inwards, each one of these layers will be introduced below, in sections 1.2.1, 1.2.2 and 1.2.3.

1.1.1 The Outer Membrane

A key distinguishing features of the Gram-negative cell envelope is the OM, since its Gram-positive counterpart usually lacks this layer (Figure 1.1). The OM is an asymmetric lipid bilayer, which is composed of phospholipids in the inner leaflet and lipopolysaccharide (LPS) and lipooligosaccharide (LOS) glycolipids in the outer leaflet

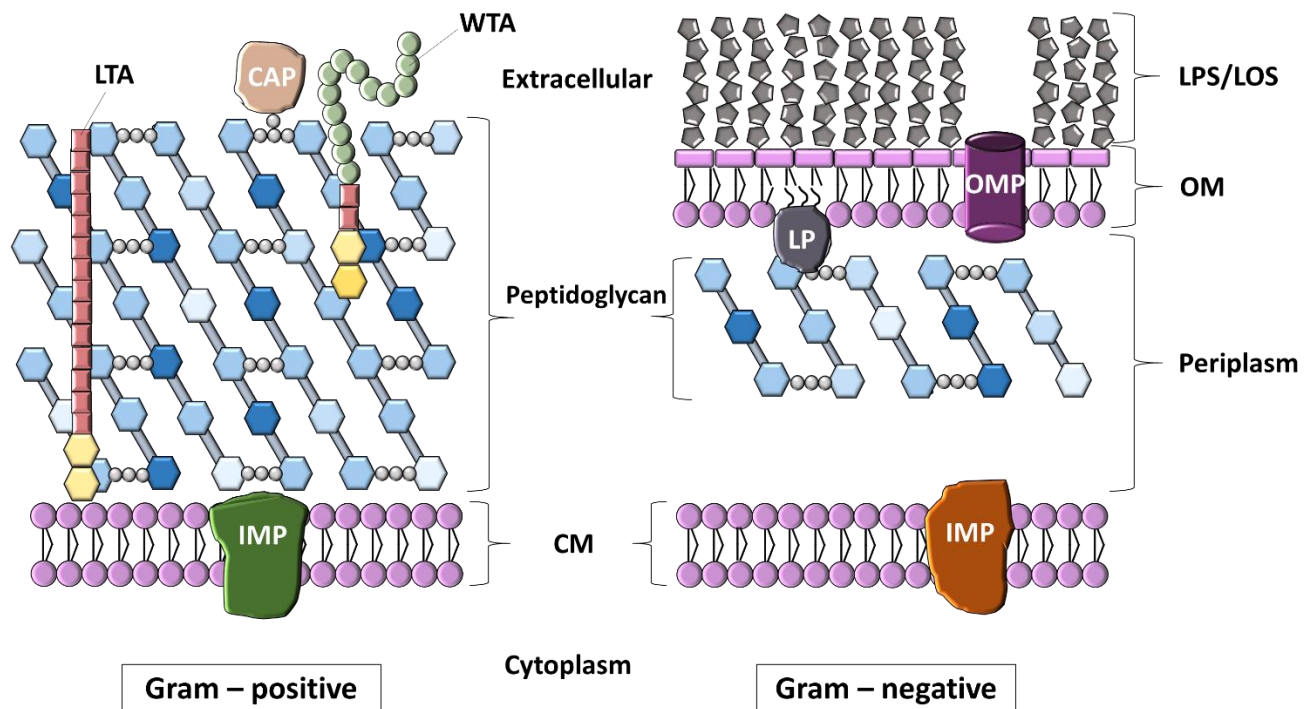


Figure 1.1. Schematic representation of Gram-positive and Gram-negative cell envelopes (adapted from reference (4)): LTA = lipoteichoic acid; CAP = covalently attached protein; WTA = wall teichoic acid; IMP = integral membrane protein; LP = lipoprotein; OMP = outer membrane protein; LPS/LOS = lipopolysaccharide/lipooligosaccharide; CM = cytoplasmic membrane; OM = outer membrane.

(5). It has been suggested that the most important function of the bacterial OM is to serve as a selective, low permeability barrier against antibiotics, detergents and other noxious agents in the environment (5, 6). The glycolipid monolayer is essential to this barrier function, as it is a highly ordered, gel-like structure of very low fluidity, which slows down the inward diffusion of lipophilic solutes (7, 8).

Although LPS/LOS cover approximately 75% of the outer surface of the OM, nearly half of the OM mass consists of protein (9, 10). These OM proteins can be divided into two classes: lipoproteins and integral proteins. Lipoproteins are peripheral proteins, which are anchored to the OM, on either the periplasmic or the outer surface side, via an N-terminal lipid moiety (11). While the presence of numerous lipoproteins in Gram-negative bacteria suggests that various membrane-associated activities are dependent on them, the function of the majority of *E. coli* lipoproteins is not known (12).

The integral OM proteins (OMPs) span the membrane bilayer in a barrel conformation, forming narrow channels for import of low molecular weight (≤ 700 Da) hydrophilic compounds, such as mono-/di-saccharides and amino acids, and export of waste products across the low-permeability OM barrier. While many of these channel-forming OMPs function as general diffusion porins, like OmpF and OmpC (13, 14), some are able recognize specific substrates, like the maltoporin LamB that only transports maltose and maltodextrins (15, 16). The β -pleated sheet is the predominant type of secondary structure of these OMPs, yet some OM barrel proteins, for example Wza, are known to be formed by hydrophobic α -helices (17, 18). Also, while the nonspecific porins and the structural protein OmpA (19, 20) are the most abundant OMPs, many other β -barrel proteins that function as enzymes, adhesins to host surfaces and bacteriophages, receptors and components of multipartite transport systems are also present in the OM (21).

1.1.2 The Peptidoglycan Cell Wall

The cell envelope of most bacteria contains a ridged peptidoglycan (also known as murein) layer, which allows the cell to maintain a certain shape and protects it from rupture, as a result of osmotic pressure of the cytoplasm (Figure 1.1). Although the chemical composition of the peptidoglycan varies between species, this exoskeleton-like structure is always made of linear glycan strands, which usually consist of alternating N-acetylglucosamine (GlcNAc) and N-acetylmuramic acid (MurNAc) residues linked by β -1 \rightarrow 4 bonds, that are cross-linked by short peptide side chains (22, 23).

Unlike Gram-positive bacteria, which contain a >20 nm-thick peptidoglycan mesh (as summarized in reference 24), Gram-negative microorganisms are not able to retain crystal violet (primary stain) used in the Gram staining method, since their peptidoglycan layer is only around 2-8 nm in thickness and their OM is dissolved by the alcohol-containing decolorizing mixture, aiding the release of the primary stain (Figure 1.1, 24, 25). Another differential aspect is the fact that the peptidoglycan from Gram-negative bacteria is “stapled” to the OM by a murein lipoprotein (LP), known as Lpp (26), and appears to interact non-covalently with various OMPs, such as OmpA and Pal (27).

1.1.3 The Cytoplasmic Membrane

The inner most layer of the Gram-negative cell envelope is the CM, which is a selectively-permeable membrane that encloses the cytoplasm (Figure 1.1). Like many biological membranes, CM is a fluid phospholipid bilayer and in *E. coli*, for example, the principal phospholipids are phosphatidylethanolamine and phosphatidylglycerol, while phosphatidylserine and cardiolipin are present in lesser amounts (as reviewed in reference

28). Also, the CM harbours a wide selection of proteins, which are involved in vital cell processes, such as trafficking of ions and molecules, cell division, environmental sensing, metabolism and biosynthesis of lipids, polysaccharides and peptidoglycan (as summarized in reference 29). In a typical *E. coli* cell, approximately a quarter of all genes are predicted to encode CM proteins and, unlike the earlier mentioned OM proteins, they all fold into α -helical bundles.

1.2 Bacterial Stress Responses

When bacteria are provided with sufficient nutrients and optimal growth temperature, pH, oxygen levels and solute concentrations, a maximum growth rate characteristic for those microorganisms is observed. Any deviation in these parameters can affect the growth rate and, consequently, can represent an environmental stress. The bacteria's ability to sense and properly respond to those spontaneous changes in the environment is critical to their survival. Since in nature (outside the laboratory) conditions that allow for maximal growth rates are few and far between, most bacteria live in a constant state of stress (30). Bacterial responses to environmental osmotic and pH stress will be discussed further in sections 1.2.1 and 1.2.2, respectively, of this chapter.

1.2.1 Osmotic Stress and Bacterial Osmoregulation

Osmotic pressure can be defined as the hydrostatic pressure required to prevent water from flowing across a semipermeable membrane into an aqueous solution of a membrane-impermeable solute (31). Bacteria maintain an osmotic pressure in the

cytoplasm that is higher than that in the surrounding environment, resulting in an outward directed pressure on the cell wall, known as the turgor pressure, which is thought to be necessary for growth. Since the bacterial cell envelope is permeable to water, due to the presence of water-selective channels (aquaporins), any fluctuations in the osmotic strength of the environment trigger the flux of water across the CM along the osmotic gradient (32). Hence, an increase in the osmolality of the surrounding environment causes the cell to lose water and turgor, while exposure to an environment with a very low osmotic strength leads to a rapid influx of water into the cell, thereby increasing turgor. This change in turgor pressure, caused by sudden osmotic upshifts or downshifts, is commonly known as osmotic stress and in order to avoid cell lysis under low-osmolality or dehydration under high-osmolality growth conditions, bacteria must possess mechanisms to efficiently re-adjust their cytoplasmic osmolality.

Bacteria respond to osmotic stress by accumulating solutes in the cytoplasm when extracellular osmolality rises and rapidly releasing those solutes from the cell when extracellular osmolality declines (33). Although, this is a universal approach among microorganisms, the types of molecules accumulated and the accumulation mechanisms used vary between species. For instance, halophilic archaea and acetogenic anaerobes accumulate large amounts of NaCl and KCl (34, 35). Bacteria that are unable to tolerate high concentrations of salt, on the other hand, prefer to build up the osmolality of the cytoplasm by accumulating organic solutes, which are often termed osmoprotectants or compatible solutes, as they accumulate to high levels without disturbing cellular functions (36, 37).

The amino acid proline and the amino acid intermediates betaine and choline are organic compounds that are commonly accumulated by *E. coli* as osmoprotectants (33, 37, 38). Since *E. coli* is unable to synthesize choline, cytoplasmic accumulation of this osmoprotectant can be achieved through import via the Bet system (39). Build-up of proline and betaine, however, can be achieved through both transport, via the unspecific transporter systems ProU and ProP (40–42), or biosynthesis from their metabolic precursors, glutamate and choline, respectively (39, 43).

Although proline, betaine and choline are preferred for accumulation, when subjected to osmotic stress in minimal medium without osmoprotectants, *E. coli* rely on K^+ uptake, via the Trk, Kdp and Kup uptake systems (44), followed by glutamate synthesis (45), to restore the cytoplasmic osmotic strength. Additionally, changing the ratio of OM porin proteins, OmpF and OmpC, is also a mechanism used by *E. coli* to survive osmotic stress. OmpF and OmpC are homologous porins that are responsible for passive diffusion of small, hydrophilic molecules across the OM (46–48). While the total number of these two proteins is fairly consistent in cells, the biosynthesis of OmpF and OmpC is inversely regulated by the osmolarity of the environment. As the osmolarity increases, the *ompC* gene is preferentially expressed and the *ompF* gene is repressed, while the opposite hold true when the osmolarity decreases. Due to a bigger pore diameter, the OmpF porin is less restrictive and allows for a faster rate of diffusion, which may account for the observed relationship between *ompF* and *ompC* gene expression (as reviewed in 49, 50).

1.2.2 pH Stress and Bacterial Alkali Tolerance

Colonization of certain sites within the human body requires for the ability to withstand extreme changes in external pH (51, 52). The enteric bacterium *E. coli*, for example, in order to grow within the human gastrointestinal tract, must be able to grow between pH 4.5 and pH 9 (53). This broad pH specificity is made possible by *E. coli*'s ability to maintain the cytoplasmic pH within the narrow range of pH 7.2– 7.8 (54, 55). Hence, it is able to acidify or alkalinize its cytoplasm relative to the external environment, thereby preserving enzyme activity, in addition to protein and nucleic acid stability and structural integrity (56, 57). While both acid and alkali pH homeostasis have been extensively studied in bacteria, only the latter will be briefly introduced in this thesis chapter.

Bacteria are known to utilize a number of strategies for maintenance of pH homeostasis under alkali stress, including increased adenosine triphosphate (ATP) synthase activity that couples H⁺ import to ATP synthesis, up-regulation of metabolic acid-generating mechanisms, such as amino acid deamination and sugar fermentation, and cell surface modifications to maximize cytoplasmic H⁺ retention (as reviewed in reference 58). However, increased expression and activity of monovalent cation/proton antiporters, which exchange intracellular cations (such as Na⁺ and K⁺) for external protons, is believed to be the leading contributing factor to alkali pH homeostasis (58, 59). Since the number of entering H⁺ is greater than the number of exiting monovalent cations during a turnover, these electrogenic antiporters catalyze a net H⁺ accumulation necessary for acidification of the cytoplasm under alkaline conditions (60).

Oftentimes, the dominant role in alkali pH homeostasis is assumed by Na^+/H^+ antiporters. *E. coli*, for example, rely on the Na^+/H^+ antiport activity of NhaB and ChaA transporters under acid and alkaline conditions, respectively, and resort to NhaA only when the low intracellular concentration of sodium ions is not maintained by other extrusion systems (61–64). However, in the absence of Na^+ or when there is a large inward directed Na^+ gradient, pH homeostasis is supported by the K^+/H^+ antiport activity of ChaA and MdfA antiporters (65, 66).

1.3 Antibiotic Resistance in Bacteria

In general, Gram-negative bacteria are more resistant to a larger number of antimicrobial agents than are Gram-positive bacteria. As introduced in section 1.1.1 of this chapter, this intrinsic (natural) resistance has long been attributed to the presence, in the Gram-negative cell envelope, of the OM permeability barrier that limits access of antimicrobial agents to their targets within the bacterial cell. Although the permeability of the OM can be further reduced through porin loss (67–69) or by lowering the fluidity of the LPS leaflet (70), equilibration across the OM barrier is achieved very rapidly (71, 72). Even in opportunistic pathogens, such as *Pseudomonas aeruginosa*, that have an OM of extremely low permeability, the intracellular drug concentration has been shown to reach half of its external concentration in just 10-20 seconds (73, 74). Therefore, since the OM barrier cannot prevent the antimicrobial agents from exerting their toxic action once they have entered the cell, additional resistance mechanisms must be involved, to ensure clinically significant levels of antibiotic resistance (75). This additional resistance is known as acquired, since bacteria must undergo changes either by chromosomal mutation

or by gene transfer from another bacterium. While a variety of acquired resistance mechanisms are currently known to be utilized by Gram-negative bacteria, including antibiotic target modification (76), antibiotic inactivation by enzymes (77) and increased cell wall (peptidoglycan and OM) impermeability (78), active efflux of antimicrobials against their concentration gradients across the membrane has been shown to play a key role in bacterial multidrug resistance (MDR) (79) and will be further discussed below.

1.3.1 Efflux-Mediated Multidrug Resistance

Active efflux as a mechanism for bacterial resistance is mediated by integral membrane transporter proteins, commonly known as drug efflux pumps, which export toxic substances, such as antibiotics and antiseptics, from the cell until the intracellular concentration is at sub-toxic levels (79). These active efflux pumps may be specific for one substrate or may transport a wide range of structurally unrelated compounds, thereby significantly contributing to MDR. Based on their energy source for drug efflux, all MDR pumps are subdivided into two major classes, shown below in Figure 1.2. Primary active transporters, which utilize the free energy of ATP binding and hydrolysis to drive transport of substrate across the membrane, belong to the ATP-binding cassette (ABC) transporter superfamily (Figure 1.2, 80). The secondary active transporters, which make up the second class, are pumps that employ the electrochemical potential gradient ($\Delta\mu$) of protons or sodium ions across the membrane to catalyze transport (81). The secondary multidrug transporters are further subdivided into distinct families, based on amino acid sequence similarities, predicted secondary protein structures, known three-dimensional (3D) crystal protein structures and phylogenetic relationships. These four different

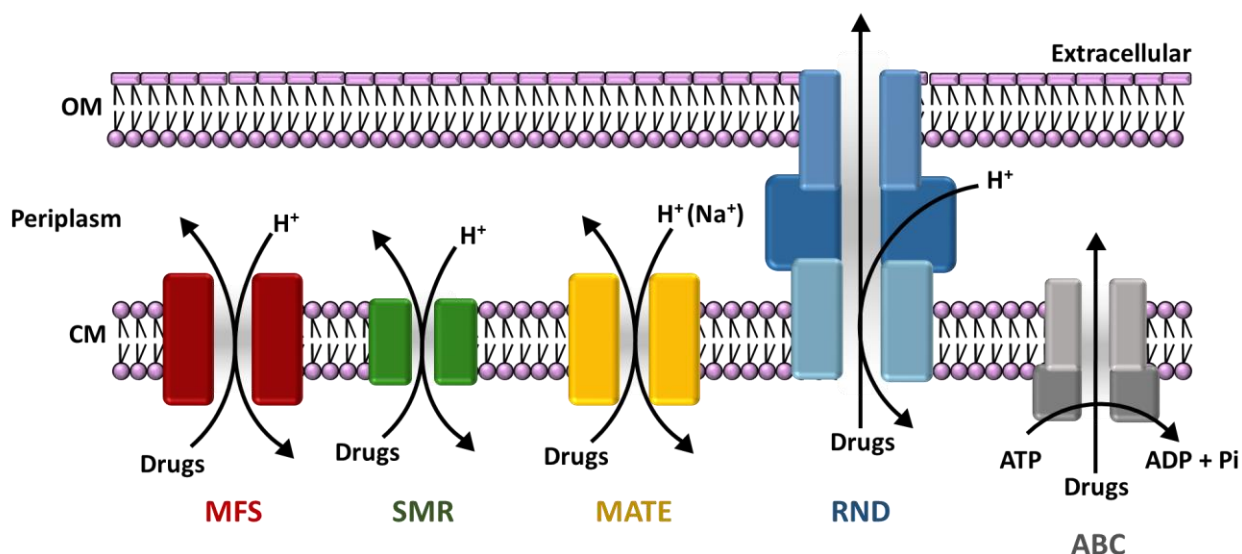


Figure 1.2. Diagrammatic comparison of the five major families of multidrug resistance transporters in bacteria (adapted from 82): MFS = major facilitator superfamily, SMR = small multidrug resistance superfamily, MATE = multidrug and toxic compound extrusion superfamily, RND = resistance-nodulation-cell division superfamily, ABC = ATP-binding cassette superfamily, OM = outer membrane and CM = cytoplasmic membrane.

superfamilies are: the major facilitator superfamily (MFS) (83), the small multidrug resistance (SMR) superfamily (84), the multidrug and toxic compound extrusion superfamily (MATE) (85) and the resistance-nodulation-cell division (RND) superfamily (86) of transporters (Figure 1.2). For the purpose of this thesis, only the SMR superfamily will be discussed further in section 1.3.2 of this chapter.

1.3.2 The Small Multidrug Resistance Family

As the name suggests, the smallest known secondary transporters belong to the SMR family. These proteins are typically between 100 and 140 amino acid residues in length and are believed to span the CM as four transmembrane (TM) α -helices (84, 87, 88). The first TM contains a highly conserved, negatively charged glutamate residue, which is believed to be the main component of the SMR protein active site, as it coordinates both substrate and proton binding (89–91). Based on various experimental data, it is thought that SMR proteins have to oligomerize in order to exhibit transport activity. The most frequently determined multimeric state of homooligomeric SMR proteins is a dimer, however, tetramers present as an arrangement of two protein dimers have also been reported (84, 91, 92).

Despite their small size, SMR proteins confer bacterial host resistance to a broad range of quaternary cationic compounds (QCCs) (89, 93, 94). QCCs are a diverse group of chemicals with the general structure XR_4^+ , where X is a positively charged ion (primarily N or P, or even As ion) and each R is a covalently bound alkyl or aryl group. Anthropogenic QCCs have been shown to have membrane-disruptive and antimicrobial activities and are widely used as cationic surfactants, disinfectants, herbicides and dyes in a variety of domestic, industrial and medical applications (95). Some common examples of these manmade QCCs are benzalkonium (antimicrobial), methyl viologen (herbicide) and ethidium bromide (lipophilic dye). The genes encoding SMR proteins have been found on chromosomes, as well as, a variety of plasmids and transposable elements that confer high levels of resistance to a wide range of antibiotics (as reviewed in 87), which

suggests a tight genetic linkage between both antibiotic and SMR resistance genes (96, 97).

SMR proteins are widespread in Bacteria and Archaea. According to the NCBI sequence database surveys, conducted five years ago using characterised SMR homologues from *Bacillus subtilis* and *E. coli* as seed sequences, a total of 685 putative chromosomally encoded SMR protein sequences are present within the two prokaryotic domains (98). While only ten Archaeal species, all of which belong to either Halobacteria or Methanomicrobia, were identified to contain SMR sequence homologues, a significantly greater SMR diversity among Bacteria was observed. Bacterial genome surveys revealed that at least 330 species have chromosomally encoded SMR sequences, with two SMR homologues per bacterium on average (98).

Based on sequence alignments and phylogenetic analysis, SMR transporter proteins can be further subdivided into three subclasses. Members of the small multidrug pumps (SMP) and suppressor of *groEL* mutation (SUG) subclasses make up the two major protein branches of the current SMR protein family tree (87), while SMR proteins grouped into the third subclass, known as the paired small multidrug resistance (PSMR), form small branches within the SMP and SUG clusters (84, 99–101). The SMP subclass members are mainly characterized by their ability to confer host resistance to a variety of QCCs in Gram-negative (EmrE from *E. coli*) and Gram-positive (Smr from *Staphylococcus aureus*) bacteria, as well as Archaea (Hsmr from *Halobacterium salinarum*) (84, 101). SUG proteins, on the other hand, can only recognize and transport a limited range of QCCs (99, 102) and are grouped together based on their ability to suppress *groEL* mutation phenotypes (103). The SUG subclass consists primarily of

SugE members, which have been identified in a variety of Bacterial and Euryarchaeal classes, although, only homologous from *E. coli* and *Citrobacter freundii* have been functionally characterized to date (84, 99, 104). Unlike SMP and SUG proteins, which confer MDR from the expression of a single gene, members of the PSMR subclass are not isogenic and require two SMR homologues to be simultaneously expressed in order to confer host resistance to toxic QCCs (105, 106). Currently, there are only five experimentally characterizes PSMR pairs: YdgE /YdgF in Proteobacteria and YkkC/YkkD, YvdR/YvdS, EbrA/EbrB, and YvaD/YvaE in Actinobacteria (as reviewed in 98).

1.3.3 Ethidium multidrug resistance protein E

The focus of this thesis work is on the ethidium multidrug resistance protein E (EmrE) from *E. coli*, the most extensively characterized member of the SMR protein family, which has been studied since the early 1990s (Figure 1.3, 84, 94, 107, 108). At 110 amino acids in length and just four TM α -helices, EmrE is the smallest known MDR transporter (84, 94, 107, 109, 110). This 12-kDa protein is highly hydrophobic and contains a total of eight charged residues, of which seven are located in the hydrophilic loops and only one, the Glu-14 residue, located in the TM domain of EmrE (91, 109). As previously mention, in section 1.3.2, this negatively charged Glu-14 residue is conserved throughout the SMR family and is believed to be absolutely required for the resistance phenotype and the transport activity of these MDR proteins (91, 92). As can be expected for a protein of such small size, EmrE functions as an oligomer. While a homodimer is believed to be the minimal functional unit (111), higher oligomeric states,

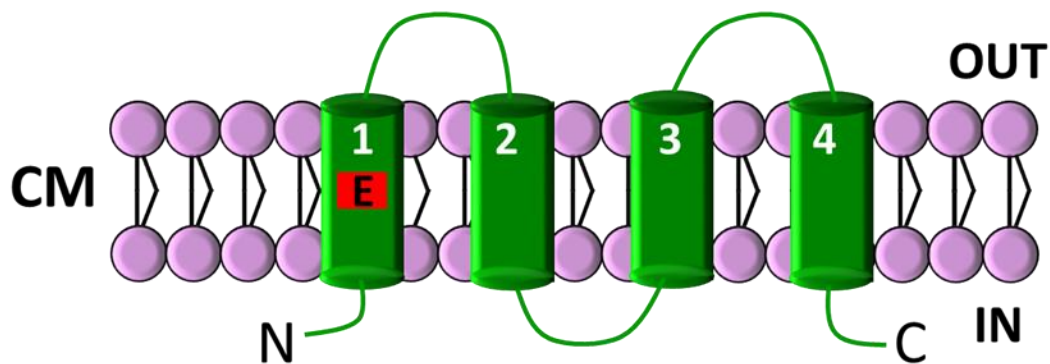


Figure 1.3. Schematic representation of the ethidium multidrug resistance protein E (EmrE) from *E. coli*; CM = cytoplasmic membrane; “E” represented the highly conserved glutamate residue located in the first transmembrane α -helix in all small multidrug resistance proteins

such as a tetramer composed of two dimers (112, 113), have also been observed. One of the most fascinating features of the EmrE, however, is its membrane topology. Unlike most membrane proteins, which follow the “positive inside rule” (114) and insert into the membrane in a particular orientation, EmrE is able to insert in two opposite orientations due to an insignificant charge bias. Hence, EmrE monomers adopt a mixed membrane orientation, known as dual-topology (87, 115–119).

As a secondary transporter, EmrE utilizes the energy of the proton gradient across the CM to extruding a wide range of toxic QCCs, thereby conferring bacterial host MDR. The stoichiometry of this exchange reaction is believed to be two protons per substrate, since EmrE is able to export both monovalent and divalent compounds (120). It has also been shown that substrate binding to EmrE induces the release of one proton per monomer, which suggests that the functional form of EmrE (dimer) exchanges two

protons per substrate molecule during each transport cycle (121). In addition to drug export, EmrE has recently been shown to participate in host osmotic regulation, by recognising betaine, choline and, under particular conditions, proline osmoprotectants as biological QCC substrates (122) and this interesting finding will be discussed further in chapters 3 and 4 of this thesis.

Although EmrE serves as the archetypical member of the SMR protein family, the nature of its transport mechanism remains uncertain and is a topic of both interest and speculation. Isogenic over-expression of *emrE* in *E. coli* confers host resistance to a variety of toxic QCC, suggesting that EmrE functions independently in the PM (87, 123). Support for this notion can be drawn from observations that SMR genes have demonstrated both chromosomal and lateral inheritance, where genes encoding EmrE homologues are frequently transmitted on mobile genetic elements (integrons) and resistance plasmids (98). However, due to its structure and accumulation site in the plasma membrane it is still not clear how exactly EmrE is able to extrude substrate completely out of the cell.

Typically, in Gram-negative bacteria, export of antimicrobial agents to the extracellular space is carried out by dedicated multipartite efflux systems, which span both the OM and the PM. Well characterized examples of such include the AcrAB–TolC (124, 125) system of the RND family and the EmrAB-TolC transporter of the MFS family (126, 127), which contain a transporter protein located in the CM, an OM channel and a periplasmic linker protein, known as the membrane fusion protein (MFP), which transiently connects the other two (69, 128, 129). These multicomponent transport systems are able produce significant levels of resistance, as their organization allows for

drug molecules to be excreted directly into the extracellular space. The SMR protein EmrE, on the other hand, appears to catalyze transport only across the PM (75, 129, 130) and the fate of QCCs that are transported into the periplasmic space by this MDR efflux pump is unknown.

Two possibilities for EmrE-mediated substrate extrusion in *E. coli* have been proposed and are shown in Figure 1.4 below. The first suggested method involves escape of QCC from the periplasmic space through the OM via an unidentified channel or porin. Alternatively, EmrE may be reliant on another assisting transporter system(s), like the multipartite AcrAB-TolC efflux complex, to capture and export its substrate completely out of the cell and, hence, delivers QCC to this efflux system. Based on the findings of Tal and Schuldiner in 2009, the involvement of an as yet unidentified OMP is far more likely, since *E. coli* strains lacking *acrAB-tolC* system genes rely on other functional MDR transporters, including EmrE, for QCC resistance (131, 132).

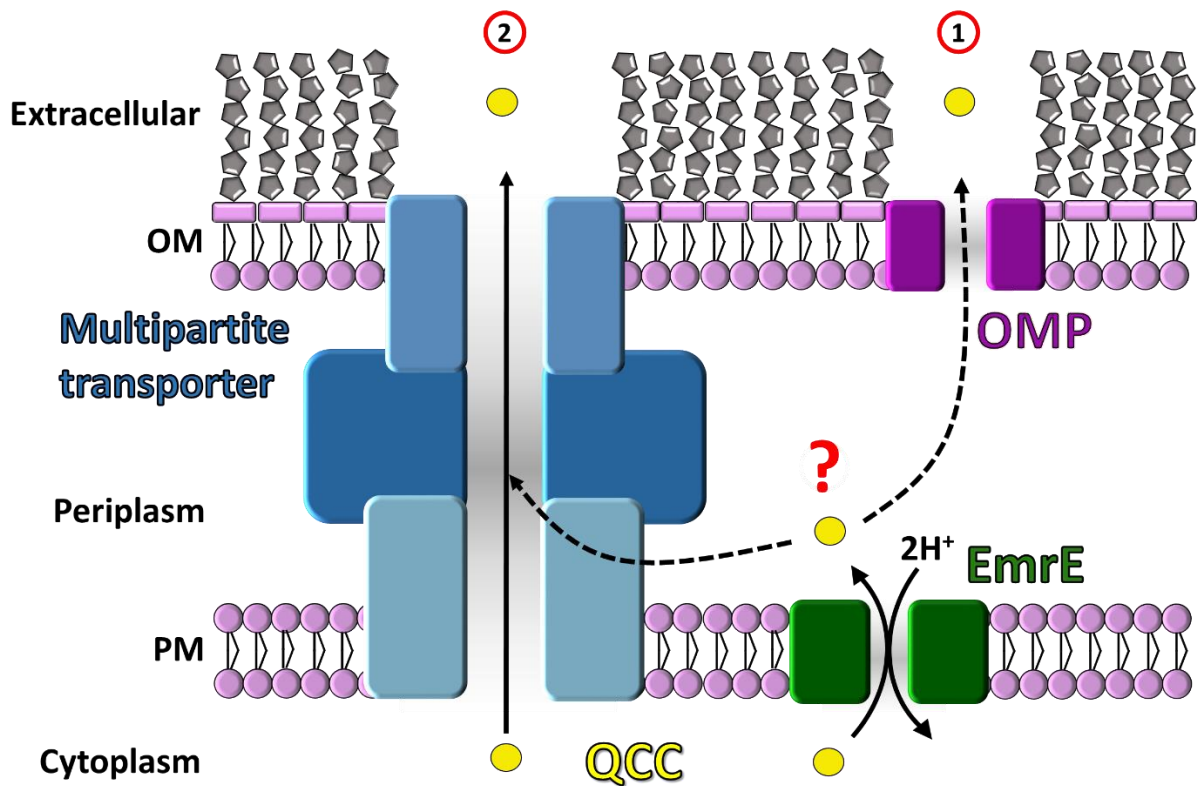


Figure 1.4. Schematic representation of the two proposed mechanism for EmrE-mediated substrate efflux in Gram-negative bacteria. According to the first hypothesis, indicated by the number 1, EmrE relies on an unidentified OMP to completely remove its substrate from the cell. According to the second hypothesis, indicated by the number 2, EmrE supplies substrate into the periplasm, where it can be accessed and removed completely from the cell by a multipartite transporter system.

1.4 Research Hypothesis and Goals

Since the complete mechanism of EmrE-mediated substrate efflux is currently not known, we set out to test the hypothesis that the SMR protein EmrE relies on an unidentified OMP to complete the extracellular efflux of its substrates in Gram-negative bacteria (Figure 1.4). In order to test our research hypothesis, the following research goals were set:

1. Design a simple and effective *in vivo* screen to look for OM candidates that are potentially involved in EmrE-mediated efflux mechanism.
2. Screen selected OMPs to identify possible candidates that potentially participate in substrate efflux with EmrE.
3. Confirm any identified OMP hits through specific cloning and complementation.
4. Confirm whether identified OMP hits confer QCC resistance.

Chapter Two: **General Experimental Methods and Materials**

2.1 Bacterial Strains

A list of all *E. coli* strains used within this thesis and their genotypes is provided below, in Table 2.1. *E. coli* wild-type (WT) strain (BW25113) and 11 selected Δ OMP mutants, each containing a single OMP gene deletion, were used in the neutral/alkaline pH phenotypic growth screens, described in chapters 3 and 4 of this thesis. Based on the experimental results generated by these screens, the *E. coli* deletion strains $\Delta ompW$ (JW1248) and $\Delta emrE$ (JW0531) were selected for further screening with plasmid complementation and reverse complementation analyses, respectively, as described in thesis chapter 5. Toxic QCC resistance assays, which are the focus of chapter 6, were performed using the *E. coli* WT and $\Delta ompW$ strains. All *E. coli* strains used in phenotypic growth screens, complementation and toxic QCC resistance assays were provided by the National BioResource Project *E. coli* K-12 single-gene-knockout Keio Collection (133). The *E. coli* DH5 α strain (134), provided by the Turner lab archive, was used for all cloning procedures.

Table 2.1. The *E. coli* K-12 single-gene knockout Keio collection mutants (133) and cloning strain DH5 α (134) used within this thesis

Strain	OMP gene deletion	Genotype*	Antibiotic resistance
BW25113	---	F ⁻ $\Delta(araD-araB)567 \Delta lacZ4787(::rrnB-3)$ $\lambda^- rph-1 \Delta(rhaD-rhaB)568 hsdR514$	---
JW0531	<i>emrE</i>	F ⁻ $\Delta(araD-araB)567 \Delta lacZ4787(::rrnB-3)$ $\lambda^- \Delta emrE750::kan rph-1 \Delta(rhaD-rhaB)568 hsdR514$	Kanamycin
JW0731	<i>pal</i>	F ⁻ $\Delta(araD-araB)567 \Delta lacZ4787(::rrnB-3)$ $\lambda^- \Delta pal-790::kan rph-1 \Delta(rhaD-rhaB)568 hsdR514$	Kanamycin
JW0799	<i>ompX</i>	F ⁻ $\Delta(araD-araB)567 \Delta lacZ4787(::rrnB-3)$ $\lambda^- \Delta ompX-786::kan rph-1 \Delta(rhaD-rhaB)568 hsdR514$	Kanamycin
JW0912	<i>ompF</i>	F ⁻ $\Delta(araD-araB)567 \Delta lacZ4787(::rrnB-3)$ $\lambda^- \Delta ompF746::kan rph-1 \Delta(rhaD-rhaB)568 hsdR514$	Kanamycin
JW0940	<i>ompA</i>	F ⁻ $\Delta(araD-araB)567 \Delta lacZ4787(::rrnB-3)$ $\lambda^- \Delta ompA772::kan rph-1 \Delta(rhaD-rhaB)568 hsdR514$	Kanamycin
JW1248	<i>ompW</i>	F ⁻ $\Delta(araD-araB)567 \Delta lacZ4787(::rrnB-3)$ $\lambda^- \Delta ompW764::kan rph-1 \Delta(rhaD-rhaB)568 hsdR514$	Kanamycin
JW1371	<i>ompN</i>	F ⁻ $\Delta(araD-araB)567 \Delta lacZ4787(::rrnB-3)$ $\lambda^- \Delta ompN740::kan rph-1 \Delta(rhaD-rhaB)568 hsdR514$	Kanamycin
JW2047	<i>wza</i>	F ⁻ $\Delta(araD-araB)567 \Delta lacZ4787(::rrnB-3)$ $\lambda^- \Delta wza-760::kan rph-1 \Delta(rhaD-rhaB)568 hsdR514$	Kanamycin

Table 2.1. *E. coli* K-12 single-gene knockout Keio collection mutants (133) and cloning strain DH5 α (134) used within this thesis continued

Strain	OMP gene deletion	Genotype*	Antibiotic resistance
JW2203	<i>ompC</i>	F- $\Delta(araD-araB)567 \Delta lacZ4787(::rrnB-3) \lambda-$ $\Delta ompC768::kan$ <i>rph-1</i> $\Delta(rhaD-rhaB)568$ <i>hsdR514</i>	Kanamycin
JW3474	<i>slp</i>	F- $\Delta(araD-araB)567 \Delta lacZ4787(::rrnB-3) \lambda-$ $\Delta slp-761::kan$ <i>rph-1</i> $\Delta(rhaD-rhaB)568$ <i>hsdR514</i>	Kanamycin
JW3698	<i>bglH</i>	F- $\Delta(araD-araB)567 \Delta lacZ4787(::rrnB-3) \lambda-$ $\Delta bglH-751::kan$ <i>rph-1</i> $\Delta(rhaD-rhaB)568$ <i>hsdR514</i>	Kanamycin
JW5503	<i>tolC</i>	F- $\Delta(araD-araB)567 \Delta lacZ4787(::rrnB-3) \lambda-$ $\Delta tolC732::kan$ <i>rph-1</i> $\Delta(rhaD-rhaB)568$ <i>hsdR514</i>	Kanamycin
DH5 α	---	F- $\Phi 80 lacZ \Delta M15 (lacZYA-argF)$ U169 <i>recA1 endA1 hsdR17(rk-, mk+) phoA supE44 -thi-1 gyrA96 relA1</i>	---

***Mutation description:** F- = lacks the F plasmid; $\Delta(araD-araB)567$ = deletion extends from ~25 bp upstream of the *araB* start codon to ~8 bp into the beginning of the *araD* gene, blocking arabinose metabolism (135); $\Delta lacZ4787(::rrnB-3)$ = 4 tandem copies of the *rrnB* transcriptional terminator inserted by gene replacement into the region extending from near the SacII site near the N-terminus of *lacZ* through the promoter, abolishing β -galactosidase activity (135); $\lambda-$ = lambda lysogen deletion; $::kan$ = kanamycin resistance gene used to confirm successful OMP gene deletion; *rph-1* = 1 bp deletion that results in frameshift over last 15 codons and has polar effect on *pyrE* leading to suboptimal pyrimidine levels on minimal medium (136); $\Delta(rhaD-rhaB)568$ = blocked rhamnose metabolism (135); *hsdR514/ hsdR17(rk-, mk+)* = inactivation of Eco

endonuclease activity, which abolishes Eco restriction but not methylation (r – m+); **Φ80** = carries the prophage Φ80; **lacZΔM15** = partial deletion of β-galactosidase gene, which allows α-complementation for blue/white selection of recombinant colonies in *lacZ* mutant hosts; **Δ(lacZYA-argF) U169** = abolished β-galactosidase and lactose permease activity and ornithine carbamoyltransferase mutation blocks ability to use arginine; **recA1** = mutation in a gene responsible for general recombination of DNA, which results in abolished homologous recombination; **endA1** = mutation in the non-specific endonuclease Endonuclease I, which eliminates non-specific endonuclease activity; **phoA** = mutation in alkaline phosphatase, which blocks phosphate utilization; **supE44** = tRNA glutamine suppressor of amber; **thi-1** = requires thiamine for growth on minimal media; **gyrA96** = DNA gyrase mutant produces resistance to nalidixic acid; **relA** = eliminates stringent factor resulting in relaxed phenotype (RNA is synthesized in absence of protein synthesis).

2.2 Growth Conditions and Chemicals

For routine overnight (16 hrs) cultures, bacterial transformation and plasmid isolation, strains were grown at 37°C under aerobic conditions in lysogeny broth (LB, 1% (w/v) yeast extract, 0.5% (w/v) sodium chloride, 0.5% (w/v) tryptone) or on LB plates (1.5% (w/v) agar), containing 100 µg/ mL of ampicillin (Amp) and/or 34 µg/ mL of chloramphenicol (Cm), as required. All strains were stored at –80°C as DMSO stocks, containing 1 part of culture and 2 parts of sterile 24% DMSO LB.

For neutral/alkaline pH phenotypic growth screens, plasmid complementation and reverse complementation analyses, strains were grown at 37°C under aerobic conditions in phosphate buffered (pH values of 7, 8 or 9) minimal 9 salts (M9) medium (1.3 % w/v $\text{NaH}_2\text{PO}_4 \cdot 7\text{H}_2\text{O}$, 0.3 % w/v K_2HPO_4 , 0.05 % w/v NaCl, 0.1 % NH_4Cl , 1.6×10^{-5} % w/v MgSO_4 , 9.0×10^{-7} % w/v CaCl_2 , 0.00015% w/v thiamine) supplemented with 0.01 % w/v glucose, containing 100 µg/mL of Amp and 34 µg/mL of Cm. For toxic QCC resistance assays, strains were grown at 37°C on M9 agar (M9 medium at pH 7 with 1.5% w/v granulated agar) with 100 µg/mL Amp, 34 µg/mL Cm and increasing concentrations of the corresponding toxic QCC, ranging from 5 µg/mL to 200 µg/mL.

All chemicals used in the preparation of media and chemical solutions for molecular biology experiments and resistance assays were supplied by Sigma (Missouri, USA), EMD (Darmstadt, Germany) or BD Biosciences (New Jersey, USA).

2.3 Plasmids and Constructs

All plasmids used and constructed in this thesis work are listed below, in Table 2.2. Plasmid pEmrE was used for expression of *E. coli emrE*. This construct was made by cloning (as described in reference 137) a hexahistidiny-tagged *emrE* gene into an Amp-resistant expression vector pMS119EHA, which permits lactose-inducible expression of cloned genes using a PtacI-inducible promoter and *rrnB* (Trp) transcription termination region. This expression system was selected because it has been previously found to exhibit “leaky” nontoxic expression of a hexahistidiny-tagged *emrE* gene without the induction by isopropyl β-D-1-thiogalactopyranoside (IPTG) (122). As a result, IPTG was

not used to induce expression in pH-based growth phenotype screens, to avoid toxic EmrE levels due to overexpression.

Table 2.2. Plasmids used and constructed within this thesis

Vector name	Antibiotic resistance	Gene cloned	Primer sequence(s) used for OMP gene cloning	Vector origin/reference
pMS119EHA	Amp	<i>bla</i>		(138)
pMS119EHC	Cm	<i>cat</i>		this study
pCA24N	Cm	<i>cat</i>		(139)
pEmrE	Amp	<i>emrE</i>		(137)
pOmpW	Cm	<i>ompW</i>	Forward: 5' ATATTCTAGAAGGAGAAATA ATATGAAAAAGTTAACAGTG 3' Reverse: 5' ATATAAGCTTTTAAAAACGA TATCCTGCTGAGAACATAAA 3'	this study
pOmpA	Cm	<i>ompA</i>	Forward: 5' ATATTCTAGAAGGAGAAATA ATATGAA 3' Reverse: 5' ATATAAGCTTTTAAGCCTGCG GCTGAG 3'	this study
pLamB	Cm	<i>lamB</i>	Forward: 5' ATATTCTAGAAGGAGAAATA ATATGAT 3' Reverse: 5' ATATAAGCTTTTACCACCAGA TTTCCCA 3'	this study

The construction of a chloramphenicol (Cm)-resistant pMS119EHC expression vector was necessary for plasmid complementation and toxic QCC resistance assays. For expression of *ompW*, *ompA* and *lamB*, the gene corresponding to each OMP was cloned into pMS119EHC, generating pOmpW, pOmpA and pLamB, respectively (Table 2.2). By using an expression vector with an alternative antibiotic marker for cloning of these OMP genes, it was possible to co-synthesize the EmrE protein with OmpW, OmpA or LamB in the same bacterial cell. Similar to neutral/alkaline pH growth phenotype screens, IPTG was not used to induce expression in complementation and resistance experiments.

2.4 Preparation of Competent *E. coli* Cells

Ultra-competent cells (high transformation efficiency) for all *E. coli* strains used throughout this thesis were prepared using a rubidium chloride method (adapted from 140). Overnight cultures were diluted 10^{-2} into 100 mL of LB medium and grown at 37°C with shaking until the optical density (OD) measurement at 600 nm (OD_{600nm}) of 0.3-0.4 was reached. Cultures were incubated on ice for 15 minutes and centrifuged for at 5000 rpm for 5 minutes at 4°C. After removing the supernatant, the cell pellet was re-suspended in 10 mL of chilled Trans Buffer 1 (1.2% w/v $RbCl_2$, 0.99% w/v $MnCl_2 \bullet 4H_2O$, 3% v/v 1 M potassium acetate, 0.11% w/v $CaCl_2$, 15% w/v glycerol; buffered to pH 5.8 with 25% v/v acetic acid) and incubated on ice for 15 minutes. Another round of centrifugation was performed at 5000 rpm for 5 minutes. After discarding the supernatant, the pellet was re-suspended in 8 mL of chilled Trans Buffer 2 (20% v/v 0.5 M MOPS buffer pH 7, 0.12% w/v $RbCl_2$, 0.83% w/v $CaCl_2$, 15% w/v glycerol) and 100

μL aliquots were made in sterile 1.5 mL microfuge tubes. All freshly prepared competent cells were frozen using liquid nitrogen and stored at -80°C .

2.5 Bacterial Transformation

Necessary transformants and co-transformants of all *E. coli* strains used throughout this thesis were generated for use in phenotypic growth screens, complementation and toxic QCC resistance assays (adapted from reference 141). For each strain, 1 μL of plasmid working stock (made as described in section 2.6.2 of this chapter) was added to 50 μL of competent cells in a sterile 1.5 mL microfuge tube. These mixtures were incubated on ice for 30 minutes, heat shocked at 42°C for 90 seconds and placed back on ice for another 5 minutes, prior to adding 1 mL of room temperature LB. The tubes were incubated with shaking at 37°C for 1 hour and 100 μL of each culture was spread plated on LB +/- Amp +/- Cm agar plates, which were incubated overnight at 37°C . Single colonies were picked from overnight plates and used for preparation of DMSO stocks.

2.6 DNA Purification from *E. coli* Cells

2.6.1 Genomic DNA isolation

Genomic DNA was isolated from *E. coli* WT (BW25113) strain, via the phenol-chloroform method (142), for use as template in amplification of selected *E. coli* OMP genes. Five 1.5 mL aliquots (in 2.0 mL microfuge tubes) of overnight *E. coli* cell culture were made and centrifuged at 14 000 rpm to pellet the cells. After removing the supernatant, each cell pellet was re-suspended in 400 μL of TES (50 mM Tris-HCl pH

7.5, 10 mM NaCl, 10 mM EDTA). Then, 17 μ L of 30% w/v SDS and 5 μ L of 10 mg/mL proteinase K were added to each microfuge tube. Tubes were incubated at 37°C for 1 hour and 400 μ L of 4 M NH₄Ac were added. A chloroform extraction step, which involved adding 844 μ L of 1:1 phenol:chloroform solution to each tube, centrifuging for 5 minutes at 14 000 rpm and transferring the aqueous layer (containing the DNA) to a new microfuge tube, was then performed twice. To remove excess phenol from DNA, 422 μ L of chloroform were added to each tube, contents were mixed by inversion and a newly formed aqueous layer was transferred to a clean tube. DNA was then precipitated by adding 422 μ L of isopropanol, incubating each sample at room temperature for 10 minutes and centrifuging at 14 000 rpm for 5 minutes. After discarding the supernatant, pellet was resuspended in 400 μ L of 0.1 M NaAc pH 6.0 and DNA was reprecipitated by adding 800 μ L of 95% ethanol and incubating for 15 minutes. All tubes were then centrifuged at 14 000 rpm for 15 minutes at room temperature and the pellets were rinsed for 5 minutes by adding 1 mL of 70% ethanol to each microfuge tube. DNA pellets were then dried for 35 minutes in the 37°C incubator and then resuspended in 200 μ L of water. Successfully isolated genomic DNA was checked by running 1 μ L aliquot on a 1% agarose gel, as described in section 2.8.1 of this chapter. Tubes were first incubated overnight at 4°C before being stored at -20°C.

2.6.2 Plasmid DNA isolation

All plasmid DNA isolations were performed using e.Z.N.A. MiniPrepII kits (Omega BioTek, USA), which yield a large quantity of purified DNA (approximately 8-12 μ g for high copy number plasmids), suitable for most downstream molecular

applications. Overnight bacterial cultures were centrifuged for 1 minute at 10 000 x g at room temperature. After discarding the medium, cell pellets were re-suspended in 250 μ L of Solution I/RNase A. 250 μ L of Solution II was added and tubes were gently mixed by inversion, until clear lysate was obtained. Then, 350 μ L of Solution III was added and tubes were mixed immediately by inversion, until white precipitate formed. After centrifuging tubes at 13 000 x g for 10 minutes at room temperature, the clear supernatant was carefully aspirated and added into HiBind® Miniprep columns assembled in 2 mL collection tubes. These tubes were then centrifuged at 13 000 x g for 1 minute at room temperature to completely pass the lysate through the column. After discarding the flow-through, 500 μ L of Buffer HB was added to wash the columns and tubes were centrifuged at 13 000 x g for 1 minute at room temperature. Flow-through was discarded and 700 μ L of DNA Wash Buffer (containing ethanol) was added. Tubes were centrifuged at 13 000 x g for 1 minute and after removing the flow-through, empty columns were centrifuged at 13 000 x g for 1 minute to dry the column matrix. Collection tubes were then discarded and columns were placed into clean 1.5 mL microfuge tubes. DNA was eluted from the columns by adding 40-60 μ L of double distilled (dd) water and centrifuging for 1 minute at 13 000 x g at room temperature. Concentration of purified plasmid DNA was estimated by comparison to a 1kb DNA ladder on a 1% agarose gel (section 2.8). All isolated plasmids were stored at -20°C as 1-10 μ g/ μ L (approximately) DNA stocks and working stocks were made to contain between 1-10 ng/ μ L of DNA.

2.7 *E. coli* DNA Amplification

2.7.1 Polymerase Chain Reaction (PCR)

PCR is a cost-effective, widely used technique for enzymatic amplification of a specific DNA sequence *in vitro* (143). In this thesis, PCR was used to amplify three selected OMP genes (*ompW*, *ompA* and *lamb*) for cloning into the pMS119EHC expression vector. All nucleotide primers used for PCR cloning were obtained from Integrated DNA Technology (Iowa, USA) and are listed in Table 2.2 of this chapter. The master mix recipe used for all PCR reactions that were set up is provided below, in Table 2.3.

Table 2.3. Contents of a 50 μ L polymerase chain reaction

Reagent	Volume (μ L)
Nuclease free water	28.5
10X Pfu Buffer with MgSO ₄	5
dNTP Mix (1.25 mM each)	5
Forward primer (10 pmol)	5
Reverse primer (10 pmol)	5
Template (1 μ g/ μ L)	0.5
Thermo Scientific <i>Pfu</i> DNA polymerase, recombinant (2.5 U/ μ L)	1

All PCR reagents were thawed on ice, transferred to 0.5 μ L PCR tubes and spun down with a centrifuge. After setting up the desired PCR cycling program, as shown in Table 2.4, all PCR tubes were placed into the thermocycler. Once the cycling program reached completion, all PCR reactions were checked by running 5 μ l of each reaction mix on a 1% w/v agarose gel (section 2.8), to determine if the PCR was successful and the desired gene was amplified.

Table 2.4. General polymerase chain reaction cycling program used

Step	Temperature ($^{\circ}$ C)	Time (minutes)	Number of cycles
Initial denaturation	95	1	---
Denaturation	95	0.5	25
Annealing	Variable (T_m^*-5)**	0.5	25
Extension	72	Variable (2 min/kb)***	25
Final extension	72	10	---

*Primer melting temperature

**Annealing temperature of 52 $^{\circ}$ C, 60 $^{\circ}$ C, and 57 $^{\circ}$ C were used for amplification of genes *ompW*, *ompA* and *lamB*, respectively.

***Extension time of 2 min, 3 min and 3 min were used for amplification of genes *ompW*, *ompA* and *lamB*, respectively.

2.7.2 Purification of Polymerase Chain Reaction Products

Since PCR reagents can interfere with other enzymatic reactions, like restriction digestion and ligation, it was necessary to purify our PCR amplicons to make them suitable for use in various downstream applications. While a number of purification methods are available, a low-cost, simple and efficient ethanol precipitation method (adapted from reference 144) was used to purify and concentrate all newly amplified PCR products within this thesis. After adding 2 volumes of 95% ethanol and 1/10 volume of 3M NaAc to the whole PCR-product volume (5-10 reactions) in a 2.0 mL microfuge tube, the tube was mixed by inversion and incubated overnight at -20°C. The tube was then centrifuged at 4°C for 10 minutes at 14 000 rpm. After discarding the supernatant, the DNA pellet was resuspended in 1 mL of 70% ethanol and mixed by inversion. Another centrifugation round was performed at 4°C for 10 minutes at 4 000 rpm. After discarding the supernatant, the DNA pellet was dried for 30 minutes in a 37°C incubator and then re-suspended in 100-200 µL of dd water. Concentration and purity of the DNA was estimated by comparison to a 1kb DNA ladder on a 1% agarose gel (section 2.8) and samples were stored at -20°C.

2.8 Agarose Gel Electrophoresis

Agarose gel electrophoresis is a commonly used laboratory method in molecular biology for analyzing, separating and purifying DNA samples (145, 146). It facilitates the separation of DNA molecules on the basis of their size or conformation and the general principle behind this technique is that samples are subjected to an electrical field, which

induces DNA molecules to migrate through an agarose gel towards the anode, due to their negatively charged backbone. Agarose is a seaweed-derived polysaccharide, composed of long chains of cross-linked D-galactose and 3, 6-anhydro-L-galactosidase residues, and agarose concentration in the gel dictates the gel's pore size, which in turn affects the resolution. After separation and staining of the gel with an intercalating dye, DNA molecules present in the sample can be visualized under ultraviolet (UV) light.

2.8.1 DNA Analysis and Separation

Agarose gel electrophoresis was used throughout this thesis for analyzing and separating plasmids, genomic DNA, digested fragments and PCR products. A 1% agarose gel was made by adding agarose to 1 x TBE buffer. The suspension was then boiled in a microwave oven until all agarose dissolved and poured into a casting tray, containing a comb. The gel was allowed to cool until solid. After removing the comb, the gel was placed into an electrophoresis chamber filled with 1 x TBE buffer. 2 µL of 1kb DNA ladder were loaded into the first well. 6 x Orange DNA Loading Dye (Thermo Scientific, USA) was added to each DNA sample in a 1:5 ratio and mixed by stirring with a pipette tip. Each DNA sample was then loading into a separate well and the gel was run at 100 V for 30-45 minutes. The gel was then removed from the chamber, stained with GelRed™ (Biotium, Inc. USA) dye for 10 minutes and visualized using a UV transilluminator.

2.8.2 DNA Purification from Agarose Gel

Purification of all PCR products and digested (with restriction endonucleases as described in section 2.9 of this chapter) DNA fragments, generated for cloning purposes,

from an agarose gel was performed using the QIAquick Gel Extraction kits (Qiagen, USA). Agarose gel electrophoresis was performed, as discussed in section 2.8.1, to separate DNA fragments. After reaching the desired band separation, a narrow vertical strip, containing the 1 kb DNA ladder and a small portion of the band of interest, was sliced off from the gel. This strip was stained with GelRed™ dye for 10 minutes and then visualised under UV light. After excising our fragment of interest from the gel strip, the strip was pieced back together with rest of the gel. This allowed us to track the position of our fragment on the gel, without exposing it to the intercalating dye or UV light, which are both known to have a denaturing effect on DNA (147, 148). Our DNA fragment of interest was then excised from the remaining gel. The excised DNA fragment was cut into multiple slices and the volume of each slice was determined by weighing it in a 1.5 mL microfuge tube. 3 volumes of Buffer QG were added to 1 volume of gel slice and all tubes were incubated at 50°C until each gel slice had completely dissolved. 1 gel volume of isopropanol was added to each tube and mixed by inversion. Samples were then applied to a QIAquick spin-column with a 2 mL collection tube and centrifuged at 13 000 rpm for 1 minute. After discarding the flow through, each column was washed with 0.75 mL of Buffer PE (containing ethanol). Columns were centrifuged at 13 000 rpm for 1 minute and after discarding the flow through, columns were dried by performing another centrifugation round. Each column was then placed into a clean 1.5 mL microfuge tube and DNA was eluted by adding 50 µL of dd water and centrifuging the columns at 13 000 rpm for 1 minute. All DNA samples were stored at -20°C.

2.9 DNA Restriction with Endonucleases

Restriction endonucleases are enzymes that recognise specific double-stranded nucleotide sequences and catalyse phosphodiester bond cleavage, at specific sites located within or in close proximity to the recognition sites, to give linear DNA fragments with terminal 5'-phosphates and 3'-hydroxyls (149, 150). While some restriction endonucleases are sticky end cutters, which cleave the DNA helix asymmetrically to produce single-stranded overhangs, others will cut both strands at the same position, generating fragments with blunt ends. In this thesis, these restriction enzymes were used to capture the chloramphenicol (Cm) resistance *cat* gene from the pCA24 plasmid, to prepare PCR amplicons and plasmids for ligation and restriction analysis, to verify the plasmid/construct identity. The restriction digestion mix was prepared according to Table 2.5, briefly centrifuged and then incubated for 2 –16 hrs at 37°C. Following restriction digestion, fragments were analysed and separated using agarose gel electrophoresis, as described in section 2.8. Digested DNA was prepared for downstream applications (i.e. ligation reactions) using ethanol precipitation (section 2.7.2).

Table 2.5. Contents of restriction endonuclease digestion reaction mix

Reagent	Volume (μL) for	
	Analytical reaction	Preparative restriction for downstream applications
DNA	5	50 – 88
10X buffer	2	10
Restriction enzymes	1 of each	2 of each
Nuclease free water to a final volume of	20	100

2.10 DNA Ligation

Joining of DNA fragments with “sticky” overhangs or blunt ends to form recombinant DNA molecules is fundamental to most cloning procedures. This process can be carried *in vitro* using a DNA ligase enzyme, which catalyzes the formation of a phosphodiester bond between the 5’ phosphate and the 3’hydroxyl groups of adjacent nucleotides (151). In this thesis work, bacteriophage T4 DNA ligase, isolated from *E. coli* lambda lysogen NM989 by Invitrogen™, was used for construction of the pMS119EHC vector and cloning of selected OMP genes (*ompW*, *ompA* and *lamB*).

2.10.1 Blunt end ligation

Blunt end ligation approach was used for construction of the pMS119EHC vector, which involved exchanging the Amp resistance gene (*bla*) in pMS119EHA for a Cm resistance gene (*cat*). The *bla* gene was excised using the DraI restriction enzyme

(section 2.9), which produced a linearized pMS119EHA vector with blunt ends. However, since a “sticky” end cutter, *Sau3AI*, was used for excision of the *cat* gene from pCA24N, the 5’ overhangs of the isolated gene had to be blunted following the restriction digestion. Due to its strong 5'-3' polymerase activity the, *E. coli* DNA polymerase I large (Klenow) fragment (New England Biolabs, Canada) was used to fill-in the 3’recessed ends of the DNA insert (152). This blunting reaction was set up in a sterile 1.5 mL microfuge tube, as shown below in Table 2.6, and incubated for 15 minutes at 25°C. The Klenow enzyme was then inactivated by adding 0.7 µL of 0.5M EDTA (to a final concentration of ~10 mM) and heating for 20 min at 75°C.

Table 2.6. Contents of 35 µL overhang blunting reaction mix

Reagent	Volume (µL)
10X Reaction Buffer	3.5
dNTP (1.25 mM)	1
DNA insert (~20 ng/µL)	30
Klenow (5 U/µL)	0.5

Since vectors with blunt ends are prone to self-ligation, dephosphorylation of the 5’ ends of our linearized vector DNA was necessary prior to ligation to the insert fragment. Calf intestinal alkaline phosphatase (CIAP) was used for vector dephosphorylation by adding 0.1 µL of CIAP to ~1 µg of vector DNA and incubating at

37°C for 45min. The dephosphorylated plasmid was then purified using ethanol precipitation (as discussed in section 2.7.2 of this chapter).

Blunt end ligation reactions, to join the linearized dephosphorylated vector DNA to the blunted DNA insert fragment, were set-up as shown in Table 2.7. Reaction contents were mixed in a sterile 1.5 mL microfuge tube by stirring with a plastic pipette tip and incubated overnight at a 37°C → 4°C temperature gradient. A 100 µL aliquot of competent DH5α cells was transformed with 2 µL of ligation mix and plated on LB+34 µg/mL Cm plates, as described in Section 2.5. Following an overnight incubation at 37°C, plates were checked for colonies.

Table 2.7. Contents of a 20 µL blunt end DNA ligation reaction mix

Reagent	Volume (µL)
5X Ligase Reaction Buffer	4
Vector DNA (3,257bp; ~0.05 µg/µL)	1
Insert DNA (975bp; ~0.1 µg/µL)	5
T4 DNA Ligase (5 U/µL)	2
Nuclease free water	8

2.10.2 Sticky End Ligation

The ligation reaction parameters used for ligating together compatible “sticky” ends, generated by cleavage with XbaI and HindIII restriction endonucleases (section

2.9), of the pMS119EHC vector and OMP gene inserts to be cloned are shown below, in Table 2.8. As recommended in the literature (153), a 3:1 molar ratio of insert to vector DNA was used for all “sticky” end ligation reactions within this thesis work. These reactions were prepared in sterile 1.5 mL microfuge tubes, gently mixed by stirring with a plastic pipette tip and incubated overnight at room temperature. A 100 μ L aliquot of competent DH5 α cells was transformed with 2 μ L of ligation mix and plated on LB+34 μ g/mL Cm plates, as described in Section 2.5. Following an overnight incubation at 37°C, plates were checked for colonies.

Table 2.8: Contents of a 20 μ L “sticky” end DNA ligation reaction mix

Reagent	Volume / Amount
5X Ligase Reaction Buffer	4 μ L
Vector DNA (4,233 bp)	3.7-37 fmol
Insert DNA (639, 1041, 1341 bp)	10-100 fmol
T4 DNA Ligase (5 U/ μ L)	1 μ L
Nuclease free water to a final volume of	20 μ L

Chapter Three: **Development of a Phenotypic Screening Method to Identify Outer Membrane Protein Candidates Involved in EmrE-Mediated Substrate Efflux**

3.1 Introduction

Although EmrE is the most studied member of the SMR protein family, the nature of its transport mechanism is not fully understood and has sparked a great deal of interest and debate in the scientific community. What is known so far is that overexpression of EmrE causes bacteria to become resistant to a variety of toxic QCC, by exporting them out of the cell, thereby reducing their cytoplasmic concentration to subtoxic levels (88, 154). However, the fate of QCC substrates transported into the periplasm by EmrE is currently unknown, suggesting one of two possibilities for EmrE-mediated QCC extrusion in *E. coli* (Figure 1.4 in thesis chapter 1). According to the first hypothesized method, EmrE is reliant on other assisting transporter system(s), such as the multipartite AcrAB-TolC efflux complex, to export its substrates completely out of the cell and delivers QCC to this efflux system. Alternatively, these substrates escape from the periplasm through a channel or a porin in the OM. While the AcrAB-TolC efflux complex is known to remove substrates from the periplasmic space and has an overlapping substrate specificity with EmrE, involvement of an unidentified OMP seems far more likely, as *E. coli* strains lacking the *acrAB-tolC* genes have been shown to rely on other functional multidrug resistance transporters, including EmrE (131, 132). Therefore, the primary goal of this thesis chapter was to design a screening method to identify any OMP that may be involved in QCC efflux with EmrE by completing substrate removal from the cell.

A previous study has revealed that *emrE* gene expression decreases pH tolerance of its host, reducing the growth of WT *E. coli* cultures in neutral and alkaline minimal medium conditions, due to the intracellular loss of QCC-based osmoprotectants, such as betaine and choline (155). Consequently, if an OMP participates in osmoprotectant efflux with EmrE by completing substrate removal from the cell, the deletion of this OMP gene should restore growth in M9 medium buffered to pH 7-9 by preventing osmoprotectant loss. Hence, a similar pH-based phenotypic growth assay can be used to screen *E. coli* single OMP gene deletion mutants transformed with pEmrE, in hopes of possibly identifying OMPs capable of rescuing this EmrE-induced loss-of-growth phenotype. In this chapter, the above mentioned *in vivo* screening method was tested by screening five *E. coli* OMP deletion mutants: $\Delta ompA$ (JW0940), $\Delta ompX$ (JW0799), $\Delta ompW$ (JW1248), $\Delta tolC$ (JW5503) and Δwza (JW2047) (Table 2.1). The bases for selection of these OMPs are explained in chapter 4 of this thesis.

3.2 Materials and Methods

3.2.1 pH 7 to 9 M9 Growth Curves of Selected E. coli Outer Membrane Protein Gene Deletion Mutants

To test if the selected growth phenotype assay was a suitable screening method, competent cells (section 2.4 of thesis chapter 2) of five *E. coli* OMP deletion mutants ($\Delta ompA$, $\Delta ompW$, $\Delta ompX$, $\Delta tolC$ and Δwza) and the WT (BW25113) strain (Table 2.1) were transformed with pEmrE or the control vector pMS119EHA (Table 2.2, Figure 3.1), as described in section 2.5 of chapter 2. These plasmid-transformed and untransformed (control) *E. coli* strains were inoculated (from DMSO stocks) into 3 mL of LB medium

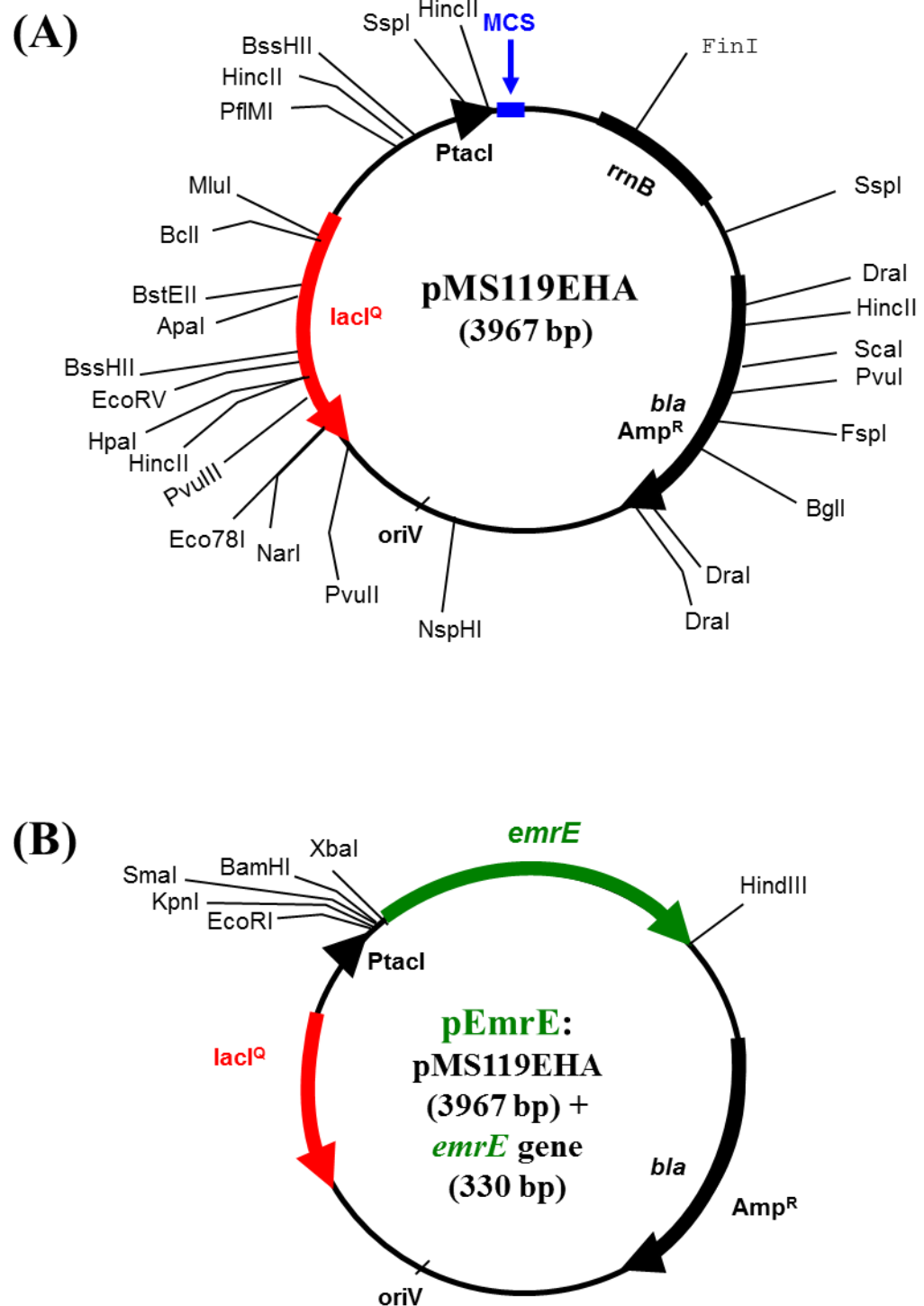


Figure 3.1. Plasmid maps of the empty control vector (A) pMS119EHA (138) and the *emrE* gene expression construct (B) pEmrE (137).

with 100 µg/mL Amp and grown overnight at 37°C with shaking at 200 rpm. Overnight cultures were standardized to an OD_{600nm} value of 1.5 using 0.9% saline (NaCl) and then diluted 10⁻³ into 3.0 ml of phosphate-buffered (pH value of 7, 8 or 9) M9 medium (please refer to section 2.2 of chapter 2 for recipe). Buffered M9 culture 10⁻² dilutions of all six *E. coli* strains (five mutants and WT), transformed with either pEmrE or pMS119EHA, were grown in a shaking incubator at 37°C and OD_{600nm} measurements were taken every 2 hrs for 16 hrs and again at the 24-hr time point. The selection of the 16- and 24-hr end points was based on the initial pH-based growth phenotype screen described in reference (155). Mean OD_{600nm} measurements at each time point were calculated from five independently inoculated pH 7 to 9 M9 phenotype growth screen trials and pairwise Student's t-test calculations were performed between empty vector (pMS119EHA)- and pEmrE-containing strains and/ or between pEmrE transformed WT and OMP deletion strains to determine significant differences (p-values ≤ 0.005).

3.3 Results and Discussion

The main objective of this study was to determine if an unidentified OMP(s) is involved in the efflux-mechanism of the *E. coli* SMR multidrug transporter EmrE. To accomplish this, a pH-based phenotypic *E. coli* growth assay was selected as a screening method to identify any OMP gene(s) capable of restoring pH-host tolerance and rescuing EmrE-induced loss-of-growth phenotypes, observed in a previous study (155), by blocking the export of osmoprotectants from the cell. This approach was an ideal screening method to identify whether an OMP was associated with EmrE efflux, since it avoided the use of QCCs potentially transported by other multidrug efflux systems, such

as AcrAB-TolC and MdfA, which possess overlapping substrate profiles with EmrE (88, 132). However, before beginning this *in vivo* screen to look for potential candidates in the OM, it was essential to determine if the same WT EmrE-induced growth phenotype could be reproduced in this study and find the optimal growth endpoint which would allow for identification of only strong OMP candidates (thereby eliminating false positives). Hence, growth curve experiments were performed for pEmrE-transformed *E. coli* WT and selected OMP gene deletion strains and growth was measured at 37°C (optimal temperature) over 24 hrs in M9 medium buffered to pH values of 7 to 9. The M9 medium was used instead of LB, since it is completely defined and its osmolarity is 100-fold lower and, thus, may identify phenotypes hidden in osmotically enriched medium (156). Untransformed strains and empty vector transformants (pMS119EHA) were also included in these growth curves to act as a positive growth control for the loss-of-growth phenotype caused by *emrE* gene expression. Based on the outcome of these growth curve experiments, the WT EmrE-induced loss-of-growth phenotype was successfully reproduced at pH 7, 8 and 9, as demonstrated in Figures 3.2, 3.3 and 3.4, respectively. The most significant reduction in growth was observed at the 16-hr time point at both neutral and alkaline conditions, making it the optimal growth endpoint when screening for growth recovery (Figure 3.4). The outcome of the five Δ OMP deletion strain growth curves also identified 16 hrs as the optimal endpoint for the pH-based growth screens, since full growth recovery is least likely to occur at that time point, as only one out of the five screened OMP produced significant growth recovery values (Figures 3.5 to 3.19). Hence, the observed Δ OMP-induced reversal of the loss-of-growth phenotype is most

significant at 16 hrs of growth, by comparison to the growth phenotype displayed by the WT strain, allowing only strong candidates to be identified.

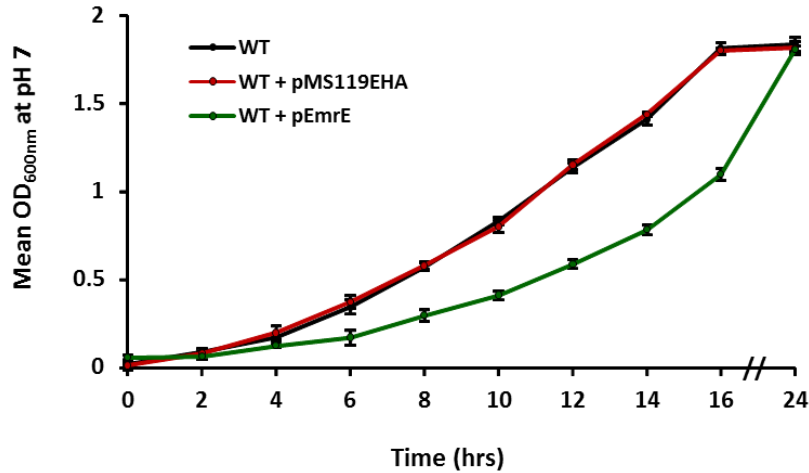


Figure 3.2. Growth curve experiments with *E. coli* WT strain transformed with the pMS119EHA and pEmrE plasmids. Mean OD_{600nm} values (y axis) represent the growth of cultures measured every 2 hrs in pH 7 M9 medium at 37°C, over a 24-hr time frame (x axis) for the *E. coli* WT strain transformed with pMS119EHA (red) or pEmrE (green) or untransformed (black). Error bars represent the standard errors determined for each mean OD_{600nm} value (n=5).

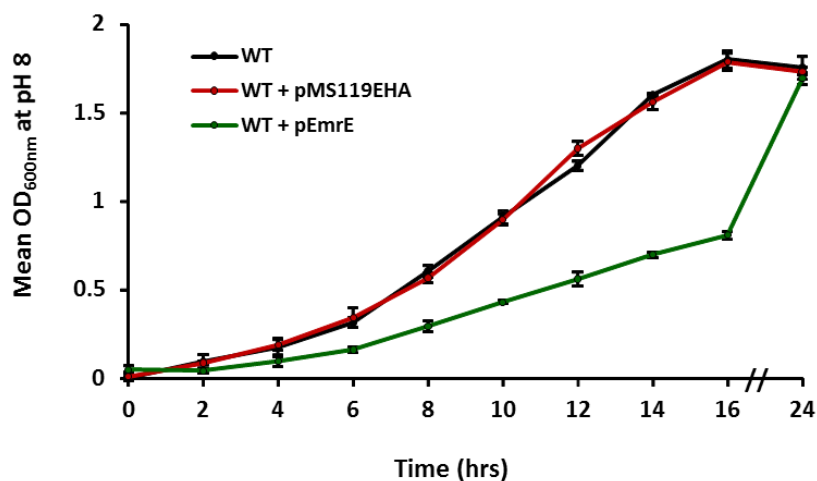


Figure 3.3. Growth curve experiments with *E. coli* WT strain transformed with the pMS119EHA and pEmrE plasmids. Mean OD_{600nm} values (y axis) represent the growth of cultures measured every 2 hrs in pH 8 M9 medium at 37°C, over a 24-hr time frame (x axis) for the *E. coli* WT strain transformed with pMS119EHA (red) or pEmrE (green) or untransformed (black). Error bars represent the standard errors determined for each mean OD_{600nm} value (n=5).

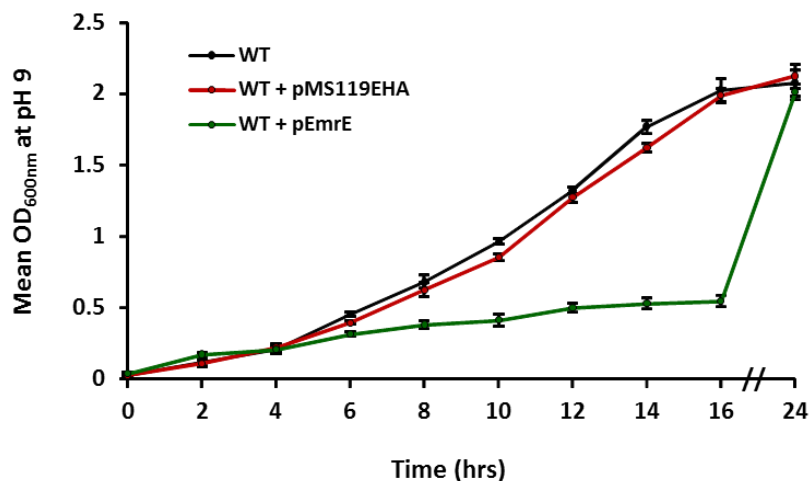


Figure 3.4. Growth curve experiments with *E. coli* WT strain transformed with the pMS119EHA and pEmrE plasmids. Mean OD_{600nm} values (y axis) represent the growth of cultures measured every 2 hrs in pH 9 M9 medium at 37°C, over a 24-hr time frame (x axis) for the *E. coli* WT strain transformed with pMS119EHA (red) or pEmrE (green) or untransformed (black). Error bars represent the standard errors determined for each mean OD_{600nm} value (n=5).

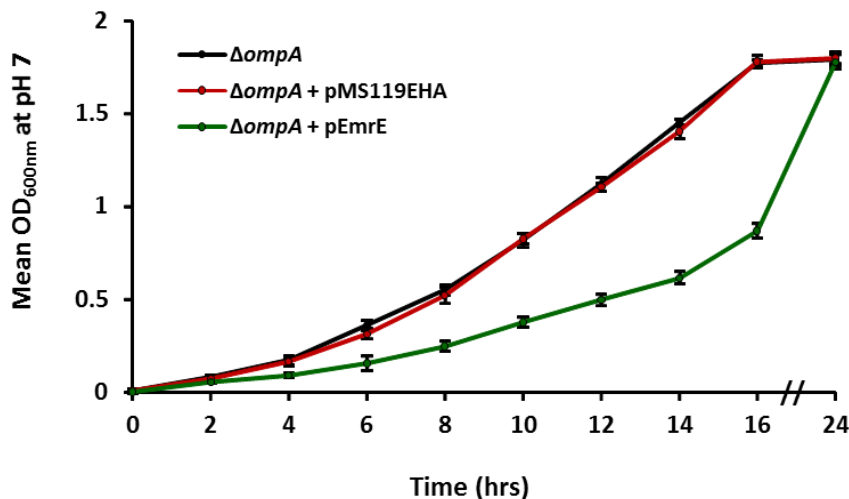


Figure 3.5. Growth curve experiments with *E. coli* $\Delta ompA$ strain transformed with the pMS119EHA and pEmrE plasmids. Mean OD_{600nm} values (y axis) represent the growth of cultures measured every 2 hrs in pH 7 M9 medium at 37°C, over a 24-hr time frame (x axis) for the *E. coli* $\Delta ompA$ strain transformed with pMS119EHA (red) or pEmrE (green) or untransformed (black). Error bars represent the standard errors determined for each mean OD_{600nm} value (n=5).

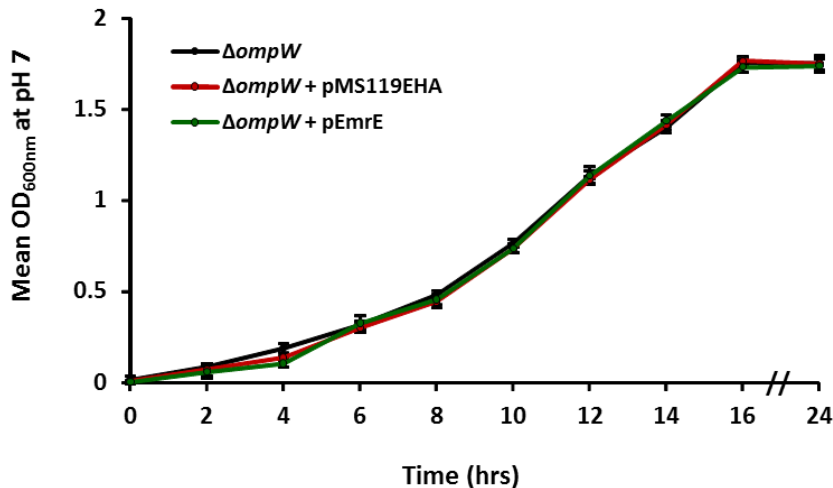


Figure 3.6. Growth curve experiments with *E. coli* $\Delta ompW$ strain transformed with the pMS119EHA and pEmrE plasmids. Mean OD_{600nm} values (y axis) represent the growth of cultures measured every 2 hrs in pH 7 M9 medium at 37°C, over a 24-hr time frame (x axis) for the *E. coli* $\Delta ompW$ strain transformed with pMS119EHA (red) or pEmrE (green) or untransformed (black). Error bars represent the standard errors determined for each mean OD_{600nm} value (n=5).

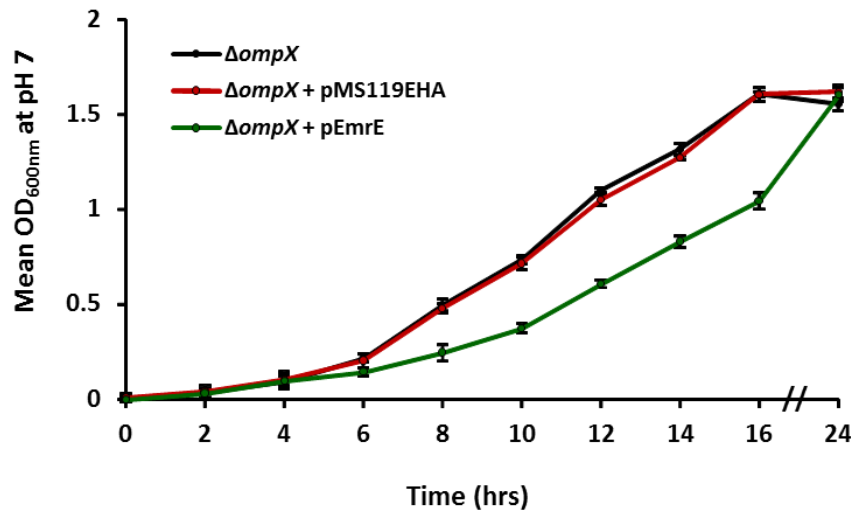


Figure 3.7. Growth curve experiments with *E. coli* $\Delta ompX$ strain transformed with the pMS119EHA and pEmrE plasmids. Mean OD_{600nm} values (y axis) represent the growth of cultures measured every 2 hrs in pH 7 M9 medium at 37°C, over a 24-hr time frame (x axis) for the *E. coli* $\Delta ompX$ strain transformed with pMS119EHA (red) or pEmrE (green) or untransformed (black). Error bars represent the standard errors determined for each mean OD_{600nm} value (n=5).

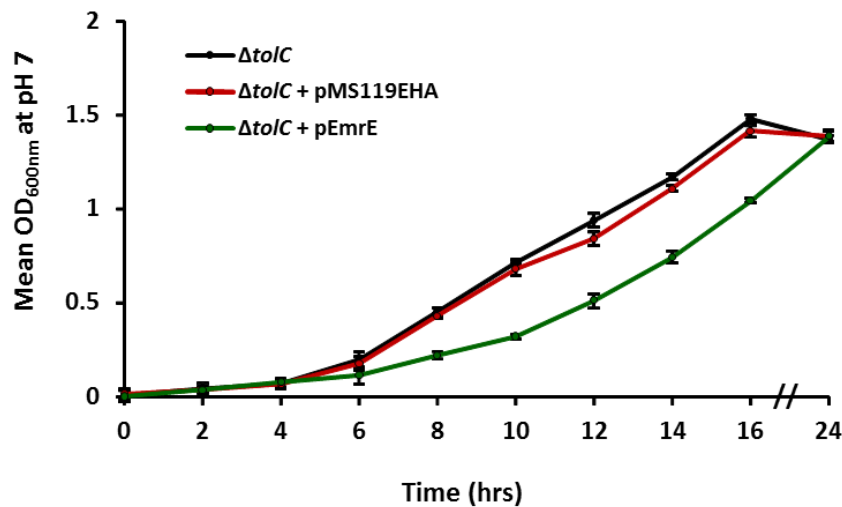


Figure 3.8. Growth curve experiments with *E. coli* $\Delta tolC$ strain transformed with the pMS119EHA and pEmrE plasmids. Mean OD_{600nm} values (y axis) represent the growth of cultures measured every 2 hrs in pH 7 M9 medium at 37°C, over a 24-hr time frame (x axis) for the *E. coli* $\Delta tolC$ strain transformed with pMS119EHA (red) or pEmrE (green) or untransformed (black). Error bars represent the standard errors determined for each mean OD_{600nm} value (n=5).

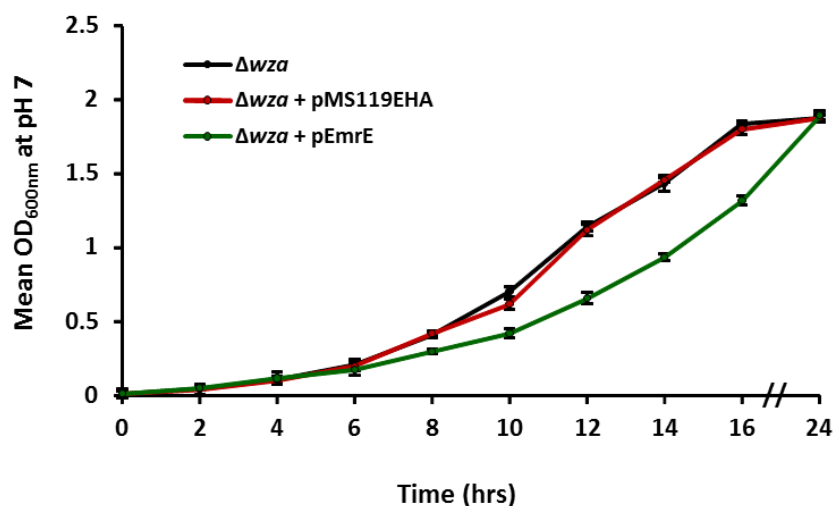


Figure 3.9. Growth curve experiments with *E. coli* Δwza strain transformed with the pMS119EHA and pEmrE plasmids. Mean OD_{600nm} values (y axis) represent the growth of cultures measured every 2 hrs in pH 7 M9 medium at 37°C, over a 24-hr time frame (x axis) for the *E. coli* Δwza strain transformed with pMS119EHA (red) or pEmrE (green) or untransformed (black). Error bars represent the standard errors determined for each mean OD_{600nm} value (n=5).

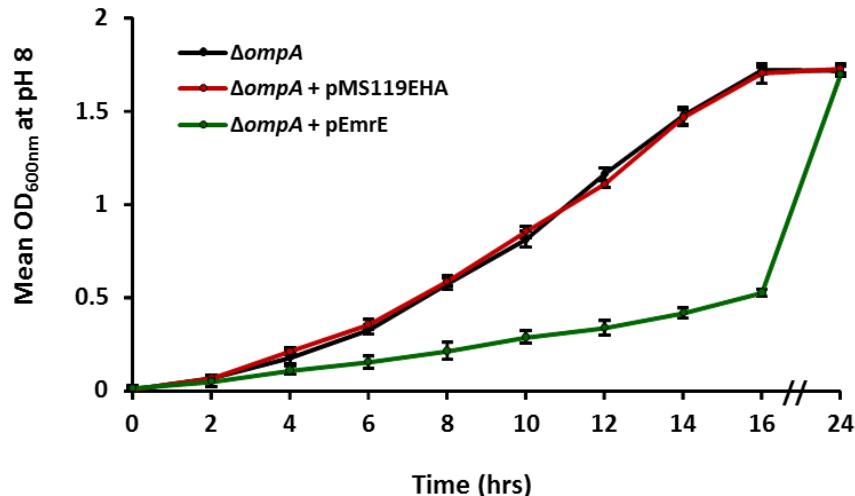


Figure 3.10. Growth curve experiments with *E. coli* $\Delta ompA$ strain transformed with the pMS119EHA and pEmrE plasmids. Mean OD_{600nm} values (y axis) represent the growth of cultures measured every 2 hrs in pH 8 M9 medium at 37°C, over a 24-hr time frame (x axis) for the *E. coli* $\Delta ompA$ strain transformed with pMS119EHA (red) or pEmrE (green) or untransformed (black). Error bars represent the standard errors determined for each mean OD_{600nm} value (n=5).

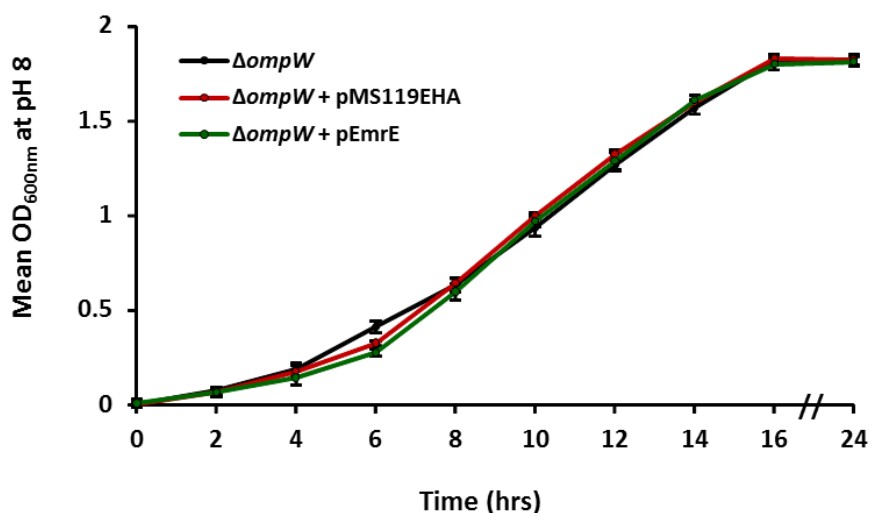


Figure 3.11. Growth curve experiments with *E. coli* $\Delta ompW$ strain transformed with the pMS119EHA and pEmrE plasmids. Mean OD_{600nm} values (y axis) represent the growth of cultures measured every 2 hrs in pH 8 M9 medium at 37°C, over a 24-hr time frame (x axis) for the *E. coli* $\Delta ompW$ strain transformed with pMS119EHA (red) or pEmrE (green) or untransformed (black). Error bars represent the standard errors determined for each mean OD_{600nm} value (n=5).

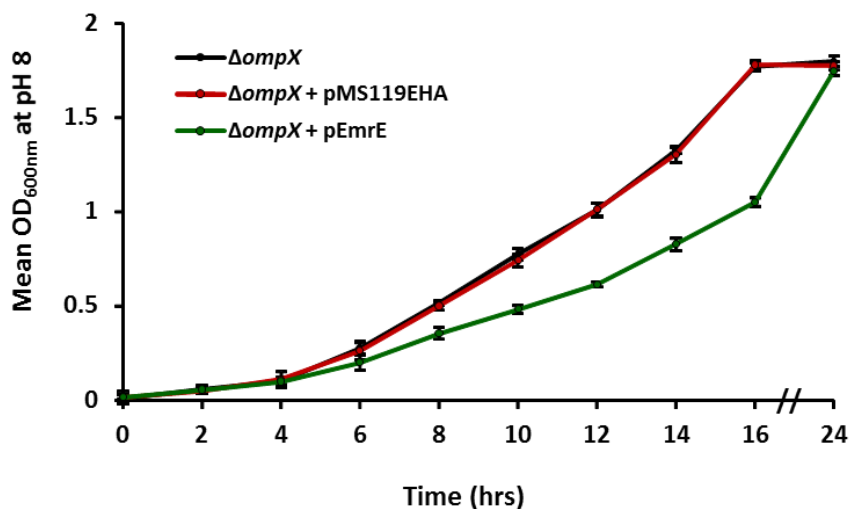


Figure 3.12. Growth curve experiments with *E. coli* $\Delta ompX$ strain transformed with the pMS119EHA and pEmrE plasmids. Mean OD_{600nm} values (y axis) represent the growth of cultures measured every 2 hrs in pH 8 M9 medium at 37°C, over a 24-hr time frame (x axis) for the *E. coli* $\Delta ompX$ strain transformed with pMS119EHA (red) or pEmrE (green) or untransformed (black). Error bars represent the standard errors determined for each mean OD_{600nm} value (n=5).

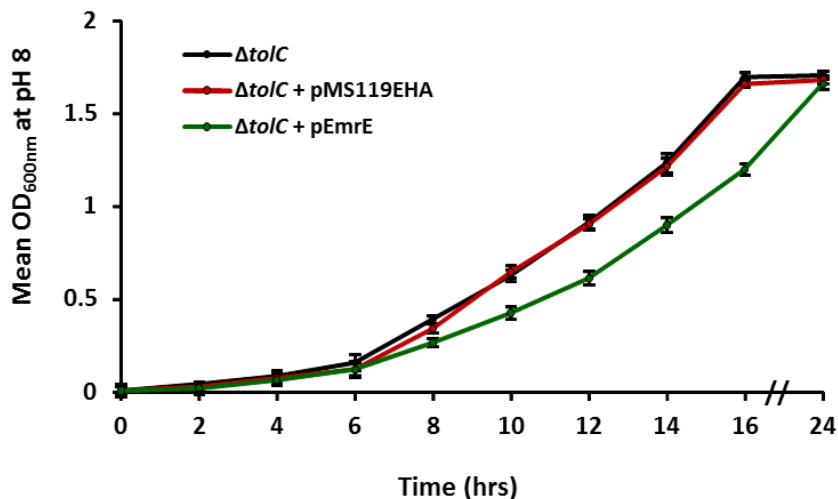


Figure 3.13. Growth curve experiments with *E. coli* $\Delta tolC$ strain transformed with the pMS119EHA and pEmrE plasmids. Mean OD_{600nm} values (y axis) represent the growth of cultures measured every 2 hrs in pH 8 M9 medium at 37°C, over a 24-hr time frame (x axis) for the *E. coli* $\Delta tolC$ strain transformed with pMS119EHA (red) or pEmrE (green) or untransformed (black). Error bars represent the standard errors determined for each mean OD_{600nm} value (n=5).

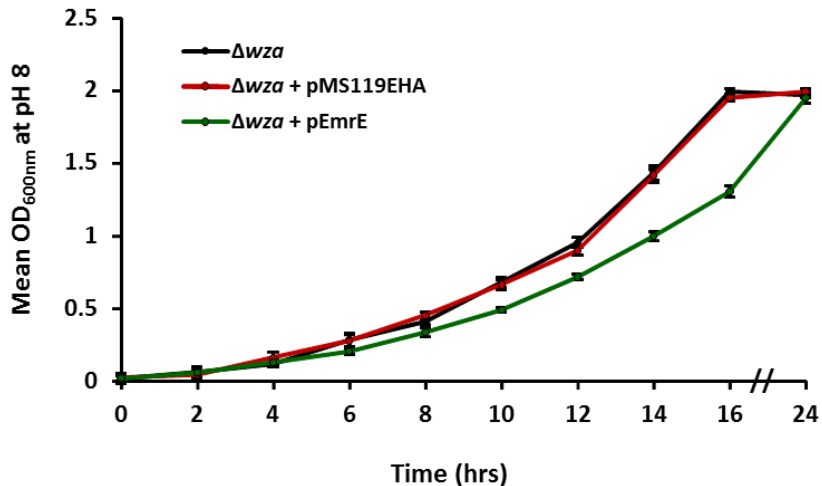


Figure 3.14. Growth curve experiments with *E. coli* Δwza strain transformed with the pMS119EHA and pEmrE plasmids. Mean OD_{600nm} values (y axis) represent the growth of cultures measured every 2 hrs in pH 8 M9 medium at 37°C, over a 24-hr time frame (x axis) for the *E. coli* Δwza strain transformed with pMS119EHA (red) or pEmrE (green) or untransformed (black). Error bars represent the standard errors determined for each mean OD_{600nm} value (n=5).

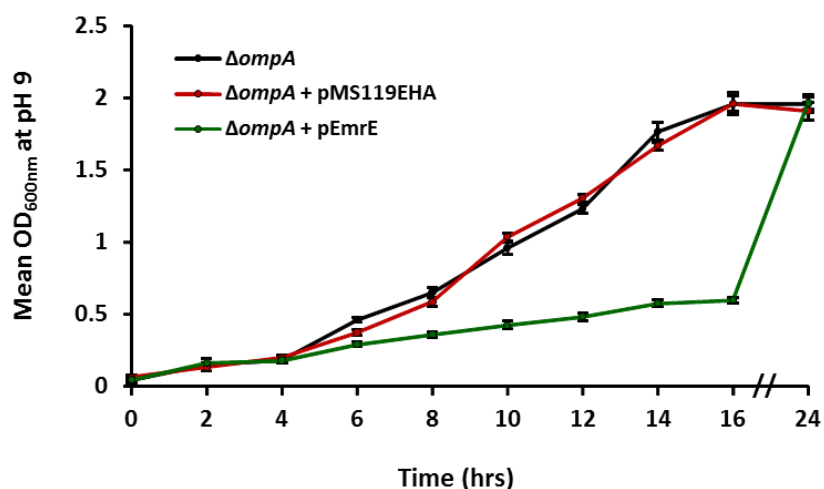


Figure 3.15. Growth curve experiments with *E. coli* $\Delta ompA$ strain transformed with the pMS119EHA and pEmrE plasmids. Mean OD_{600nm} values (y axis) represent the growth of cultures measured every 2 hrs in pH 9 M9 medium at 37°C, over a 24-hr time frame (x axis) for the *E. coli* $\Delta ompA$ strain transformed with pMS119EHA (red) or pEmrE (green) or untransformed (black). Error bars represent the standard errors determined for each mean OD_{600nm} value (n=5).

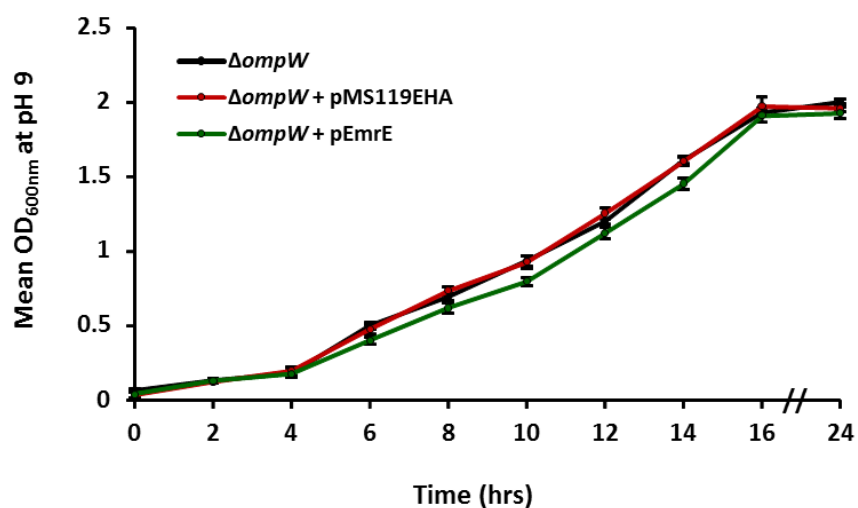


Figure 3.16. Growth curve experiments with *E. coli* $\Delta ompW$ strain transformed with the pMS119EHA and pEmrE plasmids. Mean OD_{600nm} values (y axis) represent the growth of cultures measured every 2 hrs in pH 9 M9 medium at 37°C, over a 24-hr time frame (x axis) for the *E. coli* $\Delta ompW$ strain transformed with pMS119EHA (red) or pEmrE (green) or untransformed (black). Error bars represent the standard errors determined for each mean OD_{600nm} value (n=5).

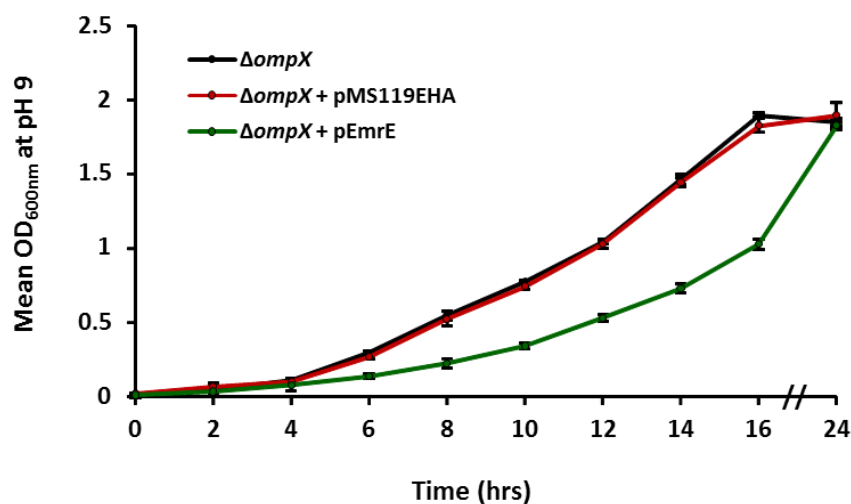


Figure 3.17. Growth curve experiments with *E. coli* $\Delta ompX$ strain transformed with the pMS119EHA and pEmrE plasmids. Mean OD_{600nm} values (y axis) represent the growth of cultures measured every 2 hrs in pH 9 M9 medium at 37°C, over a 24-hr time frame (x axis) for the *E. coli* $\Delta ompX$ strain transformed with pMS119EHA (red) or pEmrE (green) or untransformed (black). Error bars represent the standard errors determined for each mean OD_{600nm} value (n=5).

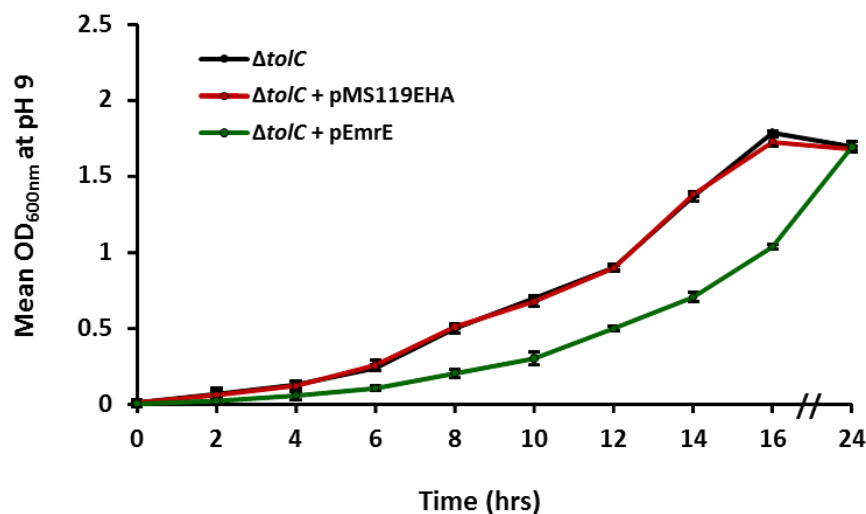


Figure 3.18. Growth curve experiments with *E. coli* $\Delta tolC$ strain transformed with the pMS119EHA and pEmrE plasmids. Mean OD_{600nm} values (y axis) represent the growth of cultures measured every 2 hrs in pH 9 M9 medium at 37°C, over a 24-hr time frame (x axis) for the *E. coli* $\Delta tolC$ strain transformed with pMS119EHA (red) or pEmrE (green) or untransformed (black). Error bars represent the standard errors determined for each mean OD_{600nm} value (n=5).

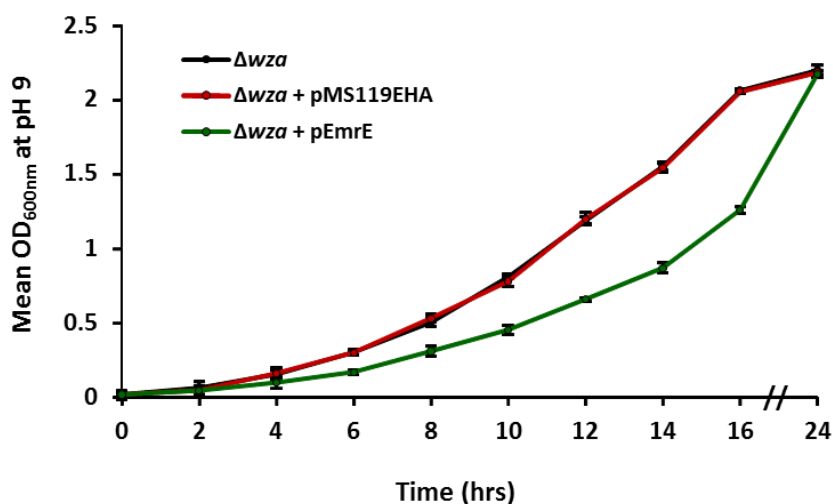


Figure 3.19. Growth curve experiments with *E. coli* Δwza strain transformed with the pMS119EHA and pEmrE plasmids. Mean OD_{600nm} values (y axis) represent the growth of cultures measured every 2 hrs in pH 9 M9 medium at 37°C, over a 24-hr time frame (x axis) for the *E. coli* Δwza strain transformed with pMS119EHA (red) or pEmrE (green) or untransformed (black). Error bars represent the standard errors determined for each mean OD_{600nm} value (n=5).

3.4 Summary

The experimental work described within this thesis chapter was aimed at designing and testing the pH-based growth phenotype assay as an *in vivo* screening method for identifying potential OMP candidates involved in the EmrE-mediated efflux mechanism. The *E. coli* WT strain and five OMP gene deletion mutants were selected, based on the criteria explained in chapter 4 of this thesis, for pH 7-9 M9 growth curve experiments, to determine if the previously observed EmrE-induced phenotype could be reproduced and at what time point would the Δ OMP-induced reversal of the loss-of-growth phenotype would be most significant, if observed. The growth of pEmrE- and pMS119EH- transformants of the selected strains was monitored every 2 hrs over a period of 24 hrs.

According to the outcome of these growth experiments, the EmrE-induced reduced growth phenotype was successfully reproduced at neutral and alkaline pH, while the reversal of this phenotype, due to prevention of osmoprotectant loss was the most significant at 16 hrs of growth, making it the optimal endpoint for screening potential OMP candidates. Also, a full recovery of loss-of-growth phenotype was only observed for the $\Delta ompW$ gene deletion mutant at the optimal growth endpoint, thus foreshadowing possible involvement of OmpW in the EmrE-mediated efflux mechanism.

Chapter Four: **pH-Based Phenotypic Growth Screens of Selected *E. coli* Outer Membrane Protein Gene Deletion Mutants**

4.1 Introduction

While the fate of QCC exported into the periplasmic space by EmrE remains a mystery, as introduced in chapter 1 of this thesis, two possibilities for EmrE-mediated substrate transport across the OM in *E. coli* have been suggested (Figure 1.4 in chapter 1). The purpose of this thesis chapter was to test the hypothesis that EmrE relies on the participation of an outer membrane protein to complete the extracellular efflux of its substrates in Gram-negative bacteria. To accomplish this, a pH-based phenotypic growth assay, developed and tested as described in chapter 3 of this thesis, was used as an *in-vivo* screening method to identify any OMP gene(s) capable of rescuing EmrE-induced loss-of-growth phenotype, due to the intracellular loss of osmoprotectants in M9 medium at pH 7-9 (122). Here we exam the possible involvement of 11 *E. coli* OMPs (listed in Table 2.1 of chapter 2), which were selected for screening based on their porin/channel forming potential (157) and/or association to drug resistance (158, 159), in the EmrE-mediated efflux of QCC based osmoprotectants.

4.2 Materials and Methods

4.2.1 Neutral/alkaline pH Growth Phenotype Screens of Candidate OMP Mutants

A total of 11 *E. coli* single OMP gene deletion strains were selected for screening using the neutral/alkaline pH phenotypic growth assays (Table 2.1). Each one of these *E. coli* OMP deletion mutants and the WT (BW25113) strain were transformed with pEmrE or the control vector pMS119EHA (please see sections 2.4 and 2.5 for component cell

preparation and transformation procedures used, respectively). These plasmid transformed *E. coli* strains were grown overnight in 3 mL of LB + 100 µg/ml Amp and standardized (with 0.9% saline to an OD_{600nm} value of 1.5) overnight cultures were used to set up pH 7, 8 and 9 M9 media growth assays, as described in section 3.2.1 of chapter 3. The OD_{600nm} measurements were taken after 16 hrs of growth (optimal endpoint as determined by growth curves discussed in thesis chapter 3) and mean OD_{600nm} values were calculated from five independently inoculated pH 7-9 M9 phenotype growth screen trials. Pairwise Student's t-test calculations were performed between empty vector (pMS119EHA) and pEmrE containing strains and/ or between pEmrE transformed WT and OMP deletion strains to determine significant differences (p-values ≤ 0.005).

4.2. Percentage Growth Recovery by pEmrE-transformed Strains

To identify OMP candidates that are associated with EmrE-mediated osmoprotection and are capable of restoring the EmrE-induced loss-of growth phenotype in M9 media buffered to pH 7, 8 and 9, percent growth recovery values were calculated using mean 16-hr OD_{600nm} values (representing cell growth) for each plasmid-transformed strain set at a particular pH M9 growth condition using the following equation:

Percent growth recovery by pEmrE-transformed *E. coli* strain at pH 7, 8 or 9 =

$$= \frac{\text{Avg OD}_{600\text{nm}} \text{Strain1} + \text{pEmrE}}{\text{Avg OD}_{600\text{nm}} \text{Strain1} + \text{pMS119EH}} \times 100\%$$

Where the mean 16-hr OD_{600nm} value for each pEmrE-transformed strain is divided by the mean 16-hr OD_{600nm} value measured for that same strain transformed with pMS119EHA (both grown in the same M9 medium at pH 7, 8, or 9) and multiplied by 100%. Any screened pEmrE-transformed OMP single-gene deletion strains that restored at least 80% of growth of the empty vector (pMS119EHA) control strain, were deemed to indicate positive OMP candidates identified in the screen. The minimum 80% threshold value used to identify OMP candidates from this screen was based on the ~80% loss of growth phenotype displayed by the pEmrE-transformed WT strain at the 16-hr time point during growth curve experiments performed at pH9 (Figure 3.4 in chapter 3), since optimal phenotypic growth differences were most significant after 16 hrs of growth in M9 media buffered to pH 9.

4.3. Results and Discussion

4.3.1 Only the ompW Gene Deletion Restored Host Alkali Tolerance and Rescued the Loss-of-Growth Phenotype Induced by EmrE at pH 9

To validate our hypothesis that an unidentified OMP is associated with EmrE-mediated substrate efflux (Figure 1.4), a pH based phenotypic growth screen of 11 *E. coli* Keio collection mutant strains (Table 2.1), each containing a single OMP gene deletion, was performed in M9 medium buffered to pH 7 to 9. It was expected that, if a specific OMP is involved in the extracellular efflux of a QCC-based osmoprotectant in neutral and alkaline buffered minimal media, the deletion of that OMP gene in an *E. coli* strain over accumulating EmrE protein should rescue the loss-of-growth phenotype by preventing QCC export across the OM.

The selection of these 11 *E. coli* OMPs was dictated by their pore- and/or channel-forming potential, based on OM proteomic experiments (157), and/or their known association to host multidrug resistance (158, 159). The membrane proteins Wza (17, 18) and TolC (124, 160) are known OMP components of multipartite PM-OM spanning efflux pumps, Wza-Wzc and AcrAB-TolC, respectively. The two major osmoregulated general diffusion porins in the *E. coli* OM, OmpF and OmpC, have been shown to be involved in antibiotic influx permeability (161–163). Additionally, the *E. coli* OMP OmpW, involved in MV resistance in Salmonella (164), and the less characterized porin OmpN, known to be expressed under superoxide stress response element SoxS (165), were also included in this screen based on their potential to transport MV, which is a powerful superoxide radical propagator (166, 167) and a substrate of EmrE (94, 168). Other OM porins, such as OmpX, which is known to promote pathogenic host cell invasion and resistance to complement-mediated killing mechanisms (169), and OmpA, which is involved in cell adhesion and plays an OM stabilizing role (170), were selected for screening, but were considered to be less likely OMP candidates to be involved in EmrE-mediated efflux. In addition to porins, the OM anchored lipoprotein Pal, which interacts with the peptidoglycan layer (171), and the carbon starvation- and stationary phase-inducible OM lipoprotein Slp, partially regulated by the multiple antibiotic resistance protein MarA (172), were also included in the screen as potential channel-linker forming complexes between the PM protein EmrE and the OM. Lastly, the carbohydrate uptake OM porin BglH, which is similar in function to the maltoporin LamB (173), was selected as a negative control for these pH-based

phenotypic growth screens, since it was the least likely OMP candidate to be involved in EmrE-mediated substrate efflux.

To conduct the neutral and alkaline M9 growth phenotype screens, all of the selected *E. coli* OMP gene deletion mutants and the WT strain (Table 2.1), included as control for phenotype reproducibility, were transformed with pEmrE or the control vector pMS119EHA (Table 2.2). All strains were diluted 10^{-3} from overnight LB cultures and grown for 16 hrs in M9 media buffered to pH 7, 8 and 9. To determine if any of the selected OMP candidates were associated with EmrE-mediated osmoprotection under tested conditions, the relative differences in mean 16-hr OD_{600nm} values were calculated between the same strain transformed with pEmrE or pMS119EH, to provide the percent growth recovery induced by OMP gene deletion. The results for these Δ OMP growth phenotype screens conducted at pH 7, 8 and 9 are provided below in Figures 4.1, 4.2 and 4.3, respectively.

As shown in Figure 4.1, all of the screened deletion mutants, except $\Delta ompC$ and Δpal , grew significantly better than the WT strain and rescued at least 80% of growth in the presence of EmrE at pH 7. According to these results, out of the 11 *E. coli* OMPs, nine showed a possible involvement in EmrE-mediated substrate efflux. The pH of the growth medium may have contributed to this unexpectedly high number of potential candidates, since *E. coli* is known to grow optimally at neutral pH (57) and hence, conducting the screen at pH 7 did not actually subject the strains to stress.

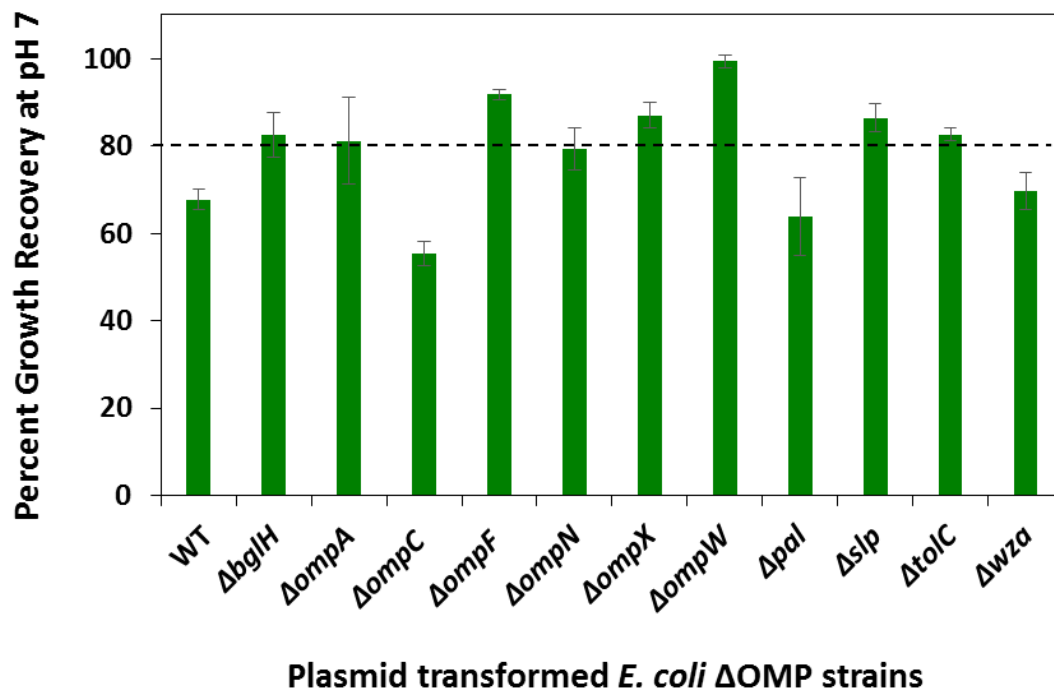


Figure 4.1. Growth recovery screens of 11 plasmid-transformed *E. coli* OMP strains in neutral pH 7 M9 media after 16 hrs at 37°C. The percentages of growth recovery, shown as a bar chart, represent the change in the mean ($n = 5$) 16 hr OD_{600nm} values (growth) of each strain transformed with pEmrE compared to results for the vector pMS119EHA. All strains except the WT, *ΔompC* and *Δpal* pEmrE transformants failed to show statistically significant reductions ($P \leq 0.005$) in growth between the pEmrE-transformed strain and the empty control vector (pMS119EHA)-containing strain.

Therefore, the EmrE-induced loss-of-growth phenotype due to the intracellular loss of osmoprotectants was not as substantial as expected, since osmoprotectant availability was not as critical to the cells for maintenance of the cytoplasmic pH homeostasis during growth. Even the pEmrE-transformed WT strain, which was predicted to display only

~20% of growth due to *emrE* over-expression (122), demonstrated a $67\% \pm 2.4\%$ growth recovery at pH 7 (Figure 4.1).

Since the phenotypic growth screen results collected at pH 7 (Figure 4.1) did not demonstrate an effective phenotype to illustrate a rescue of growth, repeating the screen under more stringent conditions was necessary. Hence, this Δ OMP screen was also conducted in M9 medium buffered to pH 8 and the results that were generated are provided below, in Figure 4.2. By increasing the pH of the growth medium and subjecting the *E. coli* deletion mutants to alkali stress, the number of potential OMP candidates was narrowed down to three. A significant rescue of the loss-of-growth phenotype caused by *emrE* was only achieved by the $\Delta ompF$, $\Delta ompW$ and Δslp mutations (Figure 4.2). The first identified OMP candidate, OmpF, is a major porin protein in *E. coli* that facilitates non-specific diffusion of hydrophilic molecules across the OM (46, 71). A $79\% \pm 6.5\%$ growth rescue was observed for the pEmrE-transformed $\Delta ompF$ strain in pH 8 M9 growth medium, which suggests the possibly this OMP gene deletion only partially restores growth, by preventing fractional osmoprotectant loss from the cell. This may be due to the fact that the level of *ompF* gene expression is affected in reciprocal manner to that of another similar porin gene, *ompC*, by the osmolarity of the growth medium (174, 175). In a medium with low osmolarity, the *ompF* gene is preferentially expressed, whereas the *ompC* gene expression predominates in media of high osmotic strength. Hence, due to the low expression level of the *E. coli ompC* gene in pH 8 M9 medium, a small portion of osmoprotectants was still able to escape from the periplasm across the OM, by diffusing along their concentration gradient through the OmpC porin, which resulted in a partial rescue-of-growth phenotype, displayed by the

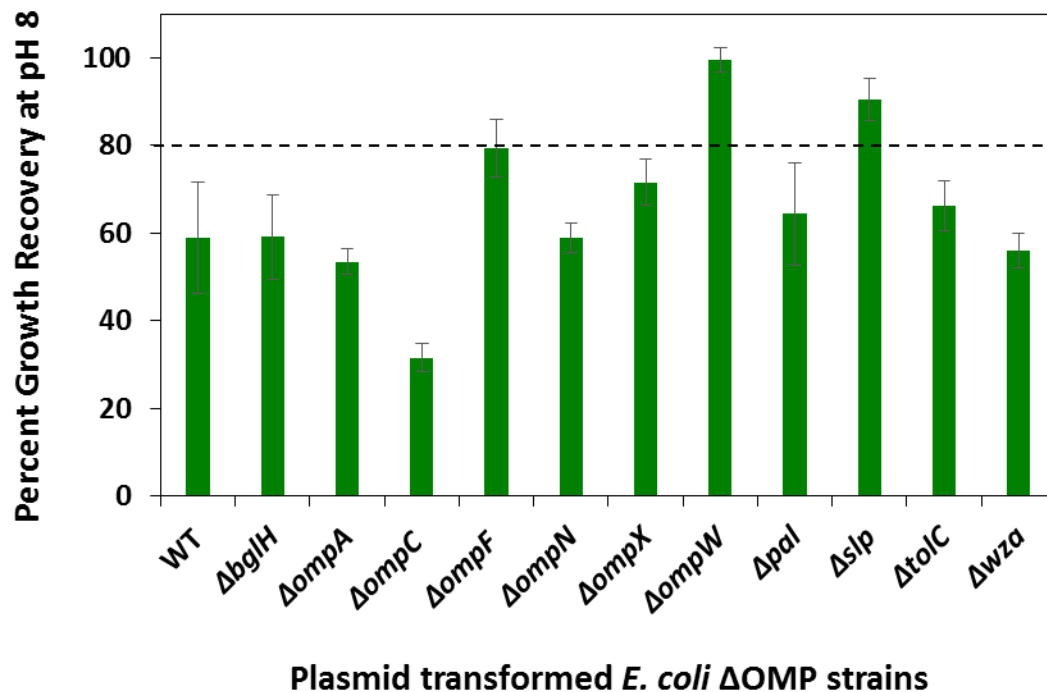


Figure 4.2. Growth recovery screens of 11 plasmid-transformed *E. coli* OMP strains in alkaline pH 8 M9 media after 16 hrs at 37°C. The percentages of growth recovery, shown as a bar chart, represent the change in the mean ($n = 5$) 16 hr OD_{600nm} values (growth) of each strain transformed with pEmrE compared to results for the vector pMS119EHA. All strains except the *ΔompF*, *ΔompW* and *Δslp* pEmrE transformants showed statistically significant reductions ($P \leq 0.005$) in growth between the pEmrE-transformed strain and the empty control vector (pMS119EHA)-containing strain.

ΔompF mutant (Figure 4.2). The *ΔompC* strain, on the other hand, did not produce a significant rescue-of-growth value ($32\% \pm 3.2\%$), since the OMP OmpF allows for a higher diffusion rate of osmoprotectants, due to a larger pore diameter and a higher gene expression level in M9 medium, in comparison to OmpC (Figure 4.2).

Similarly, a partial ($90\% \pm 4.9\%$) rescue-of-growth phenotype was also achieved by deletion of the *E. coli slp* gene, which encodes a carbon starvation-inducible OM lipoprotein, Slp, believed to play a role in the stability and permeability of the OM (176). Although this OMP is an unlikely candidate to be involved in the EmrE transport mechanism, the *slp* gene deletion may have contributed to osmoprotectant loss by reducing the overall permeability of the OM barrier. The highest growth recovery value ($99\% \pm 2.8\%$), however, was produced by the pEmrE-transformed $\Delta ompW$ strain (Figure 4.2). OmpW involvement in salinity tolerance and QCC transport, which are roles shared with EmrE, make it a highly probable OMP candidate to be functionally associated with EmrE (164, 177, 178).

In order to eliminate any false positives that may have been erroneously identified by the pH8 phenotypic growth screens, the same screening method was used to look for Δ OMP candidate capable of rescuing the EmrE-induced loss-of-growth under more alkaline (pH 9), and consequently more stressful, conditions. Based on the outcome of all growth phenotype experiments conducted within this thesis at pH 7 to 9, the pH9 OMP gene deletion growth screens produced the most significant differences in percent growth recovery values and growth phenotypes (Figure 4.1, 4.2 and 4.3). As shown in Figure 4.3, only the *E. coli ompW* gene deletion restored host alkali tolerance and significantly rescued ($102\% \pm 3.6\%$) the reduced-growth phenotype caused by *emrE* overexpression by more than 30%, in comparison to results for the WT and all other Δ OMP strains tested (Figure 4.3). Even though, none of the other OMP gene deletions were able to attain the minimum 80% threshold value used in this screen to identify positive OMP candidates,

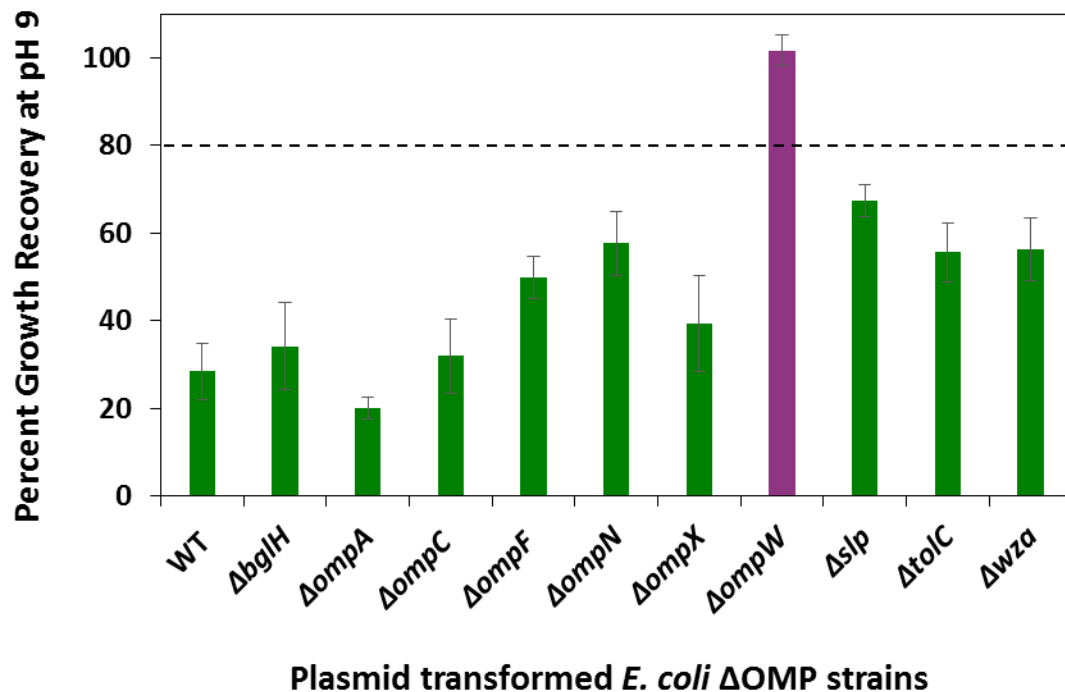


Figure 4.3. Growth recovery screens of 11 plasmid-transformed *E. coli* OMP strains in neutral pH 9 M9 media after 16 hrs at 37°C. The percentages of growth recovery, shown as a bar chart, represent the change in the mean ($n = 5$) 16-h OD_{600nm} values (growth) of each strain transformed with pEmrE compared to results for the vector pMS119EHA. Percent growth recovery value for the Δpal mutant is not shown, since this strain failed to grow at pH 9. All strains except the $\Delta ompW$ pEmrE transformant showed statistically significant reductions ($P \leq 0.005$) in growth between the pEmrE-transformed strain and the empty control vector (pMS119EHA)-containing strain.

some pEmrE-transformed Δ OMP mutants ($\Delta ompF$, $\Delta ompN$, Δslp , $\Delta tolC$ and Δwza) grew significantly better than the WT strain ($28\% \pm 6.5\%$). This “intermediate” growth phenotype may have been caused by functional association between multiple *E. coli* OMPs and EmrE. It is also important to note that the Δpal deletion strain (both

untransformed and transformed) failed to grow above pH 8 and thus, is excluded from results displayed for the pH 9 growth phenotype screens (Figure 4.3). The loss of viability may be caused by fact that this peptidoglycan-associated lipoprotein (Pal) plays a critical role in maintaining the structure, stability and function of the cell envelope (179).

Since only $\Delta ompW$ restored host alkali tolerance and rescued the loss-of-growth phenotypes in *E. coli* caused by EmrE osmoprotectant efflux under the most stringent (pH 9) growth conditions, OmpW was the only OMP candidate selected for further plasmid complementation analysis, described in chapter 5 of this thesis, to confirm its involvement.

4.4 Summary

The purpose of the experimental work described within this thesis chapter was to validate the hypothesis that the PM protein EmrE relies on the presence of an OMP to complete the extracellular release of its substrate in Gram-negative bacteria. Eleven potential OMP candidates from *E. coli* were selected for screening, using a neutral/alkaline phenotypic growth assay, to identify any OMP that may be involved in the EmrE-mediated QCC efflux mechanism. *E. coli* single OMP gene deletion strains were transformed with plasmid-carried copies of *emrE* to detect reduced-growth and rescued-growth phenotypes under pH 7 to 9 minimal medium conditions. Among the 11 OMP that were screened, only the $\Delta ompW$ strain showed rescued alkali growth tolerance, when transformed with pEmrE, at the most alkaline (pH 9) growth conditions, supporting the corresponding protein's involvement in EmrE osmoprotectant efflux.

Chapter Five: **Plasmid Complementation Alkaline Growth Assays of *E. coli* $\Delta emrE$ and $\Delta ompW$ Strains**

5.1 Introduction

Based on the experimental results generated by the neutral/alkaline pH growth phenotype screens of 11 selected *E. coli* outer membrane deletion mutant strains (described in chapter 4 of this thesis), *E. coli* deletion strain $\Delta ompW$ (JW1248) was selected for further screening to confirm possible involvement of OmpW in EmrE-mediated osmoprotectant efflux completely out of the cell. If the *ompW* gene deletion was in fact responsible for restoring host pH tolerance in M9 medium, by preventing the loss of osmoprotectant substrate from the cell, then its reintroduction back into the $\Delta ompW$ strain containing pEmrE would reverse the observed growth phenotype from rescue-of-growth back to loss-of-growth. By complementing this deleted OMP, osmoprotectant export across the OM was expected to be restored, thereby supporting potential involvement of OmpW in EmrE-mediated substrate extrusion in *E. coli*. Similarly, reintroduction of the *emrE* gene back into the pOmpW-transformed $\Delta emrE$ strain should restore the loss-of-growth phenotype, if both EmrE and OmpW are required for complete out of the cell efflux of substrate in *E. coli* and there is a phenotypic association between these two membrane proteins.

The purpose of the experiments described in this thesis chapter was to confirm our findings, generated by the pH-based growth phenotype screens (chapter 4), that the *E. coli* OMP OmpW assists in osmoprotectant efflux induced by EmrE. To do so, an alkaline (pH 9) M9 plasmid complementation analysis of the $\Delta ompW$ (JW1248) and

$\Delta emrE$ (JW0531) gene deletion strains was performed to test for a reversal of rescue-of-growth phenotype, induced by OmpW and EmrE co-expression.

5.2 Materials and Methods

5.2.1 *pMS119EHC Vector Construction*

Instead of using a previously made expression plasmid, a chloramphenicol (Cm)-resistant pMS119EHC vector (Figure 5.1) was specifically constructed in this study for *ompW* gene expression in plasmid complementation growth experiments. This expression system was selected in order to avoid toxic OmpW levels due to overexpression because, as introduced in section 2.3 of this thesis, pMS119EHA (the parental plasmid of pMS119EHC) exhibits “leaky” non-toxic expression of cloned encoding membrane proteins genes, when not induced with IPTG (122). This leakiness has turned out to be very convenient for our studies. Construction of the pMS119EHC vector involved replacing the β -lactamase gene *bla* from pMS119EHA with a chloramphenicol acetyltransferase gene *cat* from the pCA24N plasmid, since two different antibiotic resistance markers are required for maintenance of the two plasmids, of both *ompW* (cloned into pMS119EHC) and *emrE* (cloned into pMS119EHA) genes in the cell. The Amp resistance gene *bla* was “excised” from pMS119EHA using a restriction endonuclease called *DraI*, as described in section 2.9 of chapter 2. After restriction digestion, the linearized “blunt” ended pMS119EHA plasmid was separated by gel electrophoresis (section 2.8.1) and purified using the QIAquick Gel Extraction kit (section 2.8.2). Similarly, to isolate the functional *cat* gene from pCA24N, vector DNA was digested with the restriction endonuclease *Sau3AI*, digested fragments were

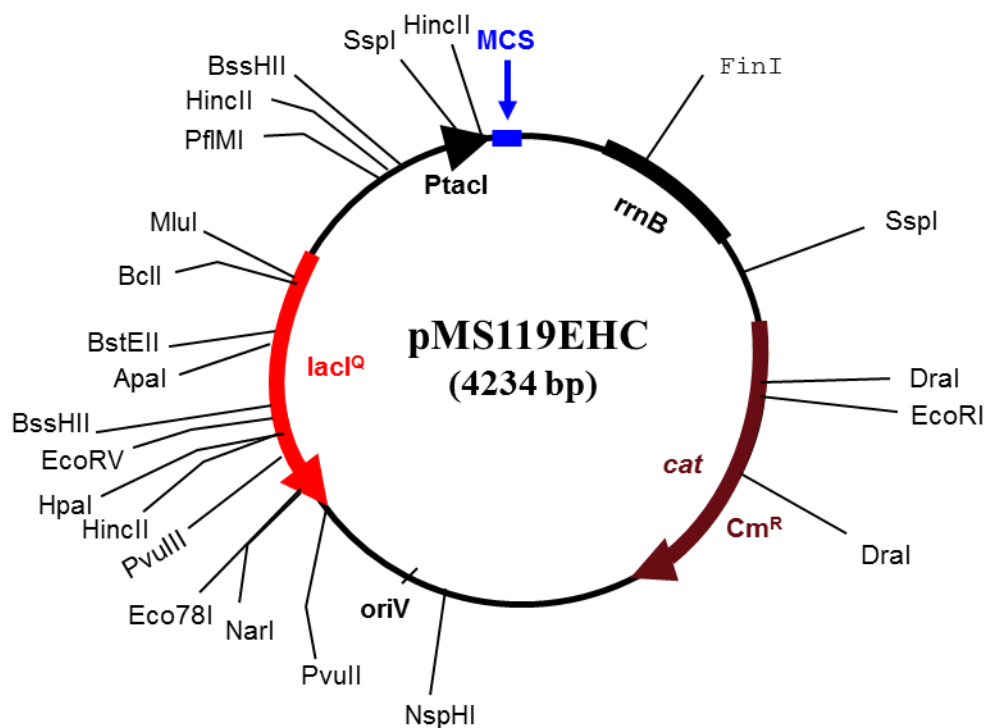


Figure 5.1. Plasmid map of the Cm-resistant control vector pMS119EHC.

separated based on size using gel electrophoresis and the gene of interest was purified using a gel extraction kit. Since *Sau3AI* is not a “sticky” end cutter, the single-strand overhangs of the “excised” *cat* gene had to be “blunted” using the Klenow enzyme, as described in section 2.10.1. Then, the prepared *cat* gene fragment was joined, via “blunt” ligation, with the linearized pMS119EH vector DNA, which was first dephosphorylated with CIAP (Table 2.6) to prevent self-ligation (section 2.10.1). Competent DH5 α cells were transformed with 2 μ l of ligation mix (Table 2.7) and successful pMS119EHC constructs were selected for using LB + 34 μ g/ml Cm agar plates.

5.2.2 Construction of *pOmpW*, *pOmpA* and *pLamB* Clones

Plasmid constructs *pOmpW*, *pOmpA*, and *pLamB* were prepared and used for growth phenotype complementation screens of *E. coli* $\Delta ompW$ (JW1248). The *pOmpW* plasmid (Figure 5.2(A)) was constructed by cloning the *ompW* gene sequence into the multiple cloning site of the newly constructed pMS119EHC vector (section 5.2.1). The *ompW* gene was amplified by PCR (as described in section 2.7.1) using *E. coli* BW25113 genomic DNA (isolated as described in section 2.6.1) with the primer pairs listed in Table 2.2. The *ompW* amplicon was separated based on size using gel electrophoresis (section 2.8.1) and isolated using the QIAquick Gel Extraction kit (section 2.8.2). To create compatible “sticky” ends, both the pMS119EHC vector and the *ompW* gene were digested with two restriction endonucleases, *Xba*I and *Hind*III, as described in section 2.9. After restriction digestion, vector and insert DNA was purified from residual enzymes and buffers with ethanol precipitation (section 2.7.2) and joined together using “sticky” end ligation (2.10.2). Similarly, the *pOmpA* (Figure 5.2(B)) and *pLamB* (Figure 5.2(C)) plasmid constructs were prepared by cloning *ompA* or *lamB* amplicons, amplified by PCR using *E. coli* WT (BW25113) genomic DNA (section 2.6.1) with primers listed in Table 2.2, into the multiple cloning site of the pMS119EHC plasmid at *Xba*I and *Hind*III restriction sites. Gene sequences of all constructs were verified using restriction digestion profiles and DNA sequencing from primers localizing to the upstream *Ptac*I to the downstream *rrnB* (*Trp*) transcription termination regions (Eurofins MWG Operon, Ebersberg, Germany).

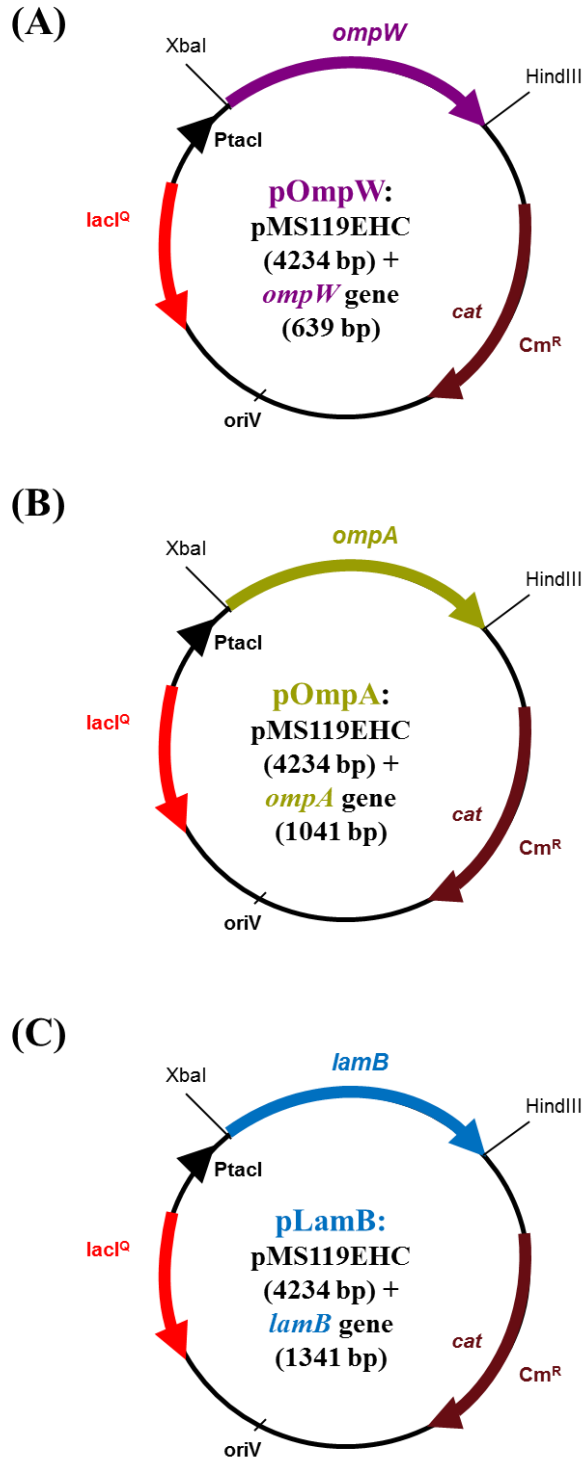


Figure 5.2. Plasmid maps of the *ompW* gene expression construct (A) pOmpW, *ompA* expression construct (B) pOmpA and *lamB* gene expression construct (C) pLamB.

5.2.3 Plasmid Complementation Alkaline Growth Assays of *E. coli* $\Delta ompW$ and $\Delta emrE$ Mutants

Based on the experimental results generated by the pH-based growth phenotype screens (described in chapter 4), the *E. coli* $\Delta ompW$ strain was selected for plasmid complementation analysis. Competent $\Delta ompW$ cells were co-transformed with the pOmpW and pEmrE plasmids to determine if the EmrE-induced loss-of-growth phenotype conferred by transformation could be produced by reintroducing *ompW* back into $\Delta ompW$ strain under alkaline (pH 9) M9 growth conditions. As a control, the $\Delta ompW$ strain was also co-transformed with the following pairwise plasmid combinations: pMS119EHA + pOmpW, pEmrE + pMS119EHC and pMS119EHA + pMS119EHC. Additionally, to ensure that the complementation was specific to *ompW* expression, plasmids carrying an unrelated *ompA* or *lamB* OMP gene (pOmpA or pLamB, respectively) were also co-transformed with pEmrE or pMS119EHA in $\Delta ompW$ strain. The *E. coli* OmpA protein was chosen as a negative control based on the results from the pH-based growth phenotype screen of selected OM proteins (chapter 4), as it was found that *ompA* gene deletion failed to rescue the loss-of-growth phenotype in pEmrE-transformed *E. coli* strain and over-expression of *ompA* gene was expected to have no significant effect on the growth phenotype of $\Delta ompW$ cultured in M9 medium at pH ≥ 7 in the presence of EmrE. Likewise, the OM protein LamB (173, 180), a sugar porin that is physiologically relevant only in the presence of maltose and maltosaccharide, was also selected as a transporter that would likely not participate in osmoprotectant efflux and reverse the rescue-of-growth phenotype.

A reverse complementation assay was also performed to confirm if the same loss of growth phenotype could be produced using the *E. coli* $\Delta emrE$ (JW0531). Similar to $\Delta ompW$ strain plasmid complementation experiments, pMS119EHA + pOmpW, pEmrE + pMS119EHC and pMS119EHA + pMS119EHC plasmid co-transformations were performed with the $\Delta emrE$ strain. To ensure that both co-transformed plasmids were maintained in the tested strains, all media used for plasmid complementation assays contained 100 $\mu\text{g/ml}$ Amp and 34 $\mu\text{g/ml}$ Cm as a selective pressure. All alkaline M9 growth phenotype complementation assays of co-transformed $\Delta ompW$ strains and reverse complementation of co-transformed $\Delta emrE$ strains were set up and monitored as described for pH-based M9 growth phenotype experiments, where mean 16 hr OD_{600nm} values were measured from five independent inoculated culturing experiments. Statistical analysis of growth differences between pEmrE + pOmpW co-transformants and control (pMS119EHA + pMS119EHC) co-transformants were determined using a Student two-tailed t test, and P values of ≤ 0.005 were considered to be significantly different.

5.2.4 Percentage Growth Recovery by Plasmid Pair Co-transformed $\Delta ompW$ and $\Delta emrE$ Strains

The conducted plasmid complementation assays were evaluated by converting mean OD_{600nm} values for all $\Delta ompW$ and $\Delta emrE$ co-transformants to percent growth recovery using calculations similar to those described in section 4.2.3 of chapter 4 for pH-based phenotypic growth screens by adjusting the following formula:

Percent growth recovery for plasmid pair co-transformed

ΔompW and *ΔemrE* strains =

$$= \frac{\text{Mean OD}_{600\text{nm}} \text{ for pEmrE or OMP-carrying-plasmid co-transformed strain}}{\text{Mean OD}_{600\text{nm}} \text{ for pMS119EHA + pMS119EHC co-transformed strain}} \times 100\%$$

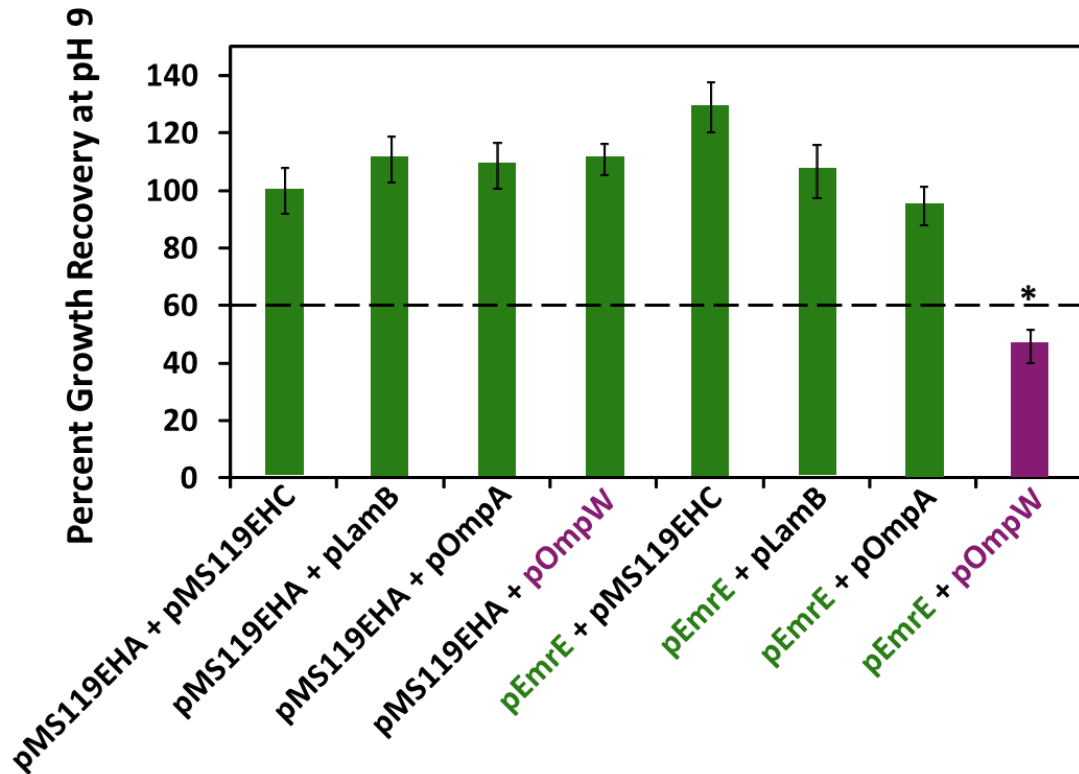
Where the mean 16 h OD_{600nm} for each plasmid pair co-transformed *ΔompW* and *ΔemrE* strain is divided by the mean value measured at 16 h OD_{600nm} for that same strain co-transformed with the empty control plasmids pMS119EHA + pMS119EHC and multiplied by 100%. The percent growth recovery values for empty control vector-containing strains were calculated by dividing mean 16 h OD_{600nm} values by the mean 16 hr OD_{600nm} values for the growth of the same strains lacking plasmids. Since the pMS119EH plasmid (derived from the parental plasmid pBR322 (138)) is present in low copy number (20 to 30 copies/cell) (181) and expression (122, 182) from each co-transformant is approximately half the amount of that for single pEmrE transformants, the cut-off value for significant complementation was set to 60%. This cut-off value is calculated by multiplying 30% by 2, since two plasmids are introduced into each strain and each plasmid is expected recover approximately 30% of growth, based on the ~30% growth recovery values observed for single pEmrE transformant in the WT *E. coli* strain (chapter 4).

5.3 Results and Discussion

5.3.1 Complementation of *E. coli* $\Delta ompW$ Strain by *pEmrE* and *pOmpW* Reproduced the Loss-of-Growth Phenotype Under Alkaline Minimal Growth Conditions

Based on the results generated by the pH-based phenotypic growth screening experiments described in chapter 4, the $\Delta ompW$ (JW1248) gene deletion strain was selected for plasmid complementation assays to confirm involvement of OmpW in osmoprotectant efflux induced by EmrE. The expected outcome for these assays was that if the *ompW* gene was in fact responsible for restoring host pH tolerance in pH 7-9 M9 media, due to the efflux of osmoprotectant substrates by EmrE, its reintroduction back into $\Delta ompW$ strain containing pEmrE would restore the loss-of-growth phenotype by complementing the deleted OMP. To ensure that the complementation was specific to *emrE* and *ompW* expression, $\Delta ompW$ strain was also co-transformed with pEmrE and plasmids encoding unrelated (to EmrE-mediated efflux) *ompA* or lamB OMP gene (pOmpA and pLamB).

The results from $\Delta ompW$ strain plasmid complementation growth assays in pH 9 M9 medium after 16 h of incubation are shown in Figure 5.3. As expected, only $\Delta ompW$ strain co-transformed with pEmrE and pOmpW resulted in a statistically significant reduction in growth when compared to all other plasmid pair co-transformation combinations (pEmrE + pMS119EHC, pMS119EHA + pOmpW and pMS119EHA + pMS119EHC). The outcome of this assays confirms that reintroduction of *ompW* with *emrE* reproduced the loss-of-growth phenotype (46% +/- 5.8%) under alkaline growth conditions, likely by resorting the efflux of osmoprotectants across the OM and completely out of the cell (Figure 5.3). Our confidence in this finding is high, since a



Plasmid pair co-transformation of $\Delta ompW$

Figure 5.3. Plasmid complementation of the *E. coli* $\Delta ompW$ strain cultured using alkaline (pH 9) M9 growth phenotype assays. The percent growth recovery of plasmid co-transformed $\Delta ompW$ strains is shown as a bar chart, reflecting the change in mean (n = 5) 16-hr OD_{600nm} values (growth) between the pEmrE-transformed strain and the pMS119EHA strain. Statistically significant reduction in percent growth recovery values ($P \leq 0.005$) was observed only for pEmrE + pOmpW co-transformant and is indicated by an asterisk. Dashed line indicates the cutoff value ($30\% \times 2 = 60\%$) used to determine significant complementation.

complementation was achieved specifically for $\Delta ompW$ pOmpW and pEmrE co-transformants. This percent complementation value is derived using the growth recovery

value ($28 \pm 6.5\%$) observed for the pEmrE-transformed WT strain (in the initial pH-based growth phenotype screen described in chapter 4), which was used to represent 100% complementation. Although 100% complementation was not attained for *ompW* gene deletion, likely due to variation in gene dosage, a complementation value of 92% still falls below the $\leq 60\%$ complementation cutoff value, which is also based on the $\sim 30\%$ growth recovery value observed for single pEmrE transformants in the WT strain (chapter 4). Transformations with either pOmpA or pLamB and pEmrE did not significantly alter percent growth recovery values, which confirms that the resulting reduced growth phenotype was caused by the addition of *ompW* and not due to a general growth alterations caused by increasing the amount of an unrelated OMP (Figure 5.3). Unexpectedly, as can be seen in Figure 5.3, the pEmrE + pMS119EHC co-transformants grew significantly better than the empty vector control (pMS119EHA + pMS119EHC). This gain-of-growth phenotype could be the result of combined activity of EmrE and the presence of the *cat* gene product that may enhance the expression of Cm induced multidrug resistant efflux pumps such as MdfA, which is known to contribute to high alkali tolerance in *E. coli* cells by coupling proton influx to export of Na^+ or K^+ ions. (65). Since $\Delta ompW$ plasmid complementation results collected at pH 9, shown in Figure 5.3, demonstrated an effective phenotype to illustrate the complementation, repeating the assay at pH 7 and 8 was not necessary.

5.3.2 Reverse complementation of *E. coli* $\Delta emrE$ strain by *pEmrE* and *pOmpW* also replicated the loss-of-growth phenotype under alkaline minimal growth conditions

Reverse complementation assays using the *E. coli* $\Delta emrE$ strain were performed as well, in order to confirm that the co-expression of both membrane proteins, EmrE and OmpW, is necessary for reducing pH host tolerance by restoring the efflux of osmoprotectants completely out of the cell. Since reintroduction of *ompW* into the *pEmrE*-transformed $\Delta ompW$ strain reproduced the loss-of-growth phenotype by complementing the deleted OMP, if OmpW is in fact involved in EmrE-mediated osmoprotectant efflux, reintroduction of *emrE* into the $\Delta emrE$ strain containing *pOmpW* should cause an analogous reversal of growth phenotype by complementing the deleted PM protein.

The results from these $\Delta emrE$ strain complementation growth assays in pH 9 M9 medium after 16 h of incubation are shown below, in Figure 5.4. Similar to the outcome of $\Delta ompW$ complementation assays, only co-transformation of *pEmrE* and *pOmpW* in the $\Delta emrE$ strain specifically resulted in reduced percent growth recovery values (58% \pm 6.2%). A 74% complementation was achieved for $\Delta emrE$ *pEmrE* and *pOmpW* co-transformants, which again fell within the 60% cut-off (Figure 5.2). Hence, the complementation of *emrE* gene deletion in the presence of OmpW successfully reproduced the loss-of-growth phenotype in pH 9 M9, thereby confirming a phenotypic association between EmrE and OmpW membrane proteins, as suggested in previous chapters of this thesis (chapters 3 and 4).

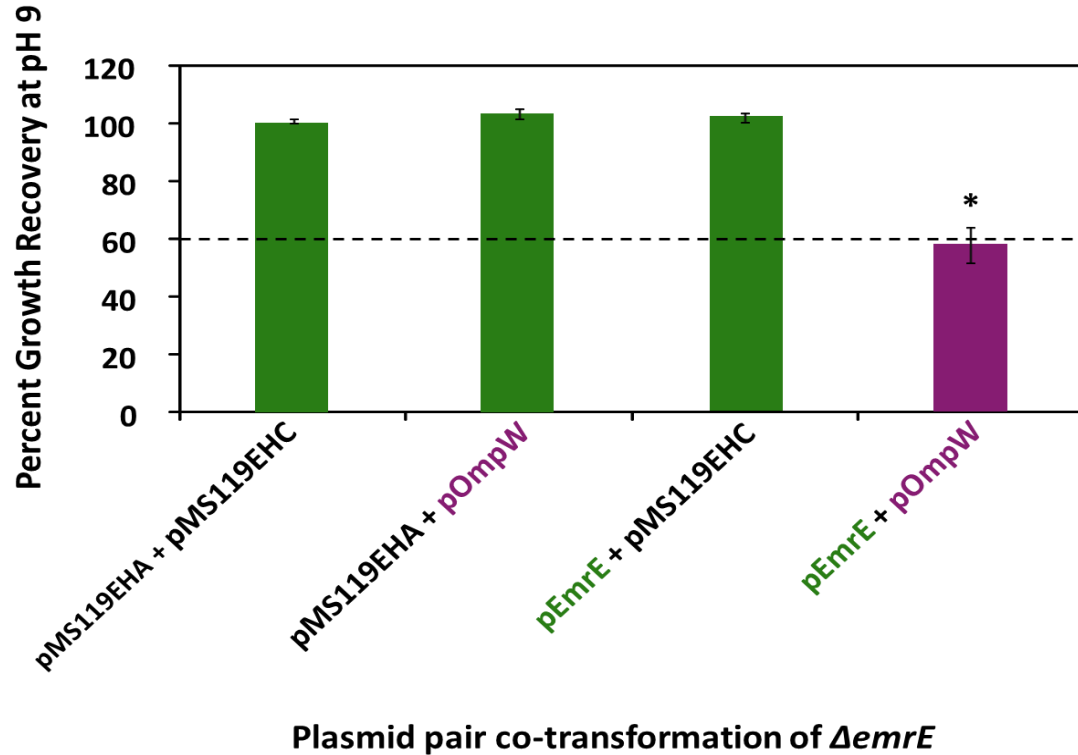


Figure 5.4. Plasmid complementation of the *E. coli ΔemrE* strain cultured using alkaline (pH 9) M9 growth phenotype assays. The percent growth recovery of plasmid co-transformed *ΔemrE* strains is shown as a bar chart, reflecting the change in mean (n = 5) 16-h OD_{600nm} values (growth) between the pOmpW-transformed strain and the pMS119EHC strain. Statistically significant reduction in percent growth recovery values ($P \leq 0.005$) was observed only for the pEmrE + pOmpW co-transformant and is indicated by an asterisks. Dashed line indicates the cutoff value ($30 \times 2 = 60\%$) used to determine significant complementation.

5.4 Summary

Based on the experimental results generated by the pH tolerance growth phenotype screens (chapter 4), *E. coli ΔompW* and *ΔemrE* gene deletion strains were

selected for further screening in order to confirm possible involvement of OMP OmpW in substrate efflux initiated by EmrE. Plasmid complementation assays were performed to test for reduced pH host tolerance and a reversal of rescue-of-growth phenotype at pH 9 in M9 media, due to restored efflux of osmoprotectant substrate completely from the cell caused by complementation of either the *ompW* or *emrE* gene deletion in the pEmrE-transformed $\Delta ompW$ or pOmpW-transformed $\Delta emrE$ strain, respectively. As expected, these complementation growth assays confirmed that only co-expression of both *emrE* and *ompW* genes in the $\Delta ompW$ or $\Delta emrE$ strain reproduced the loss-of-growth phenotype due to the efflux of osmoprotectants by both membrane proteins when the strains were grown under alkaline conditions.

Chapter Six: Toxic Quaternary Cationic Compound Minimum Inhibition Concentration Assays

6.1 Introduction

Since the majority of known EmrE substrates are antimicrobial QCCs and EmrE is a multidrug exporter, it was essential to confirm if the newly identified OmpW also participated in conferring QCC resistance when co-accumulated with EmrE. Hence, the primary goal of this thesis chapter was to test whether the co-expression of *emrE* and *ompW* increased drug tolerance in *E. coli* host, by performing drug resistance assays using a QCC, methyl viologen dichloride (MV). This compound is a well-known substrate of EmrE (94, 168) and was selected for QCC resistance experiments based on the findings of a previous study (164), which demonstrated that overexpression of *ompW* in *Salmonella enterica serovar* Typhimurium contributed to MV resistance. In order to test for substrate specificity, three additional QCC substrates of EmrE, acriflavine, cetyltrimethylammonium bromide (CTAB) and ethidium bromide (EtBr), were assayed as well (94, 109, 154).

6.2 Materials and Methods

Plasmid co-transformed *E. coli* strain QCC minimum inhibition concentration (MIC) plating assays were performed using the EmrE substrate MV to confirm if the combination of pEmrE and pOmpW co-expression increased host drug tolerance. *E. coli* $\Delta ompW$ (JW1248) and WT (BW25113) strains were co-transformed with the same plasmid combinations (pMS119EHA + pMS119EHC, pEmrE + pMS119EHC, pMS119EHA + pOmpW and pEmrE + pOmpW) used in the complementation assays

(described in chapter 5) and grown overnight in LB with 100 µg/ml Amp and 34 µg/ml Cm (to maintain both co-transformed plasmids) at 37°C with shaking. Standardized overnight cultures were spotted (5µl) at 10^0 to 10^{-5} dilutions onto M9 agar plates (pH 7 M9 medium with 1.5% [w/v] agar, 100 µg/ml Amp and 34 µg/ml Cm) containing increasing concentrations of MV, ranging from 5 µg/ml to 200 µg/ml, in addition to growth tolerance control plates lacking MV. Using the same technique, the 10^{-3} to 10^{-5} dilutions of overnight cultures of *E. coli* $\Delta ompW$ and WT strains co-transformed with the pEmrE (Amp) and pOmpW (Cm) plasmids and appropriate empty control vector combinations were also spotted onto M9 agar plates containing increasing concentrations (ranging from 5 µg/ml to 40 µg/ml) of acriflavine, CTAB or EtBr. Since previous studies demonstrate that inoculum concentration is an important factor in determination of MICs, testing a range of inoculum concentrations was necessary for generating accurate results (183). The M9 medium was selected instead of using LB plates to insure reproducibility and limit the influence of other compounds present in undefined LB medium so that only the effect of QCCs on plasmid co-transformed strain resistance was observed. All MIC assays within this thesis work were conducted at neutral pH, to minimize the amount of stress that the cultures were exposed to in addition to the toxic QCCs present in the media. Lawn growth from the 5µl spot was measured as “+” or “-” colony formation after 16, 24 and 48 h of incubation at 37°C and the MIC of the QCC for each co-transformant strain was based on results obtained from five independent plating assay trials. Statistical analysis was performed to calculate the significance of growth results, and P values of ≤ 0.005 were deemed to show significant difference according to Student’s t test calculations.

6.3 Results and Discussion

6.3.1 *E. coli* $\Delta ompW$ and WT Strains Transformed with Both *pEmrE* and *pOmpW* Conferred Host Resistance to High Concentrations of MV

Since *EmrE* is a multidrug transporter that confers host resistance to a broad range of toxic QCC, in order to confirm the involvement of *OmpW* in *EmrE*-mediated substrate efflux completely out of the cell (as suggested by pH-base growth phenotype and plasmid complementation assay results described in chapters 4 and 5 of this thesis, respectively), it was necessary to test whether *OmpW* participated in QCC resistance. Hence, QCC resistance assays were performed using the *EmrE* substrate MV, by preparing and growing cultures of *E. coli* $\Delta ompW$ and WT strains co-transformed with pMS119EHA + pMS119EHC, pEmrE + pMS119EHC, pMS119EHA + pOmpW and pEmrE + pOmpW plasmid combinations for 16 hrs on pH 7 M9 agar plates containing 5-fold-range of concentrations of MV (5 $\mu\text{g/ml}$ to 200 $\mu\text{g/ml}$) to determine the extent of host MV resistance conferred by each plasmid pair. The MV MIC values determined from these resistance experiments after 16, 24 and 48 hrs of growth in M9 media are provided below in Table 6.1, Table 6.2 and Table 6.3 respectively. Our results indicate that after 16 hrs of incubation, only 10^{-4} dilutions of both WT and $\Delta ompW$ strains co-transformed with pEmrE + pOmpW demonstrated growth on MV containing M9 agar plates (Table 6.1). While at the 10^{-3} dilution either strain transformed with pEmrE + pOmpW plasmid combination or just pEmrE displayed MV resistance, higher MV MIC values were observed for the pEmrE + pOmpW co-transformants. For low dilutions (10^{-1} and 10^{-2}) and undiluted (10^0) cultures a clear increase in MV MIC values in comparison to results for empty vector transformants was displayed by WT and $\Delta ompW$ strains co-transformed

with pEmrE + pOmpW, pEmrE + pMS119EHC or pOmpW + pMS119EHA (Table 6.1). This increase in MIC values can be attributed to the inoculum effect (IE), a phenomenon defined as the increase in MIC of an antimicrobial agent as the initial microbial inoculum is increased, possibly triggered by bacterial communication via quorum sensing or reduced effective drug exposure (183, 184).

Table 6.1. Methyl viologen minimum inhibitory concentrations for culture dilutions of *E. coli* $\Delta ompW$ and WT strain plasmid co-transformants grown on M9 medium agar for 16 hrs

Strain tested	Plasmid co-transformation combination tested	MIC ($\mu\text{g/mL}$) of spotted dilution					
		10^0	10^{-1}	10^{-2}	10^{-3}	10^{-4}	10^{-5}
WT	pMS119EHA + pMS119EHC	10	5	0	0	0	0
	pEmrE + pMS119EHC	200	200	20	10	0	0
	pMS119EHA + pOmpW	100	50	5	0	0	0
	pEmrE + pOmpW	200	200	20	15	10	0
$\Delta ompW$	pMS119EHA + pMS119EHC	10	0	0	0	0	0
	pEmrE + pMS119EHC	200	50	20	10	0	0
	pMS119EHA + pOmpW	50	10	0	0	0	0
	pEmrE + pOmpW	200	50	20	15	5	0

After 24 hrs, 10^{-4} dilutions of WT and $\Delta ompW$ strain demonstrated increased MV MIC values for strains with plasmid pairings of pEmrE + pOmpW, as well as pEmrE + pMS119EHA, indicating that resistance conferred by the various co-transformations became indistinguishable over time (Table 6.2). The 10^{-3} culture dilutions at 16 h and 24 h

indicated that strains containing pOmpW + pMS119EHA also showed increased MV resistance values, but at half the concentrations conferred by pEmrE + pMS119EHC or pEmrE + pOmpW combination (Table 6.1 and 6.2). This is likely due to variations in the copy number of pOmpW relative to that of pMS119EHA/C or to pEmrE maintained within cells.

Table 6.2. Methyl viologen minimum inhibitory concentrations for culture dilutions of *E. coli* Δ ompW and WT strain plasmid co-transformants grown on M9 medium agar for 24 hrs

Strain tested	Plasmid co-transformation combination tested	MIC (μ g/mL) of spotted dilution					
		10^0	10^{-1}	10^{-2}	10^{-3}	10^{-4}	10^{-5}
WT	pMS119EHA + pMS119EHC	100	50	10	0	0	0
	pEmrE + pMS119EHC	200	200	50	10	10	5
	pMS119EHA + pOmpW	150	50	15	5	0	0
	pEmrE + pOmpW	200	200	20	15	10	10
Δ ompW	pMS119EHA + pMS119EHC	50	10	0	0	0	0
	pEmrE + pMS119EHC	200	100	20	15	10	10
	pMS119EHA + pOmpW	150	50	10	5	0	0
	pEmrE + pOmpW	200	100	50	15	10	10

A longer incubation period of 48 hrs resulted in a small to no difference in MV resistance, even at the lowest dilutions tested (10^{-4} and 10^{-5}), except for strains with empty vector pairs (Table 6.3). This observed increase in MV resistance with incubation time is likely due to the development of resistant bacterial subpopulations caused by

stress-induced mutations (185). Overall, the findings of these MV resistance assays confirmed that the presence of both *emrE* and *ompW* genes conferred host resistance to the highest concentrations of MV and that both membrane proteins participate in MV efflux.

Table 6.3. Methyl viologen minimum inhibitory concentrations for culture dilutions of *E. coli* $\Delta ompW$ and WT strain plasmid co-transformants grown on M9 medium agar for 48 hrs

Strain tested	Plasmid co-transformation combination tested	MIC ($\mu\text{g/mL}$) of spotted dilution					
		10^0	10^{-1}	10^{-2}	10^{-3}	10^{-4}	10^{-5}
WT	pMS119EHA + pMS119EHC	200	150	50	10	10	5
	pEmrE + pMS119EHC	200	200	200	10	10	10
	pMS119EHA + pOmpW	200	150	50	10	10	10
	pEmrE + pOmpW	200	200	200	20	10	10
$\Delta ompW$	pMS119EHA + pMS119EHC	150	100	25	10	10	0
	pEmrE + pMS119EHC	200	200	50	20	10	10
	pMS119EHA + pOmpW	200	150	50	10	10	10
	pEmrE + pOmpW	200	200	100	20	15	15

6.3.2 Co-expression of *emrE* and *ompW* gGenes in *E. coli* $\Delta ompW$ and WT Strains did not Increase Host Resistance to Acriflavine, EtBr or CTAB.

To determine if both OmpW and EmrE contribute to toxic QCC, other than MV, resistance in *E. coli*, QCC MIC plating assays were also performed using other well-known EmrE substrates (94, 154), acriflavine (dye and antiseptic), CTAB (detergent and antiseptic) and EtBr (DNA intercalating dye). Cultures of the same plasmid co-

transformed *E. coli* $\Delta ompW$ and WT strains used in MV resistance assays were grown on pH 7 M9 plated containing 5-fold-increasing concentrations of one of the three selected QCC (ranging from 5 $\mu\text{g/ml}$ to 40 $\mu\text{g/ml}$), to test the degree of host resistance conferred over a 16-h to 24-h incubation period. The results that were generated by these resistance assays, shown below in Tables 6.4, 6.5 and 6.6, revealed that there were no differences in resistance levels for any of these other QCCs (acriflavine, EtBr or CTAB), even for the empty vector transformants. After a 16-h incubation, the 10^{-3} dilutions of all WT and $\Delta ompW$ strain co-transformants demonstrated acriflavin (Table 6.4) and EtBr (Table 6.5) MIC values of 40 $\mu\text{g/ml}$ and CTAB (Table 6.6) MIC value of 30 $\mu\text{g/ml}$. At the 10^{-4} culture dilution, MIC values of 40 $\mu\text{g/ml}$ for acriflavine and 25 $\mu\text{g/ml}$ for EtBr and CTAB were observed for all co-transformants. An MIC value of 0 $\mu\text{g/ml}$ was observed for all three tested QCCs at the 10^{-5} culture dilution for all co-transformants of the WT and $\Delta ompW$ strains.

Similarly, a longer incubation period of 24 hrs resulted in no differences in acriflavine (Table 6.4), EtBr (Table 6.5) and CTAB (Table 6.6) resistance at any of the dilutions tested. An MIC value of 40 $\mu\text{g/ml}$ was observed for acriflavine and EtBr at all three culture dilutions for all WT and $\Delta ompW$ strain co-transformants. For CTAB, MIC values of 30 $\mu\text{g/ml}$, 25 $\mu\text{g/ml}$ and 20 $\mu\text{g/ml}$ were displayed by 10^{-3} , 10^{-4} and 10^{-5} culture dilutions, respectively, for all tested co-transformants.

Table 6.4. Acriflavine minimum inhibitory concentrations for culture dilutions of *E. coli* $\Delta ompW$ and WT strain plasmid co-transformants grown on M9 medium agar for 16 and 24 hrs

Strain tested	Plasmid co-transformation combination tested	Incubation time (hrs)					
		16	16	16	24	24	24
		MIC ($\mu\text{g/ml}$) of spotted dilution					
		10^{-3}	10^{-4}	10^{-5}	10^{-3}	10^{-4}	10^{-5}
WT	pMS119EHA + pMS119EHC	40	40	0	40	40	40
	pEmrE + pMS119EHC	40	40	0	40	40	40
	pMS119EHA + pOmpW	40	40	0	40	40	40
	pEmrE + pOmpW	40	40	0	40	40	40
$\Delta ompW$	pMS119EHA + pMS119EHC	40	40	0	40	40	10
	pEmrE + pMS119EHC	40	40	0	40	40	40
	pMS119EHA + pOmpW	40	40	0	40	40	40
	pEmrE + pOmpW	40	40	0	40	40	40

Table 6.5. Ethidium bromide minimum inhibitory concentrations for culture dilutions of *E. coli* $\Delta ompW$ and WT strain plasmid co-transformants grown on M9 medium agar for 16 and 24 hrs

Strain tested	Plasmid co-transformation combination tested	Incubation time (hrs)					
		16	16	16	24	24	24
		MIC ($\mu\text{g/ml}$) of spotted dilution					
		10^{-3}	10^{-4}	10^{-5}	10^{-3}	10^{-4}	10^{-5}
WT	pMS119EHA + pMS119EHC	40	25	0	40	40	40
	pEmrE + pMS119EHC	40	25	0	40	40	40
	pMS119EHA + pOmpW	40	25	0	40	40	40
	pEmrE + pOmpW	40	25	0	40	40	40
$\Delta ompW$	pMS119EHA + pMS119EHC	40	25	0	40	40	40
	pEmrE + pMS119EHC	40	25	0	40	40	40
	pMS119EHA + pOmpW	40	25	0	40	40	40
	pEmrE + pOmpW	40	25	0	40	40	40

Table 6.6. Cetyltrimethylammonium bromide minimum inhibitory concentrations for culture dilutions of *E. coli* $\Delta ompW$ and WT strain plasmid co-transformants grown on M9 medium agar for 16 and 24 hrs

Strain tested	Plasmid co-transformation combination tested	Incubation time (hrs)					
		16	16	16	24	24	24
		MIC ($\mu\text{g/ml}$) of spotted dilution					
		10^{-3}	10^{-4}	10^{-5}	10^{-3}	10^{-4}	10^{-5}
WT	pMS119EHA + pMS119EHC	30	25	0	30	25	20
	pEmrE + pMS119EHC	30	25	0	30	25	20
	pMS119EHA + pOmpW	30	25	0	30	25	20
	pEmrE + pOmpW	30	25	0	30	25	20
$\Delta ompW$	pMS119EHA + pMS119EHC	30	25	0	30	25	20
	pEmrE + pMS119EHC	30	25	0	30	25	20
	pMS119EHA + pOmpW	30	25	0	30	25	20
	pEmrE + pOmpW	30	25	0	30	25	20

These indistinguishable MICs, presented in Tables 6.4, 6.5 and 6.6 of this chapter, values are potentially the result of acriflavine, EtBr and CTAB being transported by other MDR efflux systems that possess overlapping substrate profiles (such as AcrAB-TolC and MdfA) with EmrE, thereby masking the resistance phenotype conferred by pEmrE and pOmpW co-expression.

6.1 Summary

After identifying possible involvement of OmpW in EmrE-mediated osmoprotectant efflux (chapters 4 and 5 of this thesis), with EmrE being a MDR protein that primarily exports toxic QCC, the next logical step was to test whether OmpW also

conferred QCC resistance when co-accumulated with EmrE. Our approach involved conducting plasmid co-transformed *E. coli* $\Delta ompW$ and WT strain QCC MIC plating assays using the EmrE substrates: MV, acriflavine, CTAB and EtBr. No changes in resistance levels were found for the other three QCC that were tested, likely due to acriflavine, CTAB and EtBr also being substrates of other multidrug transporters, such as AcrAB-TolC.

The results of these QCC resistance assays revealed that co-expression of both *emrE* and *ompW* conferred host resistance to the highest concentration of MV, thereby confirming that OmpW participates in the efflux of EmrE-specific substrates across the OM.

Chapter Seven: **Final Discussion, Concluding Remarks and Future Directions**

7.1 Summary of Thesis Results

The overall objective of this thesis was to identify if EmrE relies on the presence of an outer membrane protein to complete the extracellular efflux of its substrates in Gram-negative bacteria. To accomplish this, a pH-based phenotypic *E. coli* growth assay was designed and applied as an *in-vivo* screening method to identify OMP gene(s) capable of rescuing the EmrE-induced loss-of-growth phenotypes observed in minimal media at pH 7, 8 and 9 (122). Based on the outcome of these neutral/alkaline M9 phenotype growth screens, described in chapter 4 of this thesis, we identified that only the *ompW* gene deletion in an *E. coli* strain over accumulating the EmrE protein rescued the loss-of-growth phenotype, by presumably preventing osmoprotectant loss from the cell, under both neutral and alkaline pH conditions (Figures 4.1 – 4.3). Next, in order to confirm involvement of the OMP OmpW in substrate efflux induced by EmrE, plasmid complementation alkaline growth assays were performed (chapter 5 of this thesis), which showed that only the complementation of both *emrE* and *ompW* in the $\Delta ompW$ and $\Delta emrE$ strain reproduced the loss-of-growth phenotype, due to the efflux of osmoprotectants by both membrane proteins when were grown under alkaline conditions (Figures 5.1 and 5.2). Lastly, to confirm if the newly identified OmpW assists EmrE in the efflux of toxic QCCs, plasmid co-transformed *E. coli* WT and $\Delta ompW$ strain methyl viologen MIC plating assays were conducted (chapter 6 of this thesis), which determined that the presence of both *emrE* and *ompW* conferred host resistance to the highest

concentrations of MV and that both membrane proteins participate in MV resistance (Table 6.1).

Taken altogether, this study provides the first evidence of OMP association with EmrE-mediated host drug resistance. It also confirms our hypothesis that EmrE relies on an OMP for assists in the removal of substrates, such as osmoprotectants and MV, completely from the cell.

7.2 Functional Association between OmpW and EmrE: Connecting the Dots

Prior to this study, OmpW may have been considered a highly probable OMP candidate to be associated with EmrE. This 23 kD (212 residues) OM porin was identified by Mitsuoki Morimyo in 1988. By screening MV-sensitive *E. coli* transposon insertion mutants and mapping their mutations, he came across two resistance-conferring genes, *mrvA* and *mvrB* (186), and almost 20 years later, the *ompW* gene sequence was confirmed to reside within this region of the genome (164). Moreover, examination of MV sensitive *E. coli* mutants by Morimyo also lead to the discovery of the *mvrC* gene (168), now commonly referred to as *emrE* (94, 108), although the functional connection between the two was not realized at the time.

After its discovery, OmpW has been largely pursued as a vaccine target in *Vibrio cholerae* strains (187, 188) and more recently in *E. coli* (189, 190), due to its ability to generate a high immunogenic (proinflammatory) response and confer host resistance to phagocytic mechanisms. The involvement of OmpW in host MV resistance has been mostly studied using the bacterium *Salmonella enterica* serovar Typhimurium and MV resistance assays performed with this host indicate that *ompW* gene expression increased

2 fold in the presence of MV, while deletions of this gene increased MV sensitivity by 2.5 fold (164). In this same study, the *Salmonella* MV-resistance transporter protein, SmvA, was examined with OmpW as a suspected plasma membrane efflux partner for conferring MV resistance across both membranes. However, the $\Delta smvA\Delta ompW$ double mutant could not be fully complemented by the re-introduction of the *smvA* gene and suggested an alternative PM counterpart for OmpW (164).

OmpW has also been shown to participate in a broad range of other physiological processes that include cell starvation, temperature tolerance and host dependence on environmental salinity (178, 191). Involvement of OmpW in host salinity tolerance is a role shared with EmrE, since EmrE was recently shown to efflux osmoprotectants, betaine and choline, under hypersaline growth conditions, as introduced in chapter 1 of this thesis (122). It is worth noting that the association between OmpW and a Gram-positive EmrE homologue, QacC, has been previously examined by testing whether QacC from *Staphylococcus epidermidis* required OmpW to function as a pump (192). To do this, the Gram-positive *S. epidermidis qacC* gene was over-expressed in the Gram-negative *S. enterica* Typhimurium WT and $\Delta ompW$ strains and the susceptibility of these derivatives to EtBr and to β -lactam antibiotics was tested. The outcome of these resistance assays, however, demonstrated that QacC functions in an OmpW-independent manner (192), which may suggest that the EmrE–OmpW association, shown in our study, is only specific to Gram-negative bacteria and may yield its own potential multipartite efflux system.

The high resolution (2.7 Å) X-ray diffraction crystal structure of OmpW demonstrated that this protein consists of an 8 stranded β -barrel channel, with a narrow

~50-Å long hydrophobic pore, relatively short periplasmic facing turns and long extracellular loops (193). Single channel conductance experiments for OmpW reconstituted into planar lipid bilayers were also conducted in the same study and revealed that this protein was capable of transporting ions and the cationic detergent, lauryl dodecyl amine oxide (LDAO), until the channel became blocked at μM concentrations (193). Hence, the hydrophobic channel of OmpW may be an important feature for the efflux of other EmrE substrates, in addition to MV, since most are known to be lipophilic detergents (cetylpyridinium chloride), surfactants (tetraphenylphosphonium) and dyes (EtBr), that readily partition into lipid bilayers (discussed in reference 168). It is also interesting to note that the structure of OmpW protein lacks long periplasmic loop regions, commonly observed in the structures of the oligomerizing channels, like TolC (160, 195) or Wza (17, 18), which are involved in facilitating connections between the OM-PM spanning multipartite complexes. This possibly suggests that the association between EmrE and OmpW is novel and worthy of further biochemical characterization, to confirm if these two proteins function through a structural linkage or in dissociated forms. Gaining an understanding of the different export apparatuses could, in turn, help develop and design novel antibacterial agents, which would specifically target and block the efflux pumps or secretion systems of MDR bacteria

Overall, the OM-PM association between EmrE and OmpW may represent important, conditionally active branches of bacterial MDR resistance, particularly when considering the efflux of MV, since Gram-negative bacteria lacking the dominant QCC/antibiotic RND efflux system, AcrAB-TolC, showed increased resistance to MV

through the activation of other multidrug efflux systems (132, 196). This finding also suggests that other multidrug transporters, currently known to confer resistance localized only in the PM, may have unidentified OMP counterparts that could potentially be identified through phenotypic screening methods similar to those used herein. In conclusion, the research work within this thesis has demonstrated a functional association between *E. coli* EmrE and OmpW, indicating that they both participate in the extracellular efflux of QCC and osmoprotectant substrates.

7.3 Future Directions

Based on the outcome of this study, some recommendations for future research work are:

1. Finish screening the remaining 47 porin/channel forming OM proteins (based on the proteomic analysis of the *E. coli* OM (157)) for potential involvement in the EmrE-mediated efflux mechanism, using the pH-based growth phenotype assay that was developed and successfully applied in this study.
2. Repeat the MIC QCC resistance assays using the *E. coli* Δ *acrA* (JW0452) and Δ *acrA* Δ *ompW* (needs to be constructed) mutants as “background” strains, in order to prevent the MDR transporter complex AcrAB-TolC from masking the QCC resistance phenotype conferred by OmpW and EmrE. This would allow a full array of over 15 QCCs to be screened.

3. Use a similar pH-based growth phenotype *in-vivo* assay to screen for potential periplasmic proteins that may participating in the EmrE-mediated efflux mechanism by functioning as physical “linkers” between the OMP OmpW and the PM protein EmrE.

References

1. **Gram C.** 1884. The differential staining of Schizomycetes in tissue sections and in dried preparations. *Fortschritte der Med.* **2**:185–189. Translated from German.
2. **Glauert AM, Thornley MJ.** 1969. The topography of the bacterial cell wall. *Annu. Rev. Microbiol.* **23**:159–198.
3. **Costerton JW, Ingram JM, Cheng KJ.** 1974. Structure and Function of the Cell Envelope of Gram-Negative Bacteria. *Bacteriol. Rev.* **38**:87–110.
4. **Silhavy TJ, Kahne D, Walker S.** 2010. The bacterial cell envelope. *Cold Spring Harb. Perspect. Biol.* **2**:a000414.
5. **Nikaido H, Vaara M.** 1985. Molecular basis of bacterial outer membrane permeability. *Microbiol. Rev.* **49**:1–32.
6. **Nikaido H.** 2003. Molecular Basis of Bacterial Outer Membrane Permeability Revisited. *Microbiol. Mol. Biol. Rev.* **67**:593–656.
7. **Labischinski H, Barnickel G, Bradaczek H, Naumann D, Rietschel ET, Giesbrecht P.** 1985. High state of order of isolated bacterial lipopolysaccharide and its possible contribution to the permeation barrier property of the outer membrane. *J. Bacteriol.* **162**:9–20.
8. **Vaara M, Nurminen M.** 1999. Outer Membrane Permeability Barrier in *Escherichia coli* Mutants That Are Defective in the Late Acyltransferases of Lipid A Biosynthesis. *Antimicrob. Agents Chemother.* **43**:1459–1462.
9. **Osborn MJ, Gander JE, Parisi E, Carson J.** 1972. Mechanism of Assembly of the Outer Membrane of *Salmonella typhimurium*. *J. Biol. Chem.* **247**:3962–3972.
10. **Koebnik R, Locher KP, Van Gelder P.** 2000. Structure and function of bacterial outer membrane proteins: barrels in a nutshell. *Mol. Microbiol.* **37**:239–253.
11. **Sankaran K, Wus HC.** 1994. Lipid Modification of Bacterial Prolipoprotein. *J. Biol. Chem.* **269**:19701–19706.
12. **Miyadai H, Tanaka-Masuda K, Matsuyama S, Tokuda H.** 2004. Effects of lipoprotein overproduction on the induction of DegP (HtrA) involved in quality control in the *Escherichia coli* periplasm. *J. Biol. Chem.* **279**:39807–39813.
13. **Schulz GE.** 1993. Bacterial porins : structure and function. *Curr. Opin. Cell Biol.* **5**:701–707.

14. **Jap BK, Walian PJ.** 1996. Structure and functional mechanism of porins. *Physiol. Rev.* **76**:1073–1088.
15. **Randall-Hazelbauer L, Schwartz M.** 1973. Isolation of the bacteriophage lambda receptor from *Escherichia coli*. *J. Bacteriol.* **116**:1436–1446.
16. **Schirmer T.** 1998. General and specific porins from bacterial outer membranes. *J. Struct. Biol.* **121**:101–109.
17. **Drummelsmith J, Whitfield C.** 1999. Gene products required for surface expression of the capsular form of the group 1 K antigen in *Escherichia coli* (O9a:K30). *Mol. Microbiol.* **31**:1321–1332.
18. **Dong C, Beis K, Nesper J, Brunkan AL, Clarke BR, Whitfield C, Naismith JH.** 2006. The structure of Wza, the translocon for group 1 capsular polysaccharides in *Escherichia coli*, identifies a new class of outer membrane protein. *Nature.* **444**:226–229.
19. **Schweizer M, Henning U.** 1977. Action of a major outer cell envelope membrane protein in conjugation of *Escherichia coli* K-12. *J. Bacteriol.* **129**:1651–1652.
20. **Ried G, Henning U.** 1987. A unique amino acid substitution in the outer membrane protein OmpA causes conjugation deficiency in *Escherichia coli* K-12. *FEBS Lett.* **223**:387–390.
21. **DiRienzo JM, Nakamura K, Inouye M.** 1978. The outer membrane proteins of Gram-negative bacteria: biosynthesis, assembly, and functions. *Ann. Rev. Biochem.* **47**:481–532.
22. **Rogers HJ, Perkins HR, Ward JB.** 1980. *Microbial Cell Walls and Membranes.* Chapman and Hall, London.
23. **Vollmer W, Blanot D, de Pedro MA.** 2008. Peptidoglycan structure and architecture. *FEMS Microbiol. Rev.* **32**:149–167.
24. **Vollmer W, Seligman SJ.** 2010. Architecture of peptidoglycan: more data and more models. *Trends Microbiol.* **18**:59–66.
25. **Matias RF, Al-amoudi A, Dubochet J, Beveridge TJ.** 2003. Cryo-Transmission Electron Microscopy of Frozen-Hydrated Sections of *Escherichia coli* and *Pseudomonas aeruginosa*. *J. Bacteriol.* **185**:6112–6118.
26. **Braun V.** 1975. Covalent lipoprotein from the outer membrane of *Escherichia coli*. *Biochim. Biophys. Acta.* **415**:335–377.

27. **De Mot R, Vanderleyden J.** 1994. The C-terminal sequence conservation between OmpA-related outer membrane proteins and MotB suggests a common function in both Gram-positive and Gram-negative bacteria, possibly in the interaction of these domains with peptidoglycan. *Mol. Microbiol.* **12**:333–334.
28. **Raetz CR, Dowhan W.** 1990. Biosynthesis and function of phospholipids in *Escherichia coli*. *J. Biol. Chem.* **265**:1235–1238.
29. **Papanastasiou M, Orfanoudaki G, Koukaki M, Kountourakis N, Sardis MF, Aivaliotis M, Karamanou S, Economou A.** 2013. The *Escherichia coli* peripheral inner membrane proteome. *Mol. Cell. Proteomics.* **12**:599–610.
30. **Moat AG, Foster JW, Spector MP.** 2002. *Microbial Physiology*. Wiley-Liss, Inc, New York.
31. **Wood JM.** 2011. Bacterial osmoregulation: a paradigm for the study of cellular homeostasis. *Annu. Rev. Microbiol.* **65**:215–238.
32. **Romantsov T, Battle AR, Hendel JL, Martinac B, Wood JM.** 2009. Protein localization in *Escherichia coli* cells: comparison of the cytoplasmic membrane proteins ProP, LacY, ProW, AqpZ, MscS, and MscL. *J. Bacteriol.* **192**:912–924.
33. **Csonka LN.** 1989. Physiological and genetic responses of bacteria to osmotic stress. *Microbiol. Rev.* **53**:121–147.
34. **Oren A.** 1986. The ecology and taxonomy of anaerobic halophilic eubacteria. *FEMS Microbiol. Lett.* **39**:23–29.
35. **Galinski EA.** 1995. Osmoadaptation in bacteria. *Adv. Microb. Physiol.* **37**:273–328.
36. **Yancey PH, Clark ME, Hand SC, Bowlus RD, Somero GN.** 1982. Living with water stress: evolution of osmolyte systems. *Science.* **217**:1214–1222.
37. **Le Rudulier D, Strom AR, Dandekar AM, Smith LT, Valentine RC.** 1984. Molecular Biology of Osmoregulation. *Science.* **224**:1064–1068.
38. **Epstein W.** 1986. Osmoregulation by potassium transport in *Escherichia coli*. *FEMS Microbiol. Lett.* **39**:73–78.
39. **Landfald B, Strom AR.** 1986. Choline-Glycine betaine pathway confers a high level of osmotic tolerance in *Escherichia coli*. *J. Bacteriol.* **165**:849–855.
40. **Csonka LN.** 1982. A third L-Proline Permease in *Salmonella typhimurium* Which Functions in Media of Elevated Osmotic Strength. *J. Bacteriol.* **151**:1433–1443.

41. **Perroud B, Le Rudulier D.** 1985. Glycine betaine transport in *Escherichia coli*: osmotic modulation. *J. Bacteriol.* **161**:393–401.
42. **Cairney J, Booth IR, Higgins CF.** 1985. Osmoregulation of gene expression in *Salmonella typhimurium*: *proU* encodes an osmotically induced betaine transport system. *J. Bacteriol.* **164**:1224–1232.
43. **Baich A.** 1969. Proline synthesis in *Escherichia coli* a proline-inhibitable glutamic acid kinase. *Biochim. Biophys. Acta.* **192**:462–467.
44. **Dinnbier U, Limpinsel E, Schmid R, Bakker EP.** 1988. Transient accumulation of potassium glutamate and its replacement by trehalose during adaptation of growing cells of *Escherichia coli* K-12 to elevated sodium chloride concentrations. *Arch. Microbiol.* **150**:348–357.
45. **Yan D, Ikeda TP, Shauger AE, Kustu S.** 1996. Glutamate is required to maintain the steady-state potassium pool in *Salmonella typhimurium*. *Proc. Natl. Acad. Sci.* **93**:6527–6531.
46. **Inokuchi K, Mutoh N, Matsuyama S, Mizushima S.** 1982. Primary structure of the *ompF* gene that codes for a major outer membrane protein of *Escherichia coli* K-12. *Nucleic Acids Res.* **10**:6957–6968.
47. **Mizuno T, Chou M-Y, Inouye M.** 1983. A Comparative Study on the Genes for Three Porins of the *Escherichia coli* Outer Membrane. *J. Biol. Chem.* **258**:6932–6940.
48. **Nikaido H, Nakae T.** 1980. The Outer Membrane of Gram-negative Bacteria. *Adv. Drug Deliv. Rev.* **20**:163–250.
49. **Forst S, Inouye M.** 1988. Environmentally Regulated Gene Expression for Membrane proteins in *Escherichia coli*. *Annu. Rev. Cell Biol.* **4**:21–42.
50. **Mizuno T, Mizushima S.** 1990. Signal transduction and gene regulation through the phosphorylation of two regulatory components: the molecular basis for the osmotic regulation of the porin genes. *Mol. Microbiol.* **4**:1077–1082.
51. **Foster JW.** 2001. Acid Stress Responses of *Salmonella* and *E. coli*: Survival Mechanisms , Regulation , and Implications for Pathogenesis. *J. Microbiol.* **39**:89–94.
52. **Stancik LM, Stancik DM, Schmidt B, Barnhart DM, Yoncheva YN, Slonczewski JL.** 2002. pH-Dependent Expression of Periplasmic Proteins and Amino Acid Catabolism in *Escherichia coli*. *J. Bacteriol.* **184**:4246–4258.

53. **Padan E, Zilbergtein D, Rottenberg H.** 1976. The proton electrochemical gradient in *Escherichia coli* cells. *Eur. J. Biochem.* **63**:533–541.
54. **Padan E, Zilberstein D, Schuldiner S.** 1981. pH homeostasis in bacteria. *Biochim. Biophys. Acta.* **650**:151–166.
55. **Booth IR.** 1985. Regulation of cytoplasmic pH in bacteria. *Microbiol. Rev.* **49**:359–378.
56. **Salmond CV, Kroll RG, Booth IR.** 1984. The Effect of Food Preservatives on pH Homeostasis in *Escherichia coli*. *J. Gen. Microbiol.* **130**:2845–2850.
57. **Zilberstein D, Agmon V, Schuldiner S, Padan E.** 1984. *Escherichia coli* intracellular pH, membrane potential, and cell growth. *J. Bacteriol.* **158**:246–252.
58. **Padan E, Bibi E, Ito M, Krulwich TA.** 2005. Alkaline pH homeostasis in bacteria: new insights. *Biochim. Biophys. Acta.* **1717**:67–88.
59. **Brey RN, Rosen BP, Sorensen EN.** 1979. Cation / Proton Antiport Systems in *Escherichia coli*. *J. Biol. Chem.* **255**:39–44.
60. **Macnab RM, Castle AM.** 1987. A variable stoichiometry model for pH homeostasis in bacteria. *Biophys. J.* **52**:637–647.
61. **Krulwich TA.** 1983. Na⁺/H⁺ Antiporters. *Biochim. Biophys. Acta* **726**:245–264.
62. **Ohyama T, Igarashi K, Kobayashi H.** 1994. Physiological role of the *chaA* gene in sodium and calcium circulations at a high pH in *Escherichia coli*. *J. Bacteriol.* **176**:4311–4315.
63. **Padan E, Schuldiner S.** 1993. Na⁺/H⁺ Antiporters, Molecular Devices that Couple the Na⁺ and H⁺ Circulation in Cells. *J. Bioenerg. Biomembr.* **25**:647–669.
64. **Padan E, Schuldiner S.** 1994. Molecular physiology of the Na⁺/H⁺ antiporter in *Escherichia coli*. *J. Exp. Biol.* **196**:443–456.
65. **Lewinson O, Padan E, Bibi E.** 2004. Alkalitolerance: a biological function for a multidrug transporter in pH homeostasis. *Proc. Natl. Acad. Sci.* **101**:14073–14078.
66. **Radchenko MV, Tanaka K, Waditee R, Oshimi S, Matsuzaki Y, Fukuhara M, Kobayashi H, Takabe T, Nakamura T.** 2006. Potassium/proton antiport system of *Escherichia coli*. *J. Biol. Chem.* **281**:19822–19829.
67. **Gutmann L, Williamson R, Moreau N, Kitzis M-D, Collatz E, Acar JF, Goldstein FW.** 1985. Cross-Resistance to Nalidixic Acid, Trimethoprim, and

Chloramphenicol Associated with Alterations in Outer Membrane Proteins of *Klebsiella*, *Enterobacter*, and *Serratia*. J. Infect. Dis. **151**:501–507.

68. **Medeiros AA, O'Brien TF, Rosenberg EY, Nikaido H.** 1987. Loss of OmpC Porin in a Strain of *Salmonella typhimurium* Resistance to Cephalosporins During Therapy. J. Infect. Dis. **156**:751–757.
69. **Nikaido H.** 1994. Prevention of Drug Access to Bacterial Targets: Permeability Barriers and Active Efflux. Science. **264**:382–388.
70. **Vaara M.** 1992. Agents that increase the permeability of the outer membrane. Microbiol. Rev. **56**:395–411.
71. **Nikaido H, Vaara M.** 1985. Molecular basis of bacterial outer membrane permeability. Microbiol. Rev. **49**:1–32.
72. **Nikaido H.** 1989. Outer Membrane Barrier as a Mechanism of Antimicrobial Resistance. Antimicrob. Agents Chemother. **33**:1831–1836.
73. **Angus BL, Carey AM, Caron DA, Kropinski AM, Hancock RE.** 1982. Outer membrane permeability in *Pseudomonas aeruginosa*: comparison of a wild-type with an antibiotic-supersusceptible mutant. Antimicrob. Agents Chemother. **21**:299–309.
74. **Yoshimura F, Nikaido H.** 1982. Permeability of *Pseudomonas aeruginosa* outer membrane to hydrophilic solutes. J. Bacteriol. **152**:636–642.
75. **Nikaido H.** 1998. Antibiotic resistance caused by gram-negative multidrug efflux pumps. Clin. Infect. Dis. **27**:S32–41.
76. **Spratt BG.** 1994. Resistance to Antibiotics Mediated by Target Alterations. Science. **264**:388–393.
77. **Davies J.** 1994. Inactivation of antibiotics and the dissemination of resistance genes. Science. **264**:375–382.
78. **Hayes JD, Wolft CR.** 1990. Molecular mechanisms of drug resistance. Biochem. J. **272**:281–295.
79. **Levy SB.** 1992. Active Efflux Mechanisms for Antimicrobial Resistance. Antimicrob. Agents Chemother. **36**:695–703.
80. **Higgins CF.** 2007. Multiple molecular mechanisms for multidrug resistance transporters. Nature **446**:749–757.

81. **Poolman B, Konings WN.** 1993. Secondary solute transport in bacteria. *Biochim. Biophys. Acta.* **1183**:5–39.
82. **Krulwich TA, Lewinson O, Padan E, Bibi E.** 2005. Do physiological roles foster persistence of drug/multidrug-efflux transporters? A case study. *Nat. Rev. Microbiol.* **3**:566–572.
83. **Marger MD, Saier MHJ.** 1993. A major superfamily of transmembrane facilitators that catalyse uniport, symport and antiport. *Trends Biochem. Sci.* **18**:13–20.
84. **Paulsen IT, Skurray RA, Tam R, Saier MH, Turner RJ, Weiner JH, Goldberg EB, Grinius LL.** 1996. The SMR family: a novel family of multidrug efflux proteins involved with the efflux of lipophilic drugs. *Mol. Microbiol.* **19**:1167–1175.
85. **Brown MH, Paulsen IT, Skurray RA.** 1999. The multidrug efflux protein NorM is a prototype of a new family of transporters. *Mol. Microbiol.* **31**:393–395.
86. **Saier MHJ, Tam R, Reizer A, Reizer J.** 1994. Two novel families of bacterial membrane proteins concerned with nodulation , celi division and transport. *Mol. Microbiol.* **11**:841–847.
87. **Bay DC, Rommens KL, Turner RJ.** 2007. Small multidrug resistance proteins: a multidrug transporter family that continues to grow. *Biochim. Biophys. Acta.* **1778**:1814–1838.
88. **Schuldiner S.** 2009. EmrE, a model for studying evolution and mechanism of ion-coupled transporters. *Biochim. Biophys. Acta.* **1794**:748–762.
89. **Grinius LL, Goldberg EB.** 1994. Bacterial multidrug resistance is due to a single membrane protein which functions as a drug pump. *J. Biol. Chem.* **269**:29998–30004.
90. **Muth TR, Schuldiner S.** 2000. A membrane-embedded glutamate is required for ligand binding to the multidrug transporter EmrE. *EMBO J.* **19**:234–240.
91. **Yerushalmi H, Schuldiner S.** 2000. An Essential Glutamyl Residue in EmrE, a Multidrug Antiporter from *Escherichia coli*. *J. Biol. Chem.* **275**:5264–5269.
92. **Schuldiner S, Granot D, Steiner S, Ninio S, Rotem D, Soskin M, Yerushalmi H.** 2001. Precious things come in little packages. *J. Mol. Microbiol. Biotechnol.* **3**:155–162.

93. **Littlejohn TG, Paulsen IT, Gillespie MT, Tennent JM, Midgley M, Jones IG, Purewal AS, Skurray RA.** 1992. Substrate specificity and energetics of antiseptic and disinfectant resistance in *Staphylococcus aureus*. FEMS Microbiol. Lett. **74**:259–266.
94. **Yerushalmi H, Lebendiker M, Schuldiner S.** 1995. EmrE, an *Escherichia coli* 12-kDa multidrug transporter, exchanges toxic cations and H⁺ and is soluble in organic solvents. J. Biol. Chem. **270**:6856–6863.
95. **Tezel U, Pavlostathis SG.** 2011. Role of Quaternary Ammonium. Antimicrobial Resistance in the Environment. John Wiley and Sons, Inc, Atlanta.
96. **Sidhu MS, Heir E, Sørum H, Holck A.** 2001. Genetic Linkage Between Resistance to Quaternary Ammonium Compounds and β -Lactam Antibiotics in Food-Related *Staphylococcus* spp. Microb. Drug Resist. **7**:363–371.
97. **Sidhu MS, Heir E, Leegaard T, Wiger K, Holck A.** 2002. Frequency of Disinfectant Resistance Genes and Genetic Linkage with β -Lactamase Transposon Tn 552 among Clinical *Staphylococci*. Antimicrob. Agents Chemother. **46**:2797–2803.
98. **Bay DC, Turner RJ.** 2009. Diversity and evolution of the small multidrug resistance protein family. BMC Evol. Biol. **9**:140.
99. **Chung YJ, Saier MH.** 2002. Overexpression of the *Escherichia coli* *sugE* Gene Confers Resistance to a Narrow Range of Quaternary Ammonium Compounds. J. Bacteriol. **184**:2543–2545.
100. **Saier MH, Paulsen IT, Sliwinski MK, Pao SS, Skurray RA, Nikaido H.** 1998. Evolutionary origins of multidrug and drug-specific efflux pumps in bacteria. FASEB J. **12**:265–274.
101. **Saier MH, Paulsen IT.** 2001. Phylogeny of multidrug transporters. Semin. Cell Dev. Biol. **12**:205–13.
102. **Son MS, Del Castillo C, Duncalf KA, Carney D, Weiner JH, Turner RJ.** 2003. Mutagenesis of SugE, a small multidrug resistance protein. Biochem. Biophys. Res. Commun. **312**:914–921.
103. **Greener T, Govezensky D, Zamir A.** 1993. A novel multicopy suppressor of a *groEL* mutation includes two nested open reading frames transcribed from different promoters. EMBO J. **12**:889–896.
104. **Sikora CW, Turner RJ.** 2005. SMR proteins SugE and EmrE bind ligand with similar affinity and stoichiometry. Biochem. Biophys. Res. Commun. **335**:105–11.

105. **Masaoka Y, Ueno Y, Morita Y, Kuroda T, Mizushima T, Tsuchiya T.** 2000. A two-component multidrug efflux pump, EbrAB, in *Bacillus subtilis*. *J. Bacteriol.* **182**:2307–2310.
106. **Jack DL, Storms ML, Tchieu JH, Paulsen IANT, Saier MH.** 2000. A Broad-Specificity Multidrug Efflux Pump Requiring a Pair of Homologous SMR-Type Proteins. *J. Bacteriol.* **182**:2311–2313.
107. **Yerushalmi H, Lebendiker M, Schuldiner S.** 1996. Negative Dominance Studies Demonstrate the Oligomeric Structure of EmrE, a Multidrug Antiporter from *Escherichia coli*. *J. Biol. Chem.* **271**:31044–31048.
108. **Purewal AS.** 1991. Nucleotide sequence of the ethidium efflux gene from *Escherichia coli*. *FEMS Microbiol. Lett.* **82**:229–232.
109. **Schuldiner S, Lebendiker M, Yerushalmi H.** 1997. EmrE, the smallest ion-coupled transporter, provides a unique paradigm for structure-function studies. *J. Exp. Biol.* **200**:335–341.
110. **Gottschalk K-E, Soskine M, Schuldiner S, Kessler H.** 2004. A Structural Model of EmrE, a multi-drug transporter from *Escherichia coli*. *Biophys. J.* **86**:3335–3348.
111. **Tate CG, Ubarretxena-Belandia I, Baldwin JM.** 2003. Conformational Changes in the Multidrug Transporter EmrE Associated with Substrate Binding. *J. Mol. Biol.* **332**:229–242.
112. **Ubarretxena-Belandia I, Tate CG.** 2004. New insights into the structure and oligomeric state of the bacterial multidrug transporter EmrE: an unusual asymmetric homo-dimer. *FEBS Lett.* **564**:234–238.
113. **Elbaz Y, Steiner-Mordoch S, Danieli T, Schuldiner S.** 2004. In vitro synthesis of fully functional EmrE, a multidrug transporter, and study of its oligomeric state. *Proc. Natl. Acad. Sci.* **101**:1519–1524.
114. **Von Heijne G.** 1986. Net N-C Charge Imbalance May be Important for Signal Sequence Function in Bacteria. *J. Mol. Biol.* **192**:287–290.
115. **Nara T, Kouyama T, Kurata Y, Kikukawa T, Miyauchi S, Kamo N.** 2007. Anti-parallel membrane topology of a homo-dimeric multidrug transporter, EmrE. *J. Biochem.* **142**:621–625.
116. **Rapp M, Granseth E, Seppälä S, von Heijne G.** 2006. Identification and evolution of dual-topology membrane proteins. *Nat. Struct. Mol. Biol.* **13**:112–116.

117. **Seppälä S, Slusky JS, Lloris-Garcerá P, Rapp M, von Heijne G.** 2010. Control of membrane protein topology by a single C-terminal residue. *Science*. **328**:1698–700.
118. **Lloris-Garcerá P, Bianchi F, Slusky JSG, Seppälä S, Daley DO, von Heijne G.** 2012. Antiparallel dimers of the small multidrug resistance protein EmrE are more stable than parallel dimers. *J. Biol. Chem.* **287**:26052–26059.
119. **Nasie I, Steiner-Mordoch S, Gold A, Schuldiner S.** 2010. Topologically Random Insertion of EmrE Supports a Pathway for Evolution of Inverted Repeats in Ion-coupled Transporters. *J. Biol. Chem.* **285**:15234–15244.
120. **Rotem D, Schuldiner S.** 2004. EmrE, a Multidrug Transporter from *Escherichia coli*, Transports Monovalent and Divalent Substrates with the Same Stoichiometry. *J. Biol. Chem.* **279**:48787–48793.
121. **Soskine M, Adam Y, Schuldiner S.** 2004. Direct Evidence for Substrate-induced Proton Release in Detergent-Solubilized EmrE, a Multidrug Transporter. *J. Biol. Chem.* **279**:9951–9955.
122. **Bay DC, Turner RJ.** 2012. Small multidrug resistance protein EmrE reduces host pH and osmotic tolerance to metabolic quaternary cation osmoprotectants. *J. Bacteriol.* **194**:5941–8.
123. **Schuldiner S.** 2009. EmrE, a model for studying evolution and mechanism of ion-coupled transporters. *Biochim. Biophys. Acta.* **1794**:748–762.
124. **Fralick JA.** 1996. Evidence that TolC is required for functioning of the Mar/AcrAB efflux pump of *Escherichia coli*. *J. Bacteriol.* **178**:5803–5805.
125. **Ma D, Cook DN, Alberti M, Pon NG, Nikaido H, Hearst JE.** 1995. Gense *acrA* and *acrB* encode a stress-induced efflux system of *Escherichia coli*. *Mol. Microbiol.* **16**:45–55.
126. **Lomovskaya O, Lewis K.** 1992. *emr*, an *Escherichia coli* locus for multidrug resistance. *Proc. Natl. Acad. Sci.* **89**:8938–8942.
127. **Lewis K.** 2000. Translocases: a bacterial tunnel for drugs and proteins. *Curr. Biol.* **10**:R678–R681.
128. **Lewis K.** 1994. Multidrug resistance pumps in bacteria: variations on a theme. *Trends Biochem. Sci.* **19**:119–123.
129. **Nikaido H.** 1996. MINIREVIEW Multidrug Efflux Pumps of Gram-Negative Bacteria. *J. Bacteriol.* **178**:5853–5859.

130. **Thanassi DG, Suh GS, Nikaido H.** 1995. Role of outer membrane barrier in efflux-mediated tetracycline resistance of *Escherichia coli*. *J. Bacteriol.* **177**:988–1007.
131. **Sulavik MC, Houseweart C, Cramer C, Jiwani N, Murgolo N, Greene J, DiDomenico B, Shaw KJ, Miller GH, Hare R, Shimer G.** 2001. Antibiotic Susceptibility Profiles of *Escherichia coli* Strains Lacking Multidrug Efflux Pump Genes. *Antimicrob. Agents Chemother.* **45**:1126–1136.
132. **Tal N, Schuldiner S.** 2009. A coordinated network of transporters with overlapping specificities provides a robust survival strategy. *Proc. Natl. Acad. Sci.* **106**:9051–9056.
133. **Baba T, Ara T, Hasegawa M, Takai Y, Okumura Y, Baba M, Datsenko KA, Tomita M, Wanner BL, Mori H.** 2006. Construction of *Escherichia coli* K-12 in-frame, single-gene knockout mutants: the Keio collection. *Mol. Syst. Biol.* **2**:1-11.
134. **Bethesda Research Laboratories.** 1986. BRL pUC host: *E. coli* DH5 α competent cells. *Focus.* **8**:9.
135. **Datsenko KA, Wanner BL.** 2000. One-step inactivation of chromosomal genes in *Escherichia coli* K-12 using PCR products. *Proc. Natl. Acad. Sci.* **97**:6640–6645.
136. **Jensen KF.** 1993. The *Escherichia coli* K-12 “wild types” W3110 and MG1655 have an *rph* frameshift mutation that leads to pyrimidine starvation due to low *pyrE* expression levels. *J. Bacteriol.* **175**:3401–3407.
137. **Winstone TL, Duncalf K a, Turner RJ.** 2002. Optimization of expression and the purification by organic extraction of the integral membrane protein EmrE. *Protein Expr. Purif.* **26**:111–121.
138. **Fürste JP, Pansegrau W, Frank R, Blöcker H, Scholz P, Bagdasarian M, Lanka E.** 1986. Molecular cloning of the plasmid RP4 primase region in a multi-host-range *tacP* expression vector. *Gene.* **48**:119–131.
139. **Kitagawa M, Ara T, Arifuzzaman M, Ioka-Nakamichi T, Inamoto E, Toyonaga H, Mori H.** 2005. Complete set of ORF clones of *Escherichia coli* ASKA library (a complete set of *E. coli* K-12 ORF archive): unique resources for biological research. *DNA Res.* **12**:291–299.
140. **Hanahan D.** 1985. Techniques for transformation of *E. coli*. In *DNA Cloning: A Practical Approach*. IRL Press, Oxford.
141. **Hanahan D.** 1983. Studies on Transformation of *Escherichia coli* with Plasmids. *J. Mol. Biol.* **166**:557–580.

142. **Sambrook J, Russell DW.** 2006. Purification of Nucleic Acids by Extraction with Phenol:Chloroform. Cold Spring Harb. Protoc.
143. **Mullis K, Faloona F, Scharf S, Saiki R, Horn G, Erlich H.** 1987. Specific Enzyme Amplification of DNA In Vitro: The Polymerase Chain Reaction. Methods Enzymol. **155**:3350–350.
144. **Maniatis T, Fritsch EF, Sambrook J.** 1982. Cloning: A Laboratory Manual. In Cold Spring Harbor Laboratory. Cold Spring Harbor.
145. **Aaij C, Borst P.** 1972. The gel electrophoresis of DNA. Biochim. Biophys. Acta. **269**:192–200.
146. **Sharp PA, Sugden B, Sambrook J.** 1973. Detection of two restriction endonuclease activities in *Haemophilus parainfluenzae* using analytical agarose-ethidium bromide electrophoresis. Biochemistry. **12**:3055–3063.
147. **Rye HS, Glazer AN.** 1995. Interaction of dimeric intercalating dyes with single-stranded DNA. Nucleic Acids Res. **23**:1215–1222.
148. **Rastogi RP, Richa, Kumar A, Tyagi MB, Sinha RP.** 2010. Molecular mechanisms of ultraviolet radiation-induced DNA damage and repair. J. Nucleic Acids. **10**:1–32.
149. **Linn S, Arber W.** 1968. Host specificity of DNA produced by *Escherichia coli*, X. In vitro restriction of phage fd replicative form. Biochim. Biophys. Acta. **269**:192–200.
150. **Meselson M, Yuan R.** 1968. DNA restriction enzyme from *E. coli*. Nature. **217**:1110–1114.
151. **Lehman IR.** 1974. DNA Ligase : Structure , Mechanism , and Function. Science. **186**:790–797.
152. **Jacobsen H, Klenow H, Overgaard-Hansen K.** 1974. The N-terminal amino-acid sequences of DNA polymerase I from *Escherichia coli* and of the large and the small fragments obtained by a limited proteolysis. Eur. J. Biochem. **45**:623–627.
153. **Sambrook J, Fritsch EF, Maniatis T.** 1989. Molecular Cloning: A laboratory manual. Cold Spring Harbor Laboratory Press, Cold Spring Harbor.
154. **Bay DC, Rommens KL, Turner RJ.** 2008. Small multidrug resistance proteins: a multidrug transporter family that continues to grow. Biochim. Biophys. Acta. **1778**:1814–38.

155. **Bay DC, Turner RJ.** 2012. Small multidrug resistance protein EmrE reduces host pH and osmotic tolerance to metabolic quaternary cation osmoprotectants. *J. Bacteriol.* **194**:5941–8.
156. **Baldwin WW, Myer R, Kung T, Anderson E, Koch AL.** 1995. Growth and buoyant density of *Escherichia coli* at very low osmolarities. *J. Bacteriol.* **177**:235–7.
157. **Molloy MP, Herbert BR, Slade MB, Rabilloud T, Nouwens AS, Williams KL, Gooley AA.** 2000. Proteomic analysis of the *Escherichia coli* outer membrane. *Eur. J. Biochem.* **267**:2871–81.
158. **Pages JM, James CE, Winterhalter M.** 2008. The porin and the permeating antibiotic: a selective diffusion barrier in Gram-negative bacteria. *Nat. Rev. Microbiol.* **6**:893–903.
159. **Wong K, Ma J, Rothnie A, Biggin PC, Kerr ID.** 2014. Towards understanding promiscuity in multidrug efflux pumps. *Trends Biochem. Sci.* **39**:8–16.
160. **Morona R, Manning PA, Reeves P.** 1983. Identification and characterization of the TolC protein , an outer membrane protein from *Escherichia coli*. *J. Bacteriol.* **153**:693–699.
161. **Randall LP, Woodward MJ.** 2002. The multiple antibiotic resistance (*mar*) locus and its significance. *Res. Vet. Sci.* **72**:87–93.
162. **Castillo-Keller M, Vuong P, Misra R.** 2006. Novel Mechanism of *Escherichia coli* Porin Regulation. *J. Bacteriol.* **188**:576–586.
163. **Mahendran KR, Hajjar E, Mach T, Lovelle M, Kumar A, Sousa I, Spiga E, Weingart H, Gameiro P, Winterhalter M, Ceccarelli M.** 2010. Molecular basis of enrofloxacin translocation through OmpF, an outer membrane channel of *Escherichia coli* - when binding does not imply translocation. *J. Phys. Chem.* **114**:5170–5179.
164. **Gil F, Ipinza F, Fuentes J, Fumeron R, Villarreal JM, Aspée A, Mora GC, Vásquez CC, Saavedra C.** 2007. The *ompW* (porin) gene mediates methyl viologen (paraquat) efflux in *Salmonella enterica* serovar typhimurium. *Res. Microbiol.* **158**:529–536.
165. **Fàbrega A, Rosner JL, Martín RG, Solé M, Vila J.** 2012. SoxS-dependent coregulation of *ompN* and *ydbK* in a multidrug-resistant *Escherichia coli* strain. *FEMS Microbiol. Lett.* **332**:61–67.

166. **Farrington JA, Ebert M, Land EJ, Fletcher K.** 1973. Bipyridylium quaternary salts and related compounds. V. Pulse radiolysis studies of the reaction of paraquat radical with oxygen. Implications for the mode of action of bipyridyl herbicides. *Biochim. Biophys. Acta.* **314**:372–381.
167. **Hassan HM, Fridovich I.** 1978. Superoxide radical and the oxygen enhancement of the toxicity of paraquat in *Escherichia coli*. *J. Biol. Chem.* **253**:8143–8148.
168. **Morimyo M, Hongo E, Hama-Inaba H, Machida I.** 1992. Cloning and characterization of the *mvrC* gene of *Escherichia coli* K-12 which confers resistance against methyl viologen toxicity. *Nucleic Acids Res.* **20**:3159–3165.
169. **Kolodziejek AM, Sinclair DJ, Seo KS, Schnider DR, Deobald CF, Rohde HN, Viall AK, Minnich SS, Hovde CJ, Minnich SA, Bohach GA.** 2007. Phenotypic characterization of OmpX, an Ail homologue of *Yersinia pestis* KIM. *Microbiology* **153**:2941–2951.
170. **Wang Y.** 2002. The function of OmpA in *Escherichia coli*. *Biochem. Biophys. Res. Commun.* **292**:396–401.
171. **Cascales E, Bernadac A, Gavioli M, Lazzaroni J-C, Lloubes R.** 2002. Pal Lipoprotein of *Escherichia coli* Plays a Major Role in Outer Membrane Integrity. *J. Bacteriol.* **184**:754–759.
172. **Price GP, St. John AC.** 2000. Purification and analysis of expression of the stationary phase-inducible Slp lipoprotein in *Escherichia coli*: role of the Mar system. *FEMS Microbiol. Lett.* **193**:51–56.
173. **Andersen C, Rak B, Benz R.** 1999. The gene *bglH* present in the *bgl* operon of *Escherichia coli*, responsible for uptake and fermentation of beta-glucosides encodes for a carbohydrate-specific outer membrane porin. *Mol. Microbiol.* **31**:499–510.
174. **Van Alphen W, Lugtenberg B.** 1977. Influence of osmolarity of the growth medium on the outer membrane protein pattern of *Escherichia coli*. *J. Bacteriol.* **131**:623–630.
175. **Kawaji H, Mizuno T, Mizushima S.** 1979. Influence of molecular size and osmolarity of sugars and dextrans on the synthesis of outer membrane proteins O-8 and O-9 of *Escherichia coli* K-12. *J. Bacteriol.* **140**:843–847.
176. **Alexander DM, St John AC.** 1994. Characterization of the carbon starvation-inducible and stationary phase-inducible gene *sip* encoding an outer membrane lipoprotein in *Escherichia coli*. *Mol. Microbiol.* **11**:1059–1071.

177. **Xu C, Ren H, Wang S, Peng X.** 2004. Proteomic analysis of salt-sensitive outer membrane proteins of *Vibrio parahaemolyticus*. Res. Microbiol. **155**:835–842.
178. **Xu C, Wang S, Ren H, Lin X, Wu L, Peng X.** 2005. Proteomic analysis on the expression of outer membrane proteins of *Vibrio alginolyticus* at different sodium concentrations. Proteomics. **5**:3142–3152.
179. **Lazzaroni JC, Germon P, Ray MC, Vianney A.** 1999. The Tol proteins of *Escherichia coli* and their involvement in the uptake of biomolecules and outer membrane stability. FEMS Microbiol. Lett. **177**:191–197.
180. **Luckey M, Nikaido H.** 1980. Specificity of diffusion channels produced by lambda phage receptor protein of *Escherichia coli*. Proc. Natl. Acad. Sci. **77**:167–171.
181. **Beernink PT, Tolan DR.** 1992. Construction of a high-copy “ATG vector” for expression in *Escherichia coli*. Protein Expr. Purif. **3**:332–336.
182. **De Boer HA, Comstock LJ, Vasser M.** 1983. The *tac* promoter: A functional hybrid derived from the *trp* and *lac* promoter. Proc. Natl. Acad. Sci. **80**:21–25.
183. **Brook I.** 1989. Inoculum Effect. Rev. Infect. Dis. **11**:361–368.
184. **Iravani A, Welty GS, Newton BR, Richard GA.** 1985. Effects of Changes in pH , Medium , and Inoculum Size on the In Vitro Activity of Amifloxacin Against Urinary Isolates of *Staphylococcus saprophyticus* and *Escherichia coli*. Antimicrob. Agents Chemother. **27**:449–451.
185. **Ito A, Taniuchi A, May T, Kawata K, Okabe S.** 2009. Increased antibiotic resistance of *Escherichia coli* in mature biofilms. Appl. Environ. Microbiol. **75**:4093–4100.
186. **Morimyo M.** 1988. Isolation and characterization of methyl viologen-sensitive mutants of *Escherichia coli* K-12. J. Bacteriol. **170**:2136–2142.
187. **Jalajakumari MB, Manning PA.** 1990. Nucleotide sequence of the gene, *ompW*, encoding a 22kDa immunogenic outer membrane protein of *Vibrio cholerae*. Nucleic Acids Res. **18**:2180.
188. **Das M, Chopra AK, Cantu JM, Peterson JW.** 1998. Antisera to selected outer membrane proteins of *Vibrio cholerae* protect against challenge with homologous and heterologous strains of *V. cholerae*. FEMS Immunol. Med. Microbiol. **22**:303–308.

189. **Söderblom T, Oxhamre C, Wai SN, Uhlén P, Aperia A, Uhlin BE, Richter-Dahlfors A.** 2005. Effects of the *Escherichia coli* toxin cytolysin A on mucosal immunostimulation via epithelial Ca²⁺ signalling and Toll-like receptor 4. *Cell. Microbiol.* **7**:779–788.
190. **Wu X-B, Tian L-H, Zou H-J, Wang C-Y, Yu Z-Q, Tang C-H, Zhao F-K, Pan J-Y.** 2013. Outer membrane protein OmpW of *Escherichia coli* is required for resistance to phagocytosis. *Res. Microbiol.* **164**:848–855.
191. **Nandi B, Nandy RK, Sarkar A, Ghose AC.** 2005. Structural features, properties and regulation of the outer-membrane protein W (OmpW) of *Vibrio cholerae*. *Microbiology* **151**:2975–2986.
192. **Fuentes DE, Navarro CA, Tantaleán JC, Araya MA, Saavedra CP, Pérez JM, Calderón IL, Youderian PA, Mora GC, Vásquez CC.** 2005. The product of the *qacC* gene of *Staphylococcus epidermidis* CH mediates resistance to beta-lactam antibiotics in Gram-positive and Gram-negative bacteria. *Res. Microbiol.* **156**:472–477.
193. **Hong H, Patel DR, Tamm LK, van den Berg B.** 2006. The outer membrane protein OmpW forms an eight-stranded beta-barrel with a hydrophobic channel. *J. Biol. Chem.* **281**:7568–7577.
194. **Bay DC, Turner RJ.** 2012. Spectroscopic analysis of small multidrug resistance protein EmrE in the presence of various quaternary cation compounds. *Biochim. Biophys. Acta.* **1818**:1318–31.
195. **Zgurskaya HI, Krishnamoorthy G, Ntrel A, Lu S.** 2011. Mechanism and Function of the Outer Membrane Channel TolC in Multidrug Resistance and Physiology of *Enterobacteria*. *Front. Microbiol.* **2**:189.
196. **Villagra NA, Hidalgo AA, Santiviago CA, Saavedra CP, Mora GC.** 2008. SmvA, and not AcrB, is the major efflux pump for acriflavine and related compounds in *Salmonella enterica* serovar Typhimurium. *J. Antimicrob. Chemother.* **62**:1273–1276.